Semiclassical Methods for Many-Body Systems

A dissertation presented
by

Brian Robert Landry

to
The Department of Chemistry
in partial fulfillment of the requirements
for the degree of
Doctor of Philosophy
in the subject of

Chemical Physics

Harvard University
Cambridge, Massachusetts
October 2010

Thesis advisor

Eric J. Heller

Author

Brian Robert Landry

Semiclassical Methods for Many-Body Systems

Abstract

Semiclassical methods are some of the most effective for tackling the notorious many-body problem. We follow up on some inspired work in the field of semiclassical physics including the Berry random wave conjecture and its connection to statistical mechanics, and the Thomas-Fermi approximation. The main thrust of the work is a new semiclassical method based on the Thomas-Fermi approximation that shows positive results *especially* for highly correlated systems. A new way of looking at particle exchange symmetry is central to our new method, and as such we take a fresh look at permutation symmetry in many-body systems of identical particles.

Contents

Citations to Previously Published Work

Portions of Chapters 2 and 4 have appeared in the following two papers:

> "Semiclassical Ground-State Energies of Many-Electron Systems", B.R. Landry, A. Wasserman, and E.J. Heller, *Phys. Rev. Lett.*, **103**, 066401 (2009);
>
> "Statistical properties of many particle eigenfunctions", E.J. Heller and B.R. Landry, *J. Phys. A*, **40**, 9259-9274 (2007).

Acknowledgments

There are several people who I need to express my gratitude towards and without whom life would not be the same. First and foremost are my parents and brother. My parents have always believed in everything that I do. They support me in any way they can think of, and I'm truly lucky to have them. My little brother has always been supportive as well. Really there's no one in the world whose company I enjoy more. We always know how to make each other crack up like no one else.

My family has been in my life since the begining, but in these last five years I've met some great people and I hope those relationships will continue until we're old. The Heller group has been extemely supportive and a great place to work. I'll always remember the great conversations that I would have with Jamie Walls and Adam Wasserman. They would always start about some aspect of chemistry or physics, but would wander through the realms of philosophy and sometimes politics touching on different areas of science, most fertile areas of research. I also hope to never forget those late night IHOP trips with Scott Sanders during which we'd often debate who is the bigger solipsist.

I'm really grateful that I've been lucky enough to study some really interesting problems. I've always thought it amazing that two worlds can exist (classical and quantum) with such different properties, but somewhere in the middle they must meet. It is this interest that has gotten me involed in one half of the title topic of this thesis. I'm also grateful for the funding including the Petroleum Research Fund that has allowed me to do this work.

The department has been a great place to study. From what I've seen the faculty is extremely supportive, especially my comittee, and great to teach with. I'd especially

like to thank Alán Aspuru-Guzik who I feel goes out of his way to point students in the right direction. I think of him as almost a second advisor.

Lastly I want to thank my actual advisor Rick Heller. He's a truly amazing guy and working for him was a great experience. He has a really unique mind for physics. It seems like he can sometimes just see the solutions whereas I'll have to spend hours scribbling on paper or cursing at Mathematica to obtain the same level of understanding. He has so many exceptional ideas that at times meeting with him can feel like you are trying to grab onto one and wrap your mind around it before he comes up with a better one. But in my eyes it is not his considerable science skill that makes him a great advisor, it's that he really truly cares about each of his students. Sometimes the halls of academia are described as cold and uncaring. If that's the case we need more advisors like Rick.

Chapter 1

Introduction

Reductionism has a central place in science. In order to work from a scientific perspective a researcher must separate on a mental if not physicsal level what is under study, the system, from everything else, the surroundings. In truth things are never quite so simple, but this perspective has allowed us to develop most of physics.

This perspective is not without its limitations however. The main problem introduced by a reductionist point of view is punctuated understanding. We understand an atom, or molecule, or protein, or cell, or organism quite well, but we have a great deal of difficulty understanding how these individual pieces work together to form a system of the next level of complexity. For example we are not good at understanding loosely associated atoms forming a molecule or how the primary structure of a protein results in a folded enzyme. These examples are manifestations of the many body problem. We understand one or two piece quite well, but we have difficulty with more than that, and it often takes many pieces at one level to form a system on the next level.

The main manifestation of the many body problem is that by definition the problem does not have an analytical solution for the number of particles under consideration. As discussed above, this limit is important because we wish to be able to understand the physics of matter at all scales. As the exact solution becomes intractable for a certain number of particles it becomes necessary to introduce approximations. This is how the many-body problem is necessarily dealt with. The most straightforward way of introducing an approximation and the one that is probably most often used is mean-field theory.

In a mean-field approximation the explicit interactions between particles are neglected and the particles are considered to be moving in a mean field made up of the averaged interactions with all the other particles. This greatly simplifies the problem because all the particles are now only moving in a single external potential and the problem is now a single particle problem.

Along the same lines as mean-field, it is possible to consider clusters of particles that interact with each other, but only feel an averaged potential from the rest of the particles. The pair product approximation (Chapter 3) for the green function of a many particle system can be thought of in this way. It is built from the combination of two-particle Green functions. In that way two-particle interactions are taken into account, but higher order interactions are neglected.

Another way to introduce an approximation is to use a synthetic approach (which is really going against the standard reductionism) . In a synthetic approach, an approximation to the structure at the next level of sophistication is assumed and used to describe the system of interest. An important example of this method is the Laugh-

lin wavefunction [1]. The Laughlin wavefunction describes the correlated motion of several electrons and allows strongly interacting electrons to be approximated. Any approximation that assumes a thermally large number of particles necessarily falls into this synthetic approach. In the thermal limit, the individual interactions can become a small correction to the thermal noninteracting ideal system.

An additional way to introduce an approximation is to interpolate between physical theories that work on different scales. Semiclassical approximations are a prime example of this. For systems that require a quantum mechanical description, it is possible to simplify calculations by considering the system to be approximately classical. There are many ways to enact this approximation. Most involve some type of $\hbar$ expantion since in the limit $\hbar \to 0$ the system can be described exactly by classical mechanics. Another way is to take a classical quantity and introduce the important quantum mechanical properties that are affecting the system. This is the basis for the correlated Thomas-Fermi approximation discussed in Chapter 4.

A final way to deal with problems that are difficult to solve such as the many-body problem is to consider symmetries of the system of interest. Anytime a symmetry is realized, it should lead to a simplification. Any many-body system of identical particles has symmetry group S_N. We should therefore be able to exploit this in our work. Usually the required antisymmetry of the wavefuncion is the only place that particle symmetry comes into play, but our work leads to some unique uses of this well known symmetry.

This thesis is organized as follows: In the next chapter we deal with the many-body problem from the perspective of quantum statistical mechanics and use Berry's

conjecture to make some new connections. In the third chapter we follow the natural path of our statistical studies to the pair product approximation. In the fourth chapter, which is the thrust of our work, we discuss a novel semiclassical method for calculating the ground states of many-body systems. In the next chapter we discuss the symmetry group S_N and how we use it beneficially in our work and suggest new ways to use it in general.

Chapter 2

Quantum Thermalization in Many-Body systems

2.1 Introduction

Quantum statistical mechanics is the study of large numbers of quantum particles. It is therefore a natural place to start when discussing semiclassical approximations for many body systems. Quantum statistical mechanics is a relatively well explored field [2], and the most straightforward extension of classical statistical mechanics is to replace the classical density of states by the quantum density of states. Statistical mechanics then follows quite directly through the analogous equations. The determination of the expectation value of some physical property f is

$$\langle f \rangle = \frac{\text{Tr } f\rho}{\text{Tr } \rho} \tag{2.1}$$

where the trace is a phase space integral, $\int dpdq$, for classical statistical mechanics and a quantum trace for quantum statistical mechanics. The functional form of ρ,

which corresponds to the density of systems in an ensemble, is dependent on the ensemble that one uses. For the microcanonical ensemble

$$\rho(p,q) \propto \delta(E - H(p,q)) \tag{2.2}$$

and for the canonical ensemble

$$\rho(p,q) \propto \exp\left(-\beta H(p,q)\right) \tag{2.3}$$

where $\beta = \frac{1}{kT}$. For quantum statistical mechanics these equations still hold with the density functions being replaced by density operators and the classical Hamiltonian replaced by the Hamiltonian operator

$$\rho \propto \delta(E - H) \tag{2.4}$$

and

$$\rho \propto \exp\left(-\beta H\right) \tag{2.5}$$

The well known result from statistical mechanics that all equilibrium thermodynamic quantities can be calculated from the normalization integrals, $\rho(E) = \text{Tr}\ \delta(E - H)$ and $Q(\beta) = \text{Tr}\ \exp(-\beta H)$, works for both classical and quantum systems. However these equations don't reveal anything about how the system approaches equilibrium from a nonequilibrium initial condition. At equilibrium, in the microcanonical ensemble, a system is equally likely to be in any accessible microstate. For equilibrium to occur therefore it must be true that any cluster of initial points in phase space must eventually spread out to cover all accessible phase space evenly. This process is called thermalization, and the hypothesis that this can take place for any initial cluster of points is the called the ergodic hypothesis.

Chaos plays an important role in explaining the ergoditic hypothesis. For systems that are chaotic, any initial ensemble of points in phase space will eventually fill up phase space evenly. So it is clear chaos plays an important role in classical thermalization. Quantum thermalization is less well studied, but it makes sense to suggest by analogy that quantum chaos must play some role in quantum thermalization. It turns out that the Berry conjecture, a major result from quantum chaos that will be discussed in the next section, plays an important role in quantum thermalization. Srednicki was the first to suggest that Berry's conjecture plays a role in the thermalization of quantum systems, and his work will be reviewed in Section 2.3. Our work builds upon his and is discussed in Section 2.4.

2.2 Berry's Conjecture

An important result in the study of quantum chaos, that is the study of quantum systems that are classically chaotic, is Berry's conjecture (also called the Berry random plane wave (RPW) hypothesis). The origin of the Berry conjecture lies in the study of chaotic billiard systems, and is most easy to understand for these systems. A billiard is an enclosed area with perfectly reflecting walls (usually in two dimensions). A chaotic billiard is one that exhibits chaos classically. Colloquially that means that two trajectories that start near one another in phase space will separate exponetially with time. For these systems, Berry's conjecture is the idea that for high enough energy eigenstates, that is for $\hbar \to 0$, the wavefunction would be indistinguishable from a superpostion of infinitely many plane waves with random direction, amplitude, and phase but with constant wavelength that corresponds to the energy of the eigenstate.

This can be generalized to smooth potentials by considering waves that are locally plane waves with random direction, amplitude, and phase, with a constant (local) wavelength that corresponds to the local kinetic energy. Intuitively this makes sense from a semiclassical perpective. If one considers a classical trajectory in a chaotic billiard, the trajectory will eventually cover phase space. The semiclassical wavefunction is then built up by putting a phase on this classical backbone. Since any point is hit by trajectories from random directions it makes sense that the wavefunction would be made from random waves.

In two dimensions, the Berry conjecture leads to the autocorrelation function

$$\langle \psi^*(\vec{x})\psi(\vec{x}+\vec{R})\rangle = J_0(ka) \tag{2.6}$$

where k is the local wavenumber and $|\vec{R}| = a$.

Another way to look at Berry's conjecture is that the wavefunction is completely random subject to contraints (in this case just the constant total energy). The additional constraint of a having a nearby wall has been done [3]. It is possible to imagine the addition of more constraints until the limit of the exact wavefunction at some eigenenergy is reached. It is this idea that motivates our work with statistical wavefunctions.

2.2.1 Berry's conjecture in N dimensions

Berry's conjecture scales to an arbitrary number of dimensions without trouble [4]. For N dimensions the Berry conjecture leads to the autocorrelation function

$$\langle \psi(\mathbf{x})\psi^*(\mathbf{x}+\mathbf{r})\rangle \propto \left(\frac{k}{r}\right)^d \; J_d(kr) \tag{2.7}$$

where k is the local wavenumber and $d = ND/2 - 1$, with number of particles N and number of dimensions D.

The randomness and constant energy that are part of the Berry conjecture is the same as the underpinnings of the microcanonical ensemble in quantum statistical mechanics. In the microcanonical ensemble of quantum statistical mechanics, ensemble averages are taken over all states at a certain energy. With Berry's conjecture we have all waves at a certain energy. For the thermodynamic limit, $N >> 1$, the microcanonical ensemble gives the same results as the canonical ensemble. We should therefore see the canonical ensemble emerging as N gets large from the (microcanonical) Berry conjecture.

2.3 Quantum Thermalization

Srednicki has shown that Berry's conjecture is sufficient for quantum thermalization, and therefore that quatum chaos is is an important factor in quantum thermalization just as classical chaos is important in classical thermalization [5]. He discusses the case of distinguishable particles in a box ending up with their momenta being well described by a Maxwell-Boltzmann distribution,

$$f_{MB}(\mathbf{p}, T) = (2\pi mkT)^{-3/2} \, e^{-\mathbf{p}^2/2mkT} \tag{2.8}$$

independent of initial conditions. The classical case is straightforward, but requires the assumption that the system is ergotic. It is a well know result from chaos theory that for fully chaotic systems the motion is indeed ergotic. For partially chaotic systems things become more complicated, but we, as Srednicki has, limit the discussion

here to the simple case of hard spheres which is a fully chaotic system.

Srednicki's main result is that for a system of N hard spheres in a box with eigenfunction

$$\psi_\alpha(\mathbf{X}) = N_\alpha \int d^{3N}P \; A_\alpha(\mathbf{P})\, \delta\left(\mathbf{P}^2 - 2mU_\alpha\right) \exp\left(i\mathbf{P}\cdot\mathbf{X}/\hbar\right) \tag{2.9}$$

where the integral is over the domain defined by the radii of the hard spheres and U_α is the energy eigenvalue. The the requirements on $A_\alpha(\mathbf{P})$ are $A^*_\alpha(\mathbf{P}) = A_\alpha(-\mathbf{P})$ and that they are chosen so that the wavefunctions are zero on the boundaries of the hard spheres and on the box containing them.

But the Berry conjecture for this system is equivalent to taking $A_\alpha(\mathbf{P})$ to be Gaussian random with

$$\langle A_\alpha(\mathbf{P})\, A_\beta(\mathbf{P}')\rangle = \delta_{\alpha\beta}\; \delta^{3N}(\mathbf{P}+\mathbf{P}')\,/\delta\left(\mathbf{P}^2 - \mathbf{P}'^2\right) \tag{2.10}$$

That is the coefficients for different eigenstates are uncorrelated as are the same coefficients at different momenta. The expectation value is taken over an eigenstate ensemble. Individual eigenfunctions are thought of to be taken at random from this ensemble.

For high energy the requirement on $A_\alpha(\mathbf{P})$ that the wavefunctions go to zero on the boundary, the surface of the hard spheres, is not too strict. As discussed in Section 2.2 for billiards, at high energies the wavefunction is highly oscillatory and so the behavior near the boundaries is not important.

The wavefunction in momentum space is

$$\begin{aligned}
\psi_\alpha(\mathbf{P}) &= h^{-3N/2} \int_D d^{3N}X \; \psi_\alpha(\mathbf{X}) \exp\left(i\mathbf{P}\cdot\mathbf{X}/\hbar\right) &(2.11)\\
&= h^{-3N/2} N_\alpha \int_{-\infty}^{\infty} d^{3N}K \; A_\alpha(\mathbf{K})\, \delta\left(\mathbf{K}^2 - 2mU_\alpha\right) \; \delta_D^{3N}(K-P) &(2.12)
\end{aligned}$$

where

$$\delta_D^{3N}(K) = h^{-3N} \int_D d^{3N}X \exp\left(i\mathbf{K}\cdot\mathbf{X}/\hbar\right) \tag{2.13}$$

and D is the domain that the wavefunction is defined, that is outside the hard spheres, but inside the box. If D were all space $\delta_D^{3N}(K)$ would be a true delta function. As it is, in the low density limit, which we consider, it is a function highly peaked around zero.

Berry's conjecture holds if the thermal wavelength $\lambda_\alpha = \sqrt{2\pi\hbar^2/mkT_\alpha}$ defined by $U_\alpha = \frac{3}{2}NkT_\alpha$ is less than the radii of the hard spheres a. This is necessary because for Berry's conjecture to hold the average wavelength must be less than the features of the boundary. If this is not the case the boundary will become important even far from it and the assumption that the $A_\alpha(\mathbf{P})$ can produce a wavefunction that is zero on the boundary does not hold.

It is also necessary to consider the low density regime, $Na^3 << L^3$. With these two requirements, $Na^3 << L^3$ and $\lambda_\alpha < a$ it is possible to make the following approximations. First since it is a low density box $\int_D d^{3N}X \approx L^{3N}$. Since the volume of the spheres is small relative to the box volume, it is possible to neglect the spheres' volume in the integral. With this approximation we have

$$\delta_D^{3N}(0) = h^{-3N} \int_D d^{3N}X = (L/h)^{3N} \tag{2.14}$$

Again because $\lambda_\alpha < a$, the regime at the boundaries is not important in the integral $\int_D d^{3N}X \exp\left(i\mathbf{K}\cdot\mathbf{X}/\hbar\right)$ so it is possible to make the substitution

$$\delta_D^{3N}(P) = \delta^{3N}(P) \tag{2.15}$$

That is $\delta_D^{3N}(P)$ is sharply peaked enough to consider it an actual delta function.

Combining these two approximations it is possible to say

$$\left(\delta_D^{3N}(P)\right)^2 = (L/h)^{3N}\,\delta^{3N}(P) \tag{2.16}$$

Using these approximations it is possible to show that

$$\langle\psi_\alpha^*(\mathbf{P})\,\psi_\beta(\mathbf{P'})\rangle = \delta_{\alpha\beta}\;\delta\left(\mathbf{P}^2 - 2mU_\alpha\right)\delta_D^{3N}(\mathbf{P}-\mathbf{P'}) \tag{2.17}$$

Now the fraction of atoms within d^3p of $\mathbf{p}$ is $f_{QM}(p,t)d^3p$ with

$$f_{QM}(p,t) = \int d^3p_2\cdots d^3p_N\,|\psi(\mathbf{P},t)| \tag{2.18}$$

For the simplest case of the initial condition being a single energy eigenstate we have

$$f_{QM}(p,t) = \int d^3p_2\cdots d^3p_N\,|\psi_\alpha(\mathbf{P},t)| \tag{2.19}$$

Taking the ensemble average over the eigenstate ensemble the result is

$$\left\langle\int d^3p_2\cdots d^3p_N\,|\psi(\mathbf{P},t)|\right\rangle = {N_\alpha}^2 L^{3N}\int d^3p_2\cdots d^3p_N\delta\left(\mathbf{P}^2 - 2mU_\alpha\right) \tag{2.20}$$

Using the proper normalization gives

$$\left\langle\int d^3p_2\cdots d^3p_N\,|\psi(\mathbf{P},t)|\right\rangle = \frac{\Gamma(3N/2)}{\Gamma((3N-3)/2)}\,(2\pi mU_\alpha)^{-3/2}\left(1-\frac{p_1^2}{2mU_\alpha}\right)^{(3N-5)/2} \tag{2.21}$$

Setting $U_\alpha = \frac{3}{2}NkT_\alpha$ and taking the large N limit gives

$$\left\langle\int d^3p_2\cdots d^3p_N\,|\psi(\mathbf{P},t)|\right\rangle = (2\pi mkT_\alpha)^{-3/2}\,e^{-{\mathbf{p_1}}^2/2mkT_\alpha} \tag{2.22}$$

which is the correct Maxwell-Boltzmann distribution.

Srednicki shows therefore that the Berry conjecture is sufficient for quantum thermalization to occur. We continue this work on the connection between the Berry

conjecture and quantum statistical mechanics. The Berry conjecture is really equivalent to a quantum microcanonical ensemble since it is a superposition of states of the same energy. It is no surprise therefore that it can be used in the same way that the classical microcanonical ensemble can to derive the Maxwell-Boltzmann distribution. We continue the investigation of the Berry conjecture in a quantum statistical mechanics context and show that it leads to a connection between the microcanonical ensemble, which is the native form of the Berry conjecture and the canonical ensemble through a novel asymptotic form.

2.4 Connection between Microcanonical and Canonical Ensembles

The way that we approach the Berry conjecture is through the central equation

$$\langle \psi^*(\vec{x})\psi(\vec{x}')\rangle = \mathrm{Tr}\left[\delta(E-H)|\vec{x}\rangle\langle\vec{x}'|\ \right], \tag{2.23}$$

Here we are assuming a continuumn in energy, which holds for example in enclosures with walls that are far away. Since the trace is independent of the basis that you are using the basis can be taken to be a complete set of random waves, as the Berry conjecture is usually written, or any other basis such as local plane waves. The result is the same.

In fact if we use the coordinate space basis for the trace, we can show that

$$\begin{aligned} \langle \psi^*(\vec{x})\psi(\vec{x}')\rangle &= \mathrm{Tr}\left[\delta(E-H)|\vec{x}\rangle\langle\vec{x}'|\ \right] && (2.24)\\ &= \int dx''\langle x''|\delta(E-H)|x\rangle\langle x'|x''\rangle && (2.25)\end{aligned}$$

$$= \int dx'' \langle x''|\delta(E-H)|x\rangle \delta\left(x'-x''\right) \tag{2.26}$$

$$= \langle x'|\delta(E-H)|x\rangle \tag{2.27}$$

This shows that the spatial correlation function $\langle\psi^*(\vec{x})\psi(\vec{x}')\rangle$ is equivalent to the microcanonical density matrix written in a coordinate space basis, $\rho(x,x',E) = \langle x'|\delta(E-H)|x\rangle$. The microcanonical density matrix $\delta(E-H)$ is therefore central to our work. We use the fact that the imaginary part of the retarded Green function is equivalent to this delta function, $-\frac{1}{\pi}\mathrm{Im}\left[G^+(E)\right] = \delta(E-H)$. The route we take to investigate the Berry conjecture for a large number of particle uses this relation and the imaginary part of the retarded Green function is the primary tool that we use.

Before continuing it is necessary to review well known formalism to establish context and notation. The Green function completely characterizes a quantum system, whether it is interacting or not, or has few or many degrees of freedom. The retarded Green function G^+, i.e.

$$G^+ = \mathcal{P}\frac{1}{E-H} - i\pi\delta(E-H), \tag{2.28}$$

where $\mathcal{P}$ stands for the principal value of the integral, is the basis for wavefunction statistics and density matrix information, through the follow relations:

$$\langle\psi(\mathbf{x})\psi^*(\mathbf{x}')\rangle = -\frac{1}{\pi}\mathrm{Im}\langle\mathbf{x}|G^+|\mathbf{x}'\rangle/\rho(E) \tag{2.29}$$

$$= \langle\mathbf{x}|\delta(E-H)|\mathbf{x}'\rangle/\rho(E) \tag{2.30}$$

where

$$\rho(E) = \mathrm{Tr}[\delta(E-H)] \tag{2.31}$$

We have chosen the normalization so that the spatial correlation function is equal to

the coordinate space representation of the density matrix rather than just proportional to it.

There are several different equivalent interpretations of the ensemble average in 2.30. The most straightforward is to take $\langle \cdots \rangle$ as an average over degeneracies. It is always possible to do this, since for a system with no degeneracies, we can artificially open the system up to a continuum. For example, a two dimensional closed billiard does not have a degeneracy, but it acquires one if we open a hole in it and let it communicate with the outside unbounded 2D space. Of course this changes the billiard properties, and the size of the hole might be problematic, but in fact we shall never really have to open a system up in this way. The quantity $\delta(E - H)$ then implies the average over all scattering wavefunctions at fixed energy E.

Another equivalent interpretation is as an average over an ensemble of potentials. There may be an infinite number of potentials that have an eigenstate at energy E. The average can be taken to be over the ensemble of these different potentials.

Yet another way to do the average is to average over energies. If for example there are no degeneracies instead of opening up the system to create artificial degeneracies it is actually equivalent to take an average over states in a small energy range ΔE. In the limit of ΔE being very small this is again a microcanonical average, and is the same as the other interpretations [6].

As discussed above, the wavefunction correlations is equal to the matrix element in coordinate space of the constant energy density matrix:

$$\langle \psi(\mathbf{x})\psi^*(\mathbf{x}') \rangle = \langle \mathbf{x}|\delta(E - H)|\mathbf{x}'\rangle / \rho(E) = \rho(\mathbf{x}, \mathbf{x}', E) \tag{2.32}$$

Reduced matrices can also be derived from wavefunction correlations; e.g.

$$\tilde{\rho}(\vec{x}_1, \vec{x}_1', E) = \int d\vec{x}_2 d\vec{x}_3 \cdots d\vec{x}_N \ \rho(\vec{x}_1, \vec{x}_2, \cdots; \vec{x}_1', \vec{x}_2, \cdots; E), \tag{2.33}$$

the one particle reduced density matrix.

We can approach the propagator via the time domain:

$$\delta(E - H) = \frac{1}{2\pi\hbar} \int_{-\infty}^{\infty} e^{iEt/\hbar} e^{-iHt/\hbar} \ dt \tag{2.34}$$

where we have used the integral definition of the delta function. We can also write

$$\langle \psi(\mathbf{x}) \psi^*(\mathbf{x}') \rangle = \frac{1}{\rho(E) \ 2\pi\hbar} \int_{-\infty}^{\infty} e^{iEt/\hbar} K(\mathbf{x}, \mathbf{x}', t) \ dt. \tag{2.35}$$

This makes clear that the statistics, density matrices and correlations are derivable without further averaging by knowing the time propagator. It is very rewarding to expand the propagator in semiclassical terms, involving short time (zero length) and longer trajectories.

We take $K_{st}(\mathbf{x}, \mathbf{x} + \mathbf{r}, t)$, the very short time semiclassical propagator, which for an N particles each in D dimensions reads

$$K_{st}(\mathbf{x}, \mathbf{x} + \mathbf{r}, t) \approx \left(\frac{m}{2\pi i\hbar t} \right)^{ND/2} e^{imr^2/2\hbar t - iV(\mathbf{x} + \frac{\mathbf{r}}{2})t/\hbar} \tag{2.36}$$

where $r^2 = |\mathbf{r}|^2$.

It is not difficult to cast the Fourier transform of this short time version to fit the definition of a Hankel function, i.e.

$$\begin{aligned} G_{cl}^{+}(\mathbf{x}, \mathbf{x} + \mathbf{r}, E) &= \frac{-i}{\hbar} \int_0^{\infty} \left(\frac{m}{2\pi i\hbar t} \right)^{ND/2} e^{imr^2/2\hbar t - iV(\mathbf{x} + \frac{\mathbf{r}}{2})t/\hbar} e^{iEt/\hbar} \ dt & (2.37) \\ &= -\frac{im}{2\hbar^2} \left(\frac{k^2}{2\pi kr} \right)^d H_d^{(1)}(kr) & (2.38) \end{aligned}$$

where $d = ND/2 - 1$, $k = k(E, \vec{x} + \mathbf{r}/2)$ and $H_d^{(1)} = J_d(kr) + iN_d(kr)$ is the Hankel function of order d, and J_d is the regular Bessel function of order d. We have simply used the integral definition of the Hankel function

$$H_d^{(1)}(z) = \frac{1}{i\pi} \int_0^\infty \frac{e^{(z/2)(t-1/t)}}{t^{d+1}} dt \tag{2.39}$$

The wavevector k varies with the local potential, i.e. $\hbar^2 k(E, \vec{x})^2/2m = E - V(\vec{x})$. Here, using only the extreme short time version of the propagator, we must suppose $\mathbf{r}$ is not large compared to significant changes in the potential, but this restriction can be removed by using the full semiclassical propagator rather than the short time version. For the case of one particle in two dimensions, $d = 0$, and we recover Berry's original result for one particle in 2D, $\langle \psi^*(\vec{x})\psi(\vec{x} + \vec{r})\rangle = J_0(kr)$.

According to the short time approximation, for any N,

$$\langle \psi(\mathbf{x})\psi^*(\mathbf{x} + \mathbf{r})\rangle \approx -\frac{1}{\pi} \frac{\mathrm{Im}\left[G_{st}^+(\mathbf{x}, \mathbf{x} + \mathbf{r}, E)\right]}{\rho(E)} = \frac{1}{\rho(E)} \frac{m}{2\pi\hbar^2} \left(\frac{k^2}{2\pi kr}\right)^d J_d(kr) \tag{2.40}$$

where $k = k(\mathbf{x}, E)$. This result includes interparticle correlations through the potential $V(\mathbf{x})$ and the spatial dependence of $k = k(\mathbf{x}, E)$; the diagonal $r = 0$ limit (following section) is equivalent to classical statistical mechanics. The implications of this for the nondiagonal short time Green function are intriguing. The way r is defined, it does not matter whether one particle is off diagonal ($\mathbf{x}_i \neq \mathbf{x}_{i'}$) or several or all of them. For given r, the Green function will be the same, apart from changes in the potential $V(\mathbf{x} + \mathbf{r}/2)$.

It is interesting that although the short time Green function is manifestly semiclassical, the energy form, e.g. Eq. 2.40 is obtained by exact Fourier transform, rather than stationary phase. In fact there is no real time stationary phase point, for the rea-

son that classical trajectories do not simultaneously remain in place and have kinetic energy E.

Now we consider the diagonal Green function which can yield the diagonal density matrix in the coordinate space representation through Eq 2.32. Interestingly although there are quantum mechanical effects included in the short time Green function, the diagonal short time Green function gives purely classical results.

2.4.1 Diagonal (Classical) Green Function

The diagonal ($r \to 0$) N body Green function is obtained using the asymptotic form

$$\lim_{r\to 0} J_d(kr) = \frac{1}{\Gamma(d+1)} \left(\frac{kr}{2}\right)^d \approx \frac{1}{\sqrt{2\pi d}} \left(\frac{ekr}{2d}\right)^d. \tag{2.41}$$

We obtain

$$-\frac{1}{\pi}\mathrm{Im}\left[G^+_{cl}(\mathbf{x},\mathbf{x},E)\right] \approx \frac{m}{2\pi\hbar^2}\frac{1}{\Gamma(d+1)}\left(\frac{k^2}{4\pi}\right)^d \approx \frac{m}{2\pi\hbar^2}\frac{1}{\sqrt{2\pi d}}\left(\frac{ek^2}{4\pi d}\right)^d \tag{2.42}$$

where the second form uses Stirling's approximation, $n! \sim n^n e^{-n}\sqrt{2\pi n}$, and is appropriate below when we consider large N. Again as discussed above this result is proportional to the wavefunction correlation or equivalently the microcanonical density matrix. So with the short time propagator we have an approximation for the diagonal microcanonical density matrix. We note that this behaves as $k^{2d} \sim (E - V(\vec{x}))^d$. This factor is familiar from the computation of the classical density of states; tracing over all $\vec{x}$ results in

$$\int d\mathbf{x}\ \frac{m}{2\pi\hbar^2}\frac{1}{\Gamma(d+1)}\left(\frac{k^2}{4\pi}\right)^d = \int \frac{d\mathbf{x}d\mathbf{p}}{h^{ND}}\ \delta(E - H_{cl}(\mathbf{p},\mathbf{x})) = \rho_{cl}(E) \tag{2.43}$$

i.e. the classical density of states. The association of the short time propagator with the classical Hamiltonian and classical density of states is well known. The Berry RPW hypothesis, the short time propagator, and the classical or Weyl (sometimes called Thomas-Fermi) term in the quantum density of states are all closely related.

For the reader that is paying especially close attention (anyone?) it may be perplexing that the integral in 2.43 is over all coordinate space. For a classical system the integral should be over only classically allowed positions. This would be included explicitly in the integral limits for a classical system. Here we have the same thing because of a special property of the Hankle function. For forbidden positions, k is imaginary and can be written as say $i\kappa$. The identity for Hankel functions that can then be used is $i^{n+1}H_n^{(1)}(ix) = \frac{2}{\pi}K_n(x)$. This means that for imaginary k the Hankel function is purely real so the imaginary part is zero. Therefore the integrand is zero for forbidden postions. This explains why the integral is only over classically allowed positions.

As long as $\mathbf{r} = 0$ (i.e. diagonal Green function) the results obtained within the short time propagator approximation for any quantity in the presence of a potential (*including* interparticle potentials such as atom-atom interactions) will be purely classical.

Since we will be discussing the equivalence of the results from the different ensembles for $\mathbf{r} \neq 0$, it is useful to recall how the classical coordinate space densities in the different ensembles can be shown to coincide since this corresponds to the $\mathbf{r} = 0$ case.

Classically the normalized phase space density in the microcanonical ensemble

and the phase space density in the canonical ensemble are given by

$$\rho_{cl}(\mathbf{p},\mathbf{x},E) = \frac{1}{\rho_{cl}(E)}\ \delta(E - H_{cl}(\mathbf{p},\mathbf{x})) \tag{2.44}$$

and

$$\rho_{cl}(\mathbf{p},\mathbf{x},\beta) = \frac{1}{Q_{cl}(\beta)}\ e^{-\beta H_{cl}(\mathbf{p},\mathbf{x})} \tag{2.45}$$

respectively. The density of states and partition function are of course the normalization factors so that

$$\rho_{cl}(E) = \int d\mathbf{x}d\mathbf{p}\ \delta(E - H_{cl}(\mathbf{p},\mathbf{x})) \tag{2.46}$$

$$Q_{cl}(\beta) = \int d\mathbf{x}d\mathbf{p}\ e^{-\beta H_{cl}(\mathbf{p},\mathbf{x})} \tag{2.47}$$

Integrating each phase space density over momentum space allows us to compare the coordinate space densities:

$$\rho_{cl}(\mathbf{x},E) = \frac{p^{2d}}{\int d\mathbf{x}\ p^{2d}} \tag{2.48}$$

$$\rho_{cl}(\mathbf{x},\beta) = \frac{e^{-\beta V(\mathbf{x})}}{\int d\mathbf{x}\ e^{-\beta V(\mathbf{x})}} \tag{2.49}$$

with $p = \sqrt{2m(E - V(\mathbf{x}))}$.

The equipartion theorem for this system can be written as $E - \langle V\rangle = \frac{ND}{2\beta}$, where where $\langle V\rangle$ is the ensemble average of the potential in one of the statistical ensembles. It is possible to use this relation to show the connection between the ensembles. Using this equipartition relation and the definition of momentum, $p = \sqrt{2m(E - V(\mathbf{x}))}$, the coordinate space density becomes

$$p^{2d} = (2m(d+1)/\beta)^d \left(1 + \frac{(\langle V\rangle - V(\mathbf{x}))\,\beta}{d+1}\right)^d \tag{2.50}$$

In the limit $N \to \infty$ ($d \to \infty$) this is

$$p^{2d} = (2m(d+1)/\beta)^d e^{(\langle V\rangle - V(\mathbf{x}))\beta} \tag{2.51}$$

$$\frac{p^{2d}}{\int d\mathbf{x}\; p^{2d}} = \frac{e^{-V(\mathbf{x})\beta}}{\int d\mathbf{x}\; e^{-V(\mathbf{x})\beta}} \tag{2.52}$$

where we have used the well known limit $e^x = \lim_{m\to\infty}\left(1+\frac{x}{m}\right)^m$. This is one of the standard ways of establishing a connection between the ensembles [7].

Since the diagonal Green function gives classical results we can use it to study classical properties. For example, we can inquire about the average two particle spacing distribution $\rho_E(r_{12})$ or the probability density for a single particle $P_E(\vec{x}_1)$ starting with the short time semiclassical Green function and the results will coincide with classical microcanonical statistical mechanics. This statement holds for all N. Similarly, in the large N limit the canonical ensemble results for these quantities must emerge. This point becomes more interesting for the non-diagonal case, which we consider next.

2.4.2 Asymptotic Bessel Functions and a Link to the Canonical Ensemble

As yet we have found nothing too surprising or useful beyond standard classical statistical mechanics. This changes when we consider the large N limit for the non-diagonal Green function, $\mathbf{r} \neq 0$. Taking the large N limit of Eq. 2.40, we are confronted with a new question about Bessel functions. The large d limit of $J_d(x)$ is indeed well known, but this is not yet sufficient for our purposes. It reads

$$\lim_{d\to\infty}\frac{J_d(kr)}{(kr)^d} = \frac{1}{2^d\;\Gamma(d+1)} \approx \frac{1}{\sqrt{2\pi d}}\left(\frac{e}{2d}\right)^d \tag{2.53}$$

This is the standard formula given in the usual references. Eq. 2.53 should be the first term in a power series for $J_d(kr)$ in kr. Another standard result is the power series expansion, valid for all d and kr:

$$J_d(kr) = \sum_{m=0}^{\infty} \frac{(-1)^m}{m!\Gamma(m+d+1)} \left(\frac{kr}{2}\right)^{2m+d} \tag{2.54}$$

We actually require a different asymptotic result. What makes our demands unusual is that, assuming we want the energy to increase in proportion to the number of particles (appropriate to many applications of the large N limit), then $k \sim \sqrt{E} \sim \sqrt{N} \sim \sqrt{d}$; this means that for fixed r the combination (kr) is increasing as $\sqrt{d}$ as $d \to \infty$. If the argument of the Bessel function increases without bound along with its order, some new considerations come into play. We find the desired form using Eq. 2.54, after summing a series recognized as that of a Gaussian Taylor expansion,

$$\lim_{d\to\infty} \frac{1}{(kr)^d} J_d(kr) = \frac{1}{2^d\ d!} \sum_{m=0}^{\infty} \frac{1}{m!} \left(\frac{-k^2r^2}{4(d+1)}\right)^m = \frac{1}{2^d\ d!} e^{-k^2r^2/(4(d+1))}, \tag{2.55}$$

where again $\hbar^2k^2/2m = E - V(\mathbf{x})$. Note that as $d \to \infty$, the argument of the Gaussian holds fixed because of the factor of $d+1$ in the denominator of that argument. Figure 2.1 illustrates the convergence to the Gaussian as N increases. The asymptotic limit in Equation 2.55 is not in the usual references, although related results have been given for N-bead polymer random chain end-to-end distributions [8]. The connection between the path integral for the propagator and polymer chains is well known [9].

It is interesting that a Gaussian emerges from Bessel functions in the large N limit. We can put Eq. 2.55 together with Eq. 2.40 and Eq. 2.32, and express the result, as $N \to \infty$,

$$\langle \psi(\mathbf{x})\psi^*(\mathbf{x}+\mathbf{r})\rangle \ = \ \rho(\mathbf{x},\mathbf{x}',E) \ \to \ \frac{1}{\rho(E)} \frac{m}{2\pi\hbar^2 d!} \left(\frac{k^2}{4\pi}\right)^d \ e^{-k^2r^2/4(d+1)}. \tag{2.56}$$

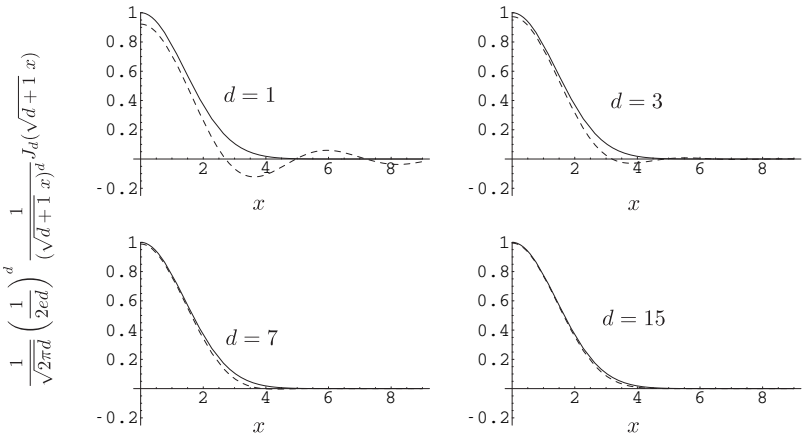

Figure 2.1: As N increases, the combination $\frac{1}{x^d} J_d(x)$, where $d = ND/2-1$, approaches a Gaussian. This is the key link between the quantum microcanonical and canonical ensembles.

For noninteracting particles moving in zero potential but confined to volume V the short time approximation becomes exact and k is constant. For this system the wavefunction correlation becomes

$$\langle \psi(\mathbf{x})\psi^*(\mathbf{x}+\mathbf{r})\rangle \;=\; \rho(\mathbf{x},\mathbf{x}',E) \;\rightarrow\; \frac{1}{V^N}\; e^{-k^2r^2/4(d+1)}. \tag{2.57}$$

Something familiar is emerging, here derived in the unfamiliar context of fixed energy (microcanonical ensemble). For comparison we recall the standard result for the ideal gas at temperature T[2]:

$$\frac{\langle \mathbf{x}|e^{-\beta H}|\mathbf{x}+\mathbf{r}\rangle}{\mathrm{Tr}[e^{-\beta H}]} = \rho(\mathbf{x},\mathbf{x}',\beta) = \frac{1}{V^N}\; e^{-\pi r^2/\lambda^2} \tag{2.58}$$

where $\lambda = h/\sqrt{2\pi m\kappa T}$ is the thermal wavelength. Indeed for the free particle case, k is fixed by E and $\langle K\rangle = (D/2)N\kappa T = \hbar^2k^2/2m$, where K is the kinetic energy and κ is Boltzmann's constant,

$$e^{-k^2r^2/4(d+1)} = e^{-\pi r^2/\lambda^2}. \tag{2.59}$$

The canonical ensemble result for the propagator has "dropped out" of the asymptotic large N limit of a microcanonical Green function, at least for noninteracting particles, and an unusual asymptotic form for the Bessel function has emerged as the link. With some caveats, the statement

$$\delta(E - H) \sim e^{-\beta H} \tag{2.60}$$

has meaning in the large N limit, where it is understood E grows as N, and a temperature extracted. In other words for large enough systems the canonical and microcanonical density matrices are equivalent. This is a necessary result of statistical mechanics, but we have shown an new way to express this qualitative result through Berry's conjecture. This means that the density matrix for a many-body quantum system that is held at a fixed energy (microcanonical) is essentially equal to the density matrix of the same system that is in contact with a bath at the proper temperature. In the case of an interaction potential, the relation between E and temperature is of course problematical.

We can say more about interacting particles using only the short time propagator introduced above. Longer time events will be discussed in Sec. 2.5.3. The short-time approximation to the correlation function for large N, which is equal to the matrix elements of the density operator in coordinate space using our normalization, (Eq. 2.56) is given by

$$\rho_{cl}(\mathbf{x}, \mathbf{x}', E) = \frac{1}{\rho(E)} \frac{m}{2\pi\hbar^2 d!} \left(\frac{k^2}{4\pi}\right)^d \; e^{-k^2 r^2/4(d+1)} \tag{2.61}$$

with $\hbar k = \sqrt{2m(E - V(\frac{\mathbf{x}+\mathbf{x}'}{2}))}$ and $r = |\mathbf{x} - \mathbf{x}'|$. Again, the Gaussian form of this expression arises from the asymptotic limit of the Bessel function. In the interacting

case this can again be brought into the same form as the equivalent expression at constant temperature:

$$\rho_{cl}(\mathbf{x}, \mathbf{x}', \beta) = \frac{1}{Z(\beta)} \left(\frac{m}{2\pi\beta\hbar^2} \right)^{d+1} e^{-\frac{mr^2}{2\hbar^2\beta} + V(\frac{\mathbf{x}+\mathbf{x}'}{2})\beta} \tag{2.62}$$

In order to make the connection we must identify the energy with a certain temperature. This relationship between E and β is

$$E - \langle V \rangle = \frac{ND}{2\beta} \tag{2.63}$$

where $\langle V \rangle$ is the ensemble average of the potential in one of the statistical ensembles. Using this relationship in Eq. 2.61 gives

$$\rho_{cl}(\mathbf{x}, \mathbf{x}', E) = \frac{1}{\rho(E)} \frac{m}{2\pi\hbar^2 d!} \left(\frac{k^2}{4\pi} \right)^d e^{-\frac{mr^2}{2\hbar^2\beta}} e^{-\frac{m(\langle V \rangle - V)r^2}{2\hbar^2(d+1)}} \tag{2.64}$$

In order for Eq. 2.64 to be equivalent to Eq. 2.62 the term with $\langle V \rangle - V$ must be negligible. This is true for configurations of particles which possess the typical (and vastly most probable) total kinetic energy. Since the typical total kinetic energy is by far the most probable, nearly all points in configuration space lead to small values of $\langle V \rangle - V$, and that term is negligible almost always. The remaining terms in Eq. 2.64 and Eq. 2.62 are shown to be the same by the equivalence of the classical ensembles as shown in Sec. 2.4.1.

This is an interesting result however. It suggests that the for interacting systems the density matrix written in the coordinate space representation may differ for the microcanonical and canonical ensembles at least at some points. It is possible to imagine a potential with a large variation in V at some point so that $\langle V \rangle$ and V differ by a large amount at that point. However, for such a system the short time

approximation will not be valid. The short time approximation is only valid for slowly varying potentials. Therefore it is possible to say that $\langle V \rangle - V$ can always be neglected for the regimes that we are considering implicitly with the use of the short time approximation. It is very likely that even these not so nice systems, if treated exactly, will also lead to the standard equivalence of the ensembles, but we really can't say anything about them using the short time approximation.

It is also telling to trace over the coordinates of all but one of the interacting particles, given by a coordinate $\vec{y}$. We thus seek the reduced density matrix, diagonal or off diagonal in $\vec{y}$. The trace will over many coordinates be overwhelmingly dominated (in the large N limit) by the most probable total kinetic energy for all the particles. Then we find

$$G(\vec{y}, \vec{y}', \beta) \sim \lambda^{-3N-2} e^{-\pi r^2/\lambda^2} \tag{2.65}$$

where $r^2 = |\vec{y} - \vec{y}'|^2$ and $\lambda = h/\sqrt{2\pi m \kappa T}$. Thus the quantum mechanical single particle Green function and density matrix make sense as their imaginary time counterparts in the $N \to \infty$ limit, in accordance with well known results for the canonical ensemble.

Even though it is a necessary consequence of the equivalence of the ensembles, it is interesting to establish the generality of the Boltzmann average over the energy of a noninteracting subsystem in the following way. Suppose $N - M$ particles are no longer interacting with the remaining M particles, but their states are correlated by having been in contact in the past with the total energy fixed at E. In the time domain and in an obvious notation we have

$$G_N^+(\mathbf{y}, \mathbf{z}; \mathbf{y}', \mathbf{z}', t) = i\hbar \, G_{N-M}^+(\mathbf{y}, \mathbf{y}', t) G_M^+(\mathbf{z}, \mathbf{z}', t) \tag{2.66}$$

Then the Fourier convolution theorem can be applied to the Fourier transform into the energy domain, i.e.

$$G_N^+(\mathbf{y},\mathbf{z};\mathbf{y}',\mathbf{z}',E) = \frac{i\hbar}{2\pi}\int_{-\infty}^{\infty} G_{N-M}^+(\mathbf{y},\mathbf{y}',E-E')G_M^+(\mathbf{z},\mathbf{z}',E')\ dE' \tag{2.67}$$

which incidentally leads to some rather unlikely looking identities for Bessel functions; the reader may easily generate them. Our purpose is served if, focussing on the subsystem of M particles, we trace over the $N-M$ $\mathbf{y}$ coordinates. This gives

$$\begin{aligned}&\mathrm{Tr}_{\mathbf{y}}[G_{N-M}^+(E-E')] \sim \\ &\lim_{\mathbf{y}'\to\mathbf{y}} -\tfrac{m}{2\hbar^2}\left(\tfrac{1}{\Gamma(d_{N-M}+1)}\left(\tfrac{{k_{N-M}}^2}{4\pi}\right)^{d_{N-M}} + i\tfrac{\Gamma(d_{N-M})}{\pi^{d_{N-M}+1}|\mathbf{y}'-\mathbf{y}|^{2d_{N-M}}}\right)\end{aligned} \tag{2.68}$$

times a volume factor, in the case of an ideal gas. The second term is not a function of E'. Therefore the integral of it times $G_M(\mathbf{z},\mathbf{z}',E)$ is proportional to $\delta(\mathbf{z}'-\mathbf{z})$. So long as $\mathbf{z}\neq\mathbf{z}'$ that term is zero. Neglecting all unimportant (for this argument) factors this leaves

$$\mathrm{Tr}_{\mathbf{y}}[G_{N-M}^+(E-E')] \propto (E-E')^{d_{N-M}} = E^{d_{N-M}}\left(1-\frac{E'}{E}\right)^{d_{N-M}} \sim E^{d_{N-M}}\ e^{-\beta E'} \tag{2.69}$$

with of course $\beta = 1/\kappa T$. In arriving at Eq. 2.69 we used $E = \frac{D}{2}N\kappa T$ for the case of particles embedded in D dimensions. Finally we arrive at

$$\mathrm{Tr}_{\mathbf{y}}[G_N^+(E)] \propto \int_{-\infty}^{\infty} e^{-\beta E'}\ G_M^+(\mathbf{z},\mathbf{z}',E')\ dE' = G_M^+(\mathbf{z},\mathbf{z}',\beta) \tag{2.70}$$

in the large N limit. This establishes the generality of the Boltzmann average over the subsystem energy for large N. This discussion establishes again the connection between the canonical and microcanonical ensembles, however in a way not involving the Bessel functions and their asymptotic form, so it is less general than other results valid for any N.

2.4.3 Stationary phase canonical limit

It is also possible to recover the Gaussian form in Eq. 2.56 by carrying out the integral in Eq. 2.38 by stationary phase, provided the real factor involving t in the denominator is taken into the exponent, as $-ND/2 \log t$ i.e.

$$G^{+}_{cl}(\mathbf{x}, \mathbf{x}+\mathbf{r}, E) = \frac{-i}{\hbar} \int_0^\infty \left(\frac{m}{2\pi i\hbar}\right)^{ND/2} e^{imr^2/2\hbar t - iV(\mathbf{x}+\frac{\mathbf{r}}{2})t/\hbar + iEt/\hbar - ND/2 \log t}\, dt. \quad (2.71)$$

The complex stationary phase point t^* in the large N limit becomes $t^* = -iND\hbar/(2(E-V))$, yielding the same result as in Eq. 2.56, with $\hbar^2 k(\mathbf{x}, E)^2/2m = E - V(\mathbf{x})$, and making this another route between the quantum microcanonical and canonical ensembles. Since the positions are arbitrary we cannot however identify the *average* kinetic energy with $E - V$, and thus without further averaging we cannot associate t^* with any inverse temperature. It is interesting nonetheless that there is a complex time t^* appropriate to every position $\mathbf{x}$, even if that time is not related to the temperature. For an ideal gas the stationary phase time is $t^* = -i\hbar/\kappa T = -i\beta\hbar$, after making the identification $E = \frac{D}{2}NkT$. A discussion about traces over most of the coordinates and the recovery of the usual temperature through $\langle K \rangle = \frac{D}{2}NkT$ proceeds as in Sec. 2.4.1.

2.5 Constraints

In the large N limit the ergodic hypothesis is strongly motivated, but statistical mechanics does not pre-suppose that ergodicity is unchecked; rather constraints are always present, such as walls and boundaries which control volume. Ergodicity is then defined with respect to these constraints. The guiding idea in this paper, i.e. the

extended Berry RPW hypothesis, is that eigenstates of the full system are "as random as possible, subject to prior constraints". In this way thermodynamic constraints arise naturally. The real time, real energy (microcanonical) semiclassical Green function approach not only automatically generates the averages required to get appropriate wavefunction statistics, it also provides a natural way to include many constraints such as walls, symmetries, and even the existence of collisions between particles by going beyond the short time limit term to include returning (not necessarily periodic) trajectories. The semiclassical Ansatz for these extended problems in the presence of constraints is

$$G(\mathbf{x},\mathbf{x}',t) \approx G_{direct}(\mathbf{x},\mathbf{x}',t) + \sum_j G_j(\mathbf{x},\mathbf{x}',t) \tag{2.72}$$

where $G_j(\mathbf{x},\mathbf{x}+\mathbf{r},t)$ is a semiclassical (Van Vleck-Morette-Gutzwiller) Green function,

$$\begin{aligned} G_j(\mathbf{x},\mathbf{x}';t) &= \left(\tfrac{1}{2\pi i\hbar}\right)^{ND/2} \left|\mathrm{Det}\left(\tfrac{\partial^2 S_j(\mathbf{x},\mathbf{x}';t)}{\partial\mathbf{x}\partial\mathbf{x}'}\right)\right|^{1/2} \\ &\quad \times \exp\left(iS_j(\mathbf{x},\mathbf{x}';t)/\hbar - \tfrac{i\pi\nu_j}{2}\right) \end{aligned} \tag{2.73}$$

corresponding to the j^{th} trajectory contributing to the path from $\mathbf{x}$ to $\mathbf{x}+\mathbf{r}$, and $G_{direct}(\mathbf{x},\mathbf{x}+\mathbf{r},t)$ is given by Eq. 2.36. The short time term $G_{direct}(\mathbf{x},\mathbf{x}+\mathbf{r},t)$, is singled out as the shortest contributing trajectory: supposing $\mathbf{r}$ to be small compared to distances to walls etc., we still have a short time, ballistic trajectory as quite distinct from trajectories which have traveled some distance away and come back. There are cases where this separation is not clean; for such cases we can adjust notation accordingly. Note that since a trace over all position is not being taken, there is no appearance semiclassically of periodic orbits as the only surviving contributors. "Closed" orbits however can play a large role semiclassically, a fact recognized long ago by Delos [10].

2.5.1 N particles and a wall

A very useful example is provided by a plane Dirichlet wall felt by all the particles (e.g. $\psi(\vec{x}_1, \vec{x}_2, \cdots \vec{x}_N) = 0$ for $y_i = 0, i = 1, \cdots N$), as in a gas confined by a rigid container. The Green function and eigenfunctions must vanish if one or more particles approaches this wall. We can use the method of images, generalized to N particles, if the particles are noninteracting. (The interacting case can in principle be handled by semiclassical trajectory techniques which we bring up in the next section.)

The Green function $G_{wall}(\mathbf{x}, \mathbf{x}')$ will consist of the shortest distance contribution for which all particles take a direct path from $\mathbf{x}$ to $\mathbf{x}'$, plus paths where one particle has bounced off the wall, paths where two particles have, etc. These histories are included automatically if we apply the symmetrization operator which imposes the image reflections. This operator can be written

$$\mathcal{R} = \prod_i^N (1 - R_i) = 1 - \sum_i R_i + \sum_{i<j} R_i R_j - \cdots \tag{2.74}$$

where R_i is the operator for reflection about the $y = 0$ axis for the i^{th} particle. Applied to the Green function $G(\mathbf{x}, \mathbf{x} + \mathbf{r}, t)$, considered as a function of the coordinates in $\mathbf{x}$ in the absence of the wall, $\mathcal{R}$ yields the series

$$G_{wall}(\mathbf{x}, \mathbf{x}', t) = G_{direct}(\mathbf{x}, \mathbf{x}', t) - \sum_i G_i(\mathbf{x}, \mathbf{x}', t) + \sum_{i<j} G_{ij}(\mathbf{x}, \mathbf{x}', t) - \cdots \tag{2.75}$$

where $G_i(\mathbf{x}, \mathbf{x}', t)$ corresponds to the i^{th} particle getting from $\vec{x}_i$ to $\vec{x}_i'$ by bouncing off the wall while the others take direct paths, etc. The Fourier transform gives an analogous equation for $G_{wall}(\mathbf{x}, \mathbf{x}', E)$. The effect of the symmetrization is to create Green function sources reflected across the wall and given proper sign, in the manner familiar from the method of images. The short time path is shown by the direct

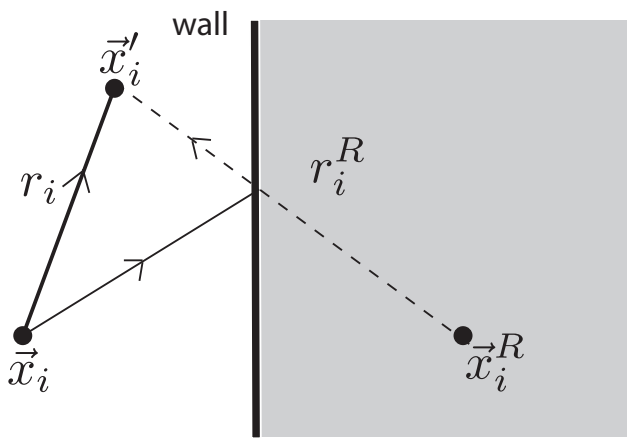

Figure 2.2: A short and a bouncing path for a particle propagating near a wall. The bounce contribution, if viewed by the image method, is equivalent to a contribution of opposite sign coming from the reflected point $\vec{x}^R$ with the wall removed.

path solid line in Fig 2.2, corresponding to the term $G_{st}(\mathbf{x}, \mathbf{x}', t)$. The bounce path is equivalent to a source reflected across the wall with an opposite sign, i.e. the method of images. Define

$$-\frac{1}{\pi}\mathrm{Im}\left[G^+_{st}(\mathbf{x}, \mathbf{x}+\mathbf{r}, E)\right] = \frac{m}{2\pi\hbar^2}\left(\frac{k^2}{2\pi}\right)^d \frac{J_d(kr)}{(kr)^d} \equiv a(k)F_d(kr) \tag{2.76}$$

Then

$$-\frac{1}{\pi}\mathrm{Im}\left[G^+_{wall}(\mathbf{x}, \mathbf{x}', E)\right] = a(k)\left(F_d(kr) - \sum_i F_d(kr_i) + \sum_{i<j} F_d(kr_{ij}) - \cdots\right). \tag{2.77}$$

This is the general result for any N. It would appear to be difficult to take it further, since all the distances, e.g.

$$r_{ij} = \sqrt{\sum_{m\neq i,j} |\vec{x}_m - \vec{x}'_m|^2 + |\vec{x}_i^R - \vec{x}'_i|^2 + |\vec{x}_j^R - \vec{x}'_j|^2}, \tag{2.78}$$

where $\vec{x}_j^R$ is the reflected j^{th} particle coordinates, involve square roots. However if we use the large N asymptotic form, we find, using $F_d(kr) \to \exp[-k^2r^2/4(d+1)]/2^d d!$,

$$-\frac{1}{\pi}\mathrm{Im}\left[G_{wall}(\mathbf{x},\mathbf{x}',E)\right]=\frac{a(k)}{2^d d!}\prod_i^N\left(e^{-\gamma r_i^2}-e^{-\gamma(r_i^R)^2}\right)=\frac{a(k)}{2^d d!}e^{-\gamma r^2}\prod_i^N\left(1-e^{-\gamma\Delta_i^2}\right) \tag{2.79}$$

where $\gamma = k^2/4(d+1) = \pi/\lambda^2$ and $\Delta_i^2 = (r_i^R)^2 - r_i^2$. Since r_i is the "direct" distance from $\vec{x}_i$ to $\vec{x}_i'$, (see Fig 2.2), Δ_i^2 records the distance change upon reflection of the i^{th} particle. We note that Δ_i^2 (and thus the Green function) vanishes as any particle approaches a wall in either $\mathbf{x}$ or $\mathbf{x}'$. It is also simple to see that the single particle density $\rho(\vec{x})$ in this noninteracting case becomes, for large N,

$$\rho(\vec{x}) = \rho_0(1 - e^{-4\gamma x^2}) \tag{2.80}$$

where x is the distance to the wall and ρ_0 is the density far from the wall.

The formulas Eq. 2.77 and Eq. 2.79 generalize Berry's result [11] for the wave-function squared of one particle in two dimensions near a wall, namely

$$\langle|\psi(\vec{x})|^2\rangle = \frac{\left(1 - J_0(k|\vec{x}^R - \vec{x}|)\right)}{\int d\vec{x}\,(1 - J_0(k|\vec{x}^R - \vec{x}|))}. \tag{2.81}$$

The Gaussian we get for large N has a very simple interpretation. First we note that for noninteracting systems in the canonical ensemble we can write the total density matrix as a product of one particle density matrices. This is essentially the form of Eq. 2.79, since we can write each one particle density matrix as

$$\rho(\vec{x},\vec{x}',\beta) = e^{-\gamma|\vec{x}-\vec{x}'|^2/N}\frac{\left(1 - e^{-\gamma(|\vec{x}^R-\vec{x}'|^2-|\vec{x}-\vec{x}'|^2)}\right)}{\int d\vec{x}\left(1 - e^{-\gamma|\vec{x}^R-\vec{x}|^2}\right)} \to \frac{\left(1 - e^{-\gamma|\vec{x}^R-\vec{x}|^2}\right)}{\int d\vec{x}\left(1 - e^{-\gamma|\vec{x}^R-\vec{x}|^2}\right)} \tag{2.82}$$

where the second form is the diagonal element.

However Eq. 2.82 also arises as the density matrix obtained from the Boltzmann average of Berry's result; i.e. averaging the fixed energy results over a canonical

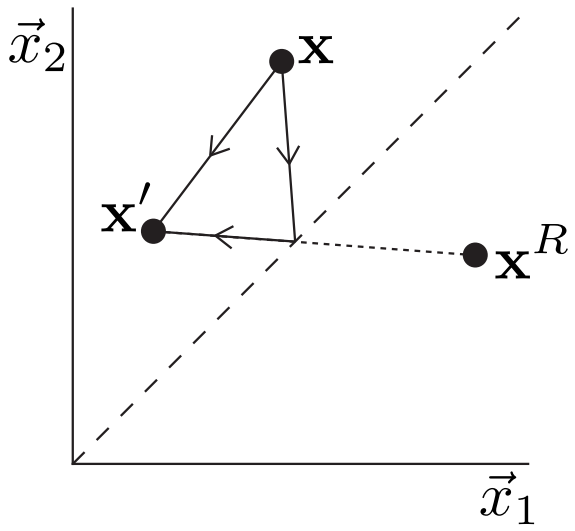

Figure 2.3: The particle symmetry or antisymmetry condition is equivalent to requiring mirror symmetry or antisymmetry across the $\vec{x}_i = \vec{x}_j$ (hyper)plane. This corresponds to having additional contributions from the images of the particles reflected over the symmetry planes.

distribution of energies, as can be seen from the integral

$$\frac{\int_0^\infty k \ \left(1 - J_0(k|\vec{x}^R - \vec{x}|)\right) \ e^{-\beta\hbar^2 k^2/2m} dk}{\int_0^\infty k \ e^{-\beta\hbar^2 k^2/2m} dk} = \left(1 - e^{-m|\vec{x}^R - \vec{x}|^2/2\beta\hbar^2}\right) \tag{2.83}$$

For $D = 2$ and $N = 1$ a Boltzmann average yields the Gaussian. Indeed this necessarily holds in any number of dimensions; i.e. the appropriate Boltzmann average of $J_d(kr)/(kr)^d$ must yield a Gaussian for any d. In the thermodynamic $N \to \infty$ limit for noninteracting particles, each particle separately is Boltzmann distributed over energy, so the result must be the same as a Boltzmann average of the one particle results for any dimension D and for any constraints.

2.5.2 Particle Exchange Symmetries - Fermions and Bosons

Particle symmetry is an essential part of the many body problem. It's effect, like other symmetries, is to generate permutations where the distances have changed due to particle exchange. Figure 2.3 shows this effect graphically. It is gratifying to see directly that permutations which induce large new distances (coming from remote pairs of particles, where "remote" is a relative term depending on the temperature) make little contribution. Consider N noninteracting Fermions or Bosons; we wish to compute the reduced density matrix for two Fermions or Bosons. This is a well known result for $N \to \infty$ [2]. The symmetric or antisymmetric Green function is

$$G_{S/A}(\mathbf{x}, \mathbf{x}+\mathbf{r}, E) = \frac{1}{N!} \sum_n \epsilon_n \frac{-im}{2\pi\hbar^2} \left(\frac{k^2}{2\pi}\right)^d \frac{H_d(kr_n)}{(kr)^d} \tag{2.84}$$

where $r_n = \sqrt{|\vec{x_1} - \vec{x_{p_1}}'|^2 + \cdots + |\vec{x_N} - \vec{x_{p_N}}'|^2}$, $\{p_1, \cdots, p_N\}$ is the nth permutation of $\{1, \cdots, N\}$, and $\epsilon_n = 1$ if the parity of the permutation is even and $\epsilon_n = \pm 1$ if the parity of the permutation is odd (with the upper sign for bosons and the lower sign for fermions).

$$\begin{aligned} \langle \psi^*(\vec{x_1} \cdots \vec{x_N}) \psi(\vec{x_1} \cdots \vec{x_N}) \rangle &= -\frac{1}{\pi} \frac{\mathrm{Im}\left(G_{S/A}(\mathbf{x}, \mathbf{x}+\mathbf{r}, E)\right)}{\rho(E)} \\ &= \frac{1}{\rho(E) N!} \sum_n \epsilon_n \frac{m}{2\pi\hbar^2} \left(\frac{k^2}{2\pi}\right)^d \frac{J_d(kr_n)}{(kr)^d} \end{aligned} \tag{2.85}$$

In the limit that N is large, this becomes

$$\langle \psi^*(\vec{x_1} \cdots \vec{x_N}) \psi(\vec{x_1} \cdots \vec{x_N}) \rangle = \frac{1}{\rho(E) N!} \sum_n^{N!} \epsilon_n \frac{m}{2\pi\hbar^2 d!} \left(\frac{k^2}{4\pi}\right)^d e^{-k^2 r_n^2/4(d+1)} \tag{2.86}$$

The diagonal component of this with the r_n's written out explicitly is

$$\begin{aligned}&\langle\psi^*(\vec{x_1}\cdots\vec{x_N})\psi(\vec{x_1}\cdots\vec{x_N})\rangle = \\ &\frac{m}{2\rho(E)N!\pi\hbar^2 d!}\left(\frac{k^2}{4\pi}\right)^d\sum_n^{N!}\epsilon_n\ e^{-k^2(\vec{x}_1-\vec{x}_{p1})^2/4(d+1)}\cdots e^{-k^2(\vec{x}_N-\vec{x}_{pN})^2/4(d+1)}\end{aligned} \tag{2.87}$$

It is important to note here that because particle symmetry is included in this result, this is not the same as for classical particles as when the diagonal limit was taken for distinguishable particles above. Up to the normalization constant this is the constant temperature density matrix for N noninteracting fermions or bosons:

$$\begin{aligned}&\langle\psi^*(\vec{x_1}\cdots\vec{x_N})\psi(\vec{x_1}\cdots\vec{x_N})\rangle = \\ &\frac{m}{2\rho(E)N!\pi\hbar^2 d!}\left(\frac{k^2}{4\pi}\right)^d\sum_n^{N!}\epsilon_n\ e^{-m(\vec{x}_1-\vec{x}_{p1})^2/2\beta\hbar^2}\cdots e^{-m(\vec{x}_N-\vec{x}_{pN})^2/2\beta\hbar^2}\end{aligned} \tag{2.88}$$

Again the identification $E = \frac{D}{2}N\kappa T$ was used. This can be rewritten as an integral over wavevectors:

$$\begin{aligned}\langle|\psi(\mathbf{x})|^2\rangle &= A\sum_n^{N!}\epsilon_n\int d\vec{k}_1\cdots d\vec{k}_N\ e^{-\beta\hbar^2{k_1}^2/2m+i\vec{k}_1\cdot(\vec{x}_1-\vec{x}_{p1})}\cdots \\ &\quad\times e^{-\beta\hbar^2{k_N}^2/2m+i\vec{k}_N\cdot(\vec{x}_N-\vec{x}_{pN})}\end{aligned} \tag{2.89}$$

where $A = \frac{m}{2\rho(E)N!\pi\hbar^2 d!}\left(\frac{k^2}{4\pi}\right)^d\left(\frac{\beta\hbar^2}{2\pi m}\right)^{d+1}$ is the normalization constant. Rearranging gives

$$\begin{aligned}\langle|\psi(\mathbf{x})|^2\rangle &= A\sum_n^{N!}\epsilon_n\int d\vec{k}_1\cdots d\vec{k}_N\ e^{-\beta\hbar^2({k_1}^2+\cdots+{k_N}^2)/m}e^{i(\vec{k}_1-\vec{k}_{p1})\cdot\vec{x}_1}\cdots \\ &\quad\times e^{i(\vec{k}_N-\vec{k}_{pN})\cdot\vec{x}_N}\end{aligned} \tag{2.90}$$

If the volume that the particles are confined to is large but finite,

$$\begin{aligned}&\int\langle|\psi(\mathbf{x})|^2\rangle d\vec{x}_3...d\vec{x}_N = \\ &AV^{N-2}\sum_n^{N!}\epsilon_n\int d\vec{\mathbf{k}}\ e^{-\beta\hbar^2\mathbf{k}^2/2m}e^{i(\vec{k}_1-\vec{k}_{p1})\cdot\vec{x}_1}e^{i(\vec{k}_2-\vec{k}_{p2})\cdot\vec{x}_2}\delta_{\vec{k}_3,\vec{k}_{p3}}\cdots\delta_{\vec{k}_N,\vec{k}_{pN}}\end{aligned} \tag{2.91}$$

For fermions if the wavevector of any two particles are the same the term is killed by the term with the wavevectors reversed in accordance with the Pauli principle. This leaves only two terms

$$\int \langle|\psi(\mathbf{x})|^2\rangle d\vec{x}_3 \cdots d\vec{x}_N = AV^{N-2} \sum_n^{N!} \epsilon_n \int d\mathbf{k}\; e^{-\beta\hbar^2\mathbf{k}^2/2m} e^{i(\vec{k}_1-\vec{k}_{p1})\cdot\vec{x}_1} e^{i(\vec{k}_2-\vec{k}_{p2})\cdot\vec{x}_2} \quad (2.92)$$

For bosons there are also only two types of terms, but each is multiplied by the same factor since like terms are added together. Either way, carrying out the integral over $\mathbf{k}$,

$$\int \langle|\psi(\mathbf{x})|^2\rangle d\vec{x}_3 \cdots d\vec{x}_N = \frac{\left(1 \pm e^{-m(\vec{x_1}-\vec{x_2})^2/\beta\hbar^2}\right)}{\int d\vec{x}_1 d\vec{x}_2 \left(1 \pm e^{-m(\vec{x_1}-\vec{x_2})^2/\beta\hbar^2}\right)} \quad (2.93)$$

This is the well known result for the density of two noninteracting fermions or bosons.

2.5.3 Scattering

A hard wall is a potential energy feature which induces a boundary condition, requiring the wavefunction or Green function to vanish as the wall is approached. Softer potentials do not induce fixed boundary conditions and require a different treatment. A potential may still however be thought of as a constraint: we consider waves as random as possible subject to the existence of a potential, be it fixed or interparticle. In practice this means we return to the Green function formulation used throughout.

Consider a soft repulsive or attractive potential somewhere in a noninteracting gas. Assuming no boundaries, mutually noninteracting particles can interact with the potential 0 or 1 times. (We assume for simplicity that the potential is short ranged. Because of the ergodicity assumption inherent to the random wave hypothesis, the

presence of remote walls would actually make no difference.) This circumstance develops along lines very similar to the wall, except that we cannot use the method of images. It illustrates the use of the full semiclassical propagator within this formalism.

Eq. 2.74 and Eq. 2.75 both hold, with the effect of R_i changed to mean "the i^{th} particle takes the path from initial to final coordinates in which it deflects from the potential, if such a path exists classically". For N particles, there is a "direct" term in Eq. 2.75 where no particle interacts with the potential, N terms where one of them does, etc. We have, in the simple case shown in Fig. 2.4, and in analogy with Eq. 2.75,

$$G(\mathbf{x},\mathbf{x}',t) = G_{direct}(\mathbf{x},\mathbf{x}',t) + \sum_i G_{bounce,i}(\mathbf{x},\mathbf{x}',t) + \sum_{i,j} G_{bounce,i,j}(\mathbf{x},\mathbf{x}',t) + \cdots \quad (2.94)$$

with $G_{direct}(\mathbf{x},\mathbf{x}',t)$ given by Eq. 2.36, and e.g.

$$\begin{aligned} G_{bounce,i}(\mathbf{z},\mathbf{y}_i,\mathbf{z}+\mathbf{r},\mathbf{y}_i',t) \quad &\approx \quad \left(\tfrac{m}{t}\right)^{\frac{(N-1)D}{2}} \left(\tfrac{1}{2\pi i\hbar}\right)^{\frac{ND}{2}} \left|\tfrac{\partial^2 S_i(\mathbf{y}_i,\mathbf{y}_i';t)}{\partial \mathbf{y}_i \partial \mathbf{y}_i'}\right|^{\frac{1}{2}} \\ &\quad \times e^{imr^2/2\hbar t - iV(\mathbf{z}+\frac{\mathbf{r}}{2})t/\hbar + iS_i(\mathbf{y}_i,\mathbf{y}_i';t)/\hbar - \frac{i\pi\nu_i}{2}} \end{aligned} \quad (2.95)$$

Considering this term where only the i^{th} particle with coordinate $\mathbf{y}_i$ interacts with the potential, we have $N-1$ "spectator" $\mathbf{z}$ particles, and the propagator becomes a product of the noninteracting Green function for $N-1$ particles and a more complicated Van Vleck semiclassical term for the colliding particle. The noninteracting part contributes a term $(N-1)D/2 \log t$ in the exponent along with the one particle classical action of the i^{th} particle. For sufficiently large N, and tracing over the $\mathbf{z}$ particles, this factor leads again to the usual time condition $t^* = -i\beta\hbar$ and a thermal average of the one particle energy Green function under the Fourier transform from

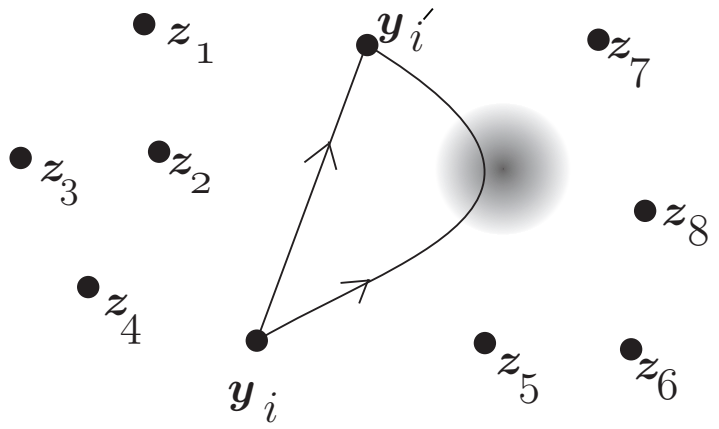

Figure 2.4: A short ballistic and a colliding path both lead to the same final point for a particle propagating near a localized repulsive potential. The colliding path cannot be treated by the short time approximation; rather, a Van Vleck Green function is required. In this term, all but the i^{th} particle remain in place.

time to energy, as in Equation 2.70:

$$\begin{aligned} G(\mathbf{y},\mathbf{y}',E) \approx G(\mathbf{y},\mathbf{y}',\beta) &= G_{direct}(\mathbf{y},\mathbf{y}',\beta) + \sum_i G_{bounce,i}(\mathbf{y},\mathbf{y}',\beta) \\ &\quad + \sum_{i,j} G_{bounce,i,j}(\mathbf{y},\mathbf{y}',\beta) + \cdots \end{aligned} \tag{2.96}$$

$t^* = -i\beta\hbar$ becomes the imaginary time over which the action for the $\mathbf{y}$ coordinates are evaluated.

2.5.4 Canonical Random Waves

Based on our understanding of the Berry conjecture, through

$$\langle \psi^*(\vec{x})\psi(\vec{x}')\rangle = \mathrm{Tr}\left[\delta(E-H)|\vec{x}\rangle\langle\vec{x}'|\ \right], \tag{2.97}$$

and the connection that we have made between

$$\delta(E-H) \sim e^{-\beta H} \tag{2.98}$$

through the both the equivalence of the ensembles and the asymptotic form of the Bessel function, it would make some sense to think of an analogous conjecture to Berry's conjecture for the canonical ensemble. Namely:

$$\langle \psi^*(\vec{x})\psi(\vec{x}')\rangle = \mathrm{Tr}\left[e^{-\beta H}|\vec{x}\rangle\langle\vec{x}'|\ \right], \tag{2.99}$$

If the trace is taken over random waves as with the Berry conjecture you have a superposition of random plane waves with the probability of having any plane wave as $e^{(-\beta\hbar^2k^2/2)}$. In the limit of $N \to \infty$ this will be equivalent to the Berry conjecture. The Berry conjecture is a useful way to look at high lying wavefunctions, namely that their statistics look like random plane waves. This would be a slightly different way of looking at things. This is just a preliminary idea, and it is not clear if it will yield fruit.

2.6 Conclusion

In this chapter we have made the semiclassical idea of Berry's conjecture the central focus, but we have gone beyond what is normally done by considering very large number of particles. Our main result is a novel way of showing the connection between the quantum statistical microcanonical and canonical ensembles. In other results we look at how constraints affect statistical properties. We continue this line of thinking into the next chapter as we study the pair product approximation.

Chapter 3

Pair Product Approximation

One interpretation of the Berry Conjecture as discussed in Chapter 2 is the idea that a wavefunction can be thought of as being as random as possible subject to constraints. This idea led us to think about the form of approximate wavefunctions. The idea is that having some functional form can be thought to be a constraint on the wavefunction. For example, information about two particle collisions can be considered while higher order collisions are ignored. This chapter explores this idea. Having the correct two particle collisions would be a type of contraint. This thinking led us to study the pair product approximation, which is essentially how an approximation to the N body Green function can be built up from exact two body Green functions.

The pair product approximation (PPA) has been used for a wide variety of systems in order to make calculations for a large number of systems tractable. It has been used for liquid parahydrogen, for liquid helium, and for bosons in a harmonic trap with contact interactions [12],[13]. The thermodynamics of these systems are of great

interest and the pair product approximation has allowed simulations to come closer to the thermodynamic limit without leaving out too much detail. The key factor in this improvement is that the pair product approximation takes into account only two-body interactions neglecting three-body and higher order interactions. These interactions are less important because they occur less often and therefore contribute less to the properties of the system overall.

The formulation of the pair product approximation includes only two body interactions by building up the full propagator from a combination of two-body and single-body propagators. Our disscussion must therefore start with the simplest system that is not trivial: two interacting particles without an external potential. It is important to note here that the only requirement on the external potential in the pair product approximation is that it be separable, although nearly all applications of PPA have used no external potential. This section discusses that standard formulation. In the next section we discuss how a harmonic external potential can be added.

We start from the Hamiltonian for two interacting particles without a confining potential:

$$\hat{H}_2 = \hat{T}_1 + \hat{T}_2 + \hat{V}_{12}(|\mathbf{r}'_1 - \mathbf{r}'_2|) \tag{3.1}$$

In this case the propagator is

$$K_2(\mathbf{r}_1, \mathbf{r}_2, \mathbf{r}'_1, \mathbf{r}'_2; t) = \langle \mathbf{r}_1 \mathbf{r}_2 | \exp(-i\hat{H}_2 t/\hbar) | \mathbf{r}'_1 \mathbf{r}'_2 \rangle, \tag{3.2}$$

In order to isolate the two body interaction we change to center of mass and relative

coordinates:

$$\mathbf{R}_{12} = \frac{\mathbf{r}_1 + \mathbf{r}_2}{2} \tag{3.3}$$

$$\mathbf{r}_{12} = \mathbf{r}_1 - \mathbf{r}_2 \tag{3.4}$$

This gives,

$$K_{2,cm}(\mathbf{r}_1, \mathbf{r}_2, \mathbf{r}_1', \mathbf{r}_2'; t) = K_0^{(\mathbf{R}_{12})}(\mathbf{R}_{12}, \mathbf{R}_{12}'; t) K_{int}^{(\mathbf{r}_{12})}(\mathbf{r}_{12}, \mathbf{r}_{12}'; t) \tag{3.5}$$

where

$$K_0^{(\mathbf{R}_{12})}(\mathbf{R}_{12}, \mathbf{R}_{12}'; t) = \langle \mathbf{R}_{12}| \exp(-i\hat{T}_{\mathbf{R}_{12}} t/\hbar) |\mathbf{R}_{12}'\rangle \tag{3.6}$$

For two free particles it is not hard to show:

$$K_0(\mathbf{r}_1, \mathbf{r}_1'; t) K_0(\mathbf{r}_2, \mathbf{r}_2'; t) = K_0(\mathbf{R}_{12}, \mathbf{R}_{12}'; t) K_0(\mathbf{r}_{12}, \mathbf{r}_{12}'; t). \tag{3.7}$$

In other words the product of two single body propagators can be written as the product of a propagator that is a function of the center of mass of the two particles and a propagator that is a function of the relative distance between the particles. Using this to eliminate $K_0^{(\mathbf{R}_{12})}(\mathbf{R}_{12}, \mathbf{R}_{12}'; t)$ from Eq. 3.5 allows the propagator to be written in a form that has clear one particle and two particle terms:

$$K_{2,pp}(\mathbf{r}_1, \mathbf{r}_2, \mathbf{r}_1', \mathbf{r}_2'; t) = K_0^{(1)}(\mathbf{r}_1, \mathbf{r}_1'; t) K_0^{(2)}(\mathbf{r}_2, \mathbf{r}_2'; t) \exp[-u(\mathbf{r}_{12}, \mathbf{r}_{12}'; t)]. \tag{3.8}$$

with

$$\exp[-u(\mathbf{r}_{12}, \mathbf{r}_{12}'; t)] = \frac{K_{int}(\mathbf{r}_{12}, \mathbf{r}_{12}', t)}{K_0(\mathbf{r}_{12}, \mathbf{r}_{12}', t)} = \frac{\langle \mathbf{r}_{12}| \exp(-i\hat{H}_{\mathbf{r}_{12}} t/\hbar) |\mathbf{r}_{12}'\rangle}{\langle \mathbf{r}_{12}| \exp(-i\hat{T}_{\mathbf{r}_{12}} t/\hbar) |\mathbf{r}_{12}'\rangle}. \tag{3.9}$$

The many body pair product propagator is then built up from this form as the product over one particle and interaction terms.

$$K_{N,pp}(\underline{\mathbf{R}}, \underline{\mathbf{R}}'; t) \approx \prod_{i=1}^{N} K_0^{(i)}(\mathbf{r}_i, \mathbf{r}_i'; t) \prod_{i<j}^{N} \exp[-u(\mathbf{r}_{ij}, \mathbf{r}_{ij}', t)]. \tag{3.10}$$

An important check to ensure that this approximation makes sense is to check what happens in the short time limit. For short times Eq. 3.20 reduces to

$$K_{N,pp,st}(\underline{\mathbf{R}}, \underline{\mathbf{R}}'; t) \approx \prod_{i=1}^{N} K_0^{(i)}(\mathbf{r}_i, \mathbf{r}_i'; t) \prod_{i<j}^{N} \exp[-iV(\mathbf{r}_{ij})t/\hbar]. \tag{3.11}$$

which is the correct form of the short time propagator for many particles interacting via $V_{12}(\mathbf{r}_{12})$.

Since the pair product approximation is built up from exact two-particle propagators, two-particle collisions are included in the approximation, but collisions involving more than two particles are neglected. Paths involving multiple collisions between the same two particles are included, but they do not happen without a confining potential. We discuss this further in the next section. Successive collisions of a single particle with two or more other particles are also not included in this approximation.

The pair product approximation works very well for low densities. This is because in the low density limit three particle collisions are less likely. Three particle collisions therefore do not greatly affect the propagator for low densities, and their neglect does not hurt the pair product approximation very much.

3.1 Harmonic Confining Potentials

As discussed in the previous section, it is possible to include confining potentials that are separable in the pair product approximation. In this section we discuss one such potentential: a harmonic confining potential. Even though many potentials are not separable, the ability to include some type of potential is of benefit since it allows for the pair product approximation to be used for more than just free particles.

Also the harmonic confining potential is an important case because most potentials are at least approximately harmonic. Harmonic potentials are often considered in chemical and physical systems such as Harmonium and atoms in a harmonic trap [14]. Therefore it is useful to consider using the pair product approximation for a harmonic confining potential. This has been considered for bosons interacting via hard-core potentials [15].

For two particles in a harmonic confining potential the Hamiltonian is

$$\hat{H}_{harm} = \hat{T}_1 + \hat{T}_2 + \frac{1}{2}m\omega^2\mathbf{r}_1^2 + \frac{1}{2}m\omega^2\mathbf{r}_2^2 + V_{12}(|\mathbf{r}_1 - \mathbf{r}_2|), \tag{3.12}$$

Again we can change to center of mass and relative coordinates, and the Hamiltonian becomes

$$\hat{H}_{harm} = \hat{H}_{\mathbf{R}_{12}} + \hat{H}_{\mathbf{r}_{12}}. \tag{3.13}$$

with

$$\hat{H}_{\mathbf{R}_{12}} = \frac{|\hat{\mathbf{P}}_{12}|^2}{2M_{12}} + \frac{1}{2}M_{12}\omega^2\mathbf{R}_{12}^2 \tag{3.14}$$

and

$$\hat{H}_{\mathbf{r}_{12}} = \frac{|\hat{\mathbf{p}}_{12}|^2}{2\mu_{12}} + \frac{1}{2}\mu_{12}\omega^2\mathbf{r}_{12}^2 + \hat{V}_{12}(|\mathbf{r}'_{12}|). \tag{3.15}$$

The separability of the Hamiltonian in center of mass and relative coordinates allows the propagator to be factored:

$$K_{harm}(\mathbf{r}_1, \mathbf{r}_2, \mathbf{r}'_1, \mathbf{r}'_2; t) = K_{osc}(\mathbf{R}_{12}, \mathbf{R}'_{12}; t)K_{\mathbf{r}_{12}}(\mathbf{r}_{12}, \mathbf{r}'_{12}; t) \tag{3.16}$$

with $K_{osc}(\mathbf{r}, \mathbf{r}'; t)$ the propagator for a particle in a harmonic potential which is

$$\begin{aligned} K_{osc}(\mathbf{r}, \mathbf{r}'; t) &= \left(\tfrac{m\omega}{2\pi i\hbar \sin(\omega t)}\right)^{D/2} \\ &\quad \times \exp\left(\tfrac{im\omega}{2\hbar \sin(\omega t)}\left[\left(r^2 + r'^2\right)\cos(\omega t) - 2\mathbf{r}\cdot\mathbf{r}'\right]\right). \end{aligned} \tag{3.17}$$

The form of Eq. 3.17 allows us to factor the propagator in Eq. 3.16 into a form analogous to Eq. 3.8:

$$K_{harm,pp}(\mathbf{r}_1, \mathbf{r}_2, \mathbf{r}_1', \mathbf{r}_2'; t) = K_{osc}^{(1)}(\mathbf{r}_1, \mathbf{r}_1'; t) K_{osc}^{(2)}(\mathbf{r}_2, \mathbf{r}_2'; t) \exp[-u(\mathbf{r}_{12}, \mathbf{r}_{12}'; t)]. \quad (3.18)$$

with

$$\exp[-u(\mathbf{r}_{12}, \mathbf{r}_{12}'; t)] = \frac{\langle \mathbf{r}_{12}| \exp(-i\hat{H}_{\mathbf{r}_{12}} t/\hbar) |\mathbf{r}_{12}'\rangle}{\langle \mathbf{r}_{12}| \exp(-i\hat{H}_{osc} t/\hbar) |\mathbf{r}_{12}'\rangle}. \quad (3.19)$$

Again the many-body pair product propagator is then built up from this form as the product over one particle and interaction terms.

$$K_{harm,pp}(\underline{\mathbf{R}}, \underline{\mathbf{R}}'; t) \approx \prod_{i=1}^{N} K_{osc}^{(i)}(\mathbf{r}_i, \mathbf{r}_i'; t) \prod_{i<j}^{N} \exp[-u(\mathbf{r}_{ij}, \mathbf{r}_{ij}', t)]. \quad (3.20)$$

This allows the propagator for an N particle system to be reduced to calculating $u(\mathbf{r}_{12}, \mathbf{r}_{12}'; t)$. Because the pair product propagator is built up from exact two-particle propagator it includes multiple collisions between two particles. The exact two-particle propagator must include these types of collisions because when a harmonic potential is included it is possible for classical trajectories to exist that involve two particles colliding and then being turned around by the harmonic potential in such a way that they collide again. A path involving a successive collision between one particle and two different particles is neglected in this approximation because it is not possible for the two-body propagators to include this three-body type process. Again these processes are less important and their relative importance decreases with the density.

3.2 Semiclassical Pair Product Approximation

The benefit of that pair product approximation is that it can greatly speed up many body computations because it reduces the collisions for a many body propagator by considering only two body collisions, although the two body collisions are still considered exactly. It is also possible to use another approximation even for the two body collisions. We discuss one possible method in this section.

In this section we discuss using semiclassical methods within the pair product approximation. We start from the most basic semiclassical method for approximating the time dependent propagator, the Van Vleck propagator:

$$K_{sc}(\underline{\mathbf{R}}, \underline{\mathbf{R}}'; t) = \left(\frac{1}{2\pi i\hbar}\right)^{ND/2} \sum_{paths} \left|\frac{\partial \underline{\mathbf{P}}}{\partial \underline{\mathbf{R}}'}\right|_{\underline{\mathbf{R}}}^{ND/2} \exp\left(\frac{iS(\underline{\mathbf{R}}, \underline{\mathbf{R}}'; t)}{\hbar} - \frac{i\nu}{2}\right) \tag{3.21}$$

where $S(\underline{\mathbf{R}}, \underline{\mathbf{R}}'; t)$ is the classical action, and the sum is over classical paths. As with the quantum Hamiltonian, the classical Hamiltonian for two interacting particles with no external potential is also separable in center of mass and relative coordinates. Since the Hamiltonian is separable the action is also separable allowing the propagator to be factored as in Eq. 3.5.

$$K_{2,cm,sc}(\mathbf{r}_1, \mathbf{r}_2, \mathbf{r}_1', \mathbf{r}_2'; t) = K_{0,sc}^{(\mathbf{R}_{12})}(\mathbf{R}_{12}, \mathbf{R}_{12}'; t) K_{int,sc}^{(\mathbf{r}_{12})}(\mathbf{r}_{12}, \mathbf{r}_{12}'; t) \tag{3.22}$$

This leads to the same result as Eq. 3.20 except with the propagator in $u(\mathbf{r}_{12}, \mathbf{r}_{12}'; t)$ evaluated semiclassically.

Using the pair product approximation in combination with a semiclassical propagator reduces the number of dimensions that the classical trajectories must be run in. Since the pair product approximation breaks down the propagator into one and two

body terms, trajectories for only two particles at a time need to be considered. Additionally for two particles without a confining potential, the potential only depends on the relative coordinate, which is confined to a plane. Therefore it is only necessary to run trajectories in two dimensions. This is a reduction of the dimensionality of the problem of calculating the propagator from $2DN$ dimensional phase space to 4 dimensional phase space.

Many standard ways to evaluate the semiclassical propagator can lead to difficulties due to the root search problem [16]. The root search problem signifies the difficulty of finding all classical trajectories between r and r' in time t. For one dimension the problem can be solved easily, since only two such trajectories exist between two points. In higher dimensions the problem becomes cumbersome since a large number trajectories must be launched in all directions from r in order to find ones that are at r' in time t. For this reason we choose to use one of the initial value methods. Initial value methods use the information from trajectories from specific initial points in phase space to avoid the root search problem. Here we choose to use the cellular dynamics method [16], although any method for determining the semiclassical propagator can be used .

3.2.1 Cellular Dynamics

In this section we discuss the cellular dynamics method and more specifically the details of its use in the problem at hand. The cellular dynamics method starts from the standard semiclassical propagator that is based on the action of classical paths

between the points of the propagator

$$G_{\rm SC}(x,x_0,t)=\left(\frac{1}{2\pi i\hbar}\right)^{1/2}\sum\left|\frac{\partial p_0}{\partial x}\right|^{1/2}_{x_0}\exp\left(i\frac{S(x,x_0)}{\hbar}-i\frac{\nu\pi}{2}\right) \tag{3.23}$$

where $S(x,x_0)=\int Ldt$ is the classical action The next step is to write the propagator in the suggestive form

$$\begin{aligned} G_{\rm SC}(x,x_0,t) &= \left(\tfrac{1}{2\pi i\hbar}\right)^{1/2}\int dp_0\left|\left(\tfrac{\partial x_t}{\partial p_0}\right)\delta\left(x-x_t(x_0,p_0)\right)\right| \\ &\quad\times\exp\left(i\tfrac{S(x,x_0)}{\hbar}-i\tfrac{\nu\pi}{2}\right) \end{aligned} \tag{3.24}$$

From (3.24) the key is to split up the propagator trajectories into trajectories from many different phase space cells by inserting a sum of Gaussians centered at the phase space cells in the form

$$1\approx\eta\sum_n exp\left[-\beta(y-na)^2\right] \tag{3.25}$$

where the width and positions of the Gaussians are chosen so that the approximation holds.

The linearized action becomes (for two dimensions)

$$\begin{aligned} S(x_0^1,x_0^2,p_0^1,p_0^2) &= S(x_k^1,x_l^2,p_m^1,p_n^2)+\tfrac{\partial S}{\partial x_0^1}(x_0^1-x_k^1)+\tfrac{\partial S}{\partial x_0^2}(x_0^2-x_l^2) \\ &+ \tfrac{\partial S}{\partial p_0^1}(p_0^1-p_m^1)+\tfrac{\partial S}{\partial p_0^2}(p_0^2-p_n^2) \\ &+ \tfrac{1}{2}\tfrac{\partial^2 S}{\partial x_0^{1^2}}(x_0^1-x_k^1)^2+\tfrac{1}{2}\tfrac{\partial^2 S}{\partial x_0^{2^2}}(x_0^2-x_l^2)^2+ \\ &+ \tfrac{1}{2}\tfrac{\partial^2 S}{\partial p_0^{1^2}}(p_0^1-p_m^1)^2+\tfrac{1}{2}\tfrac{\partial^2 S}{\partial p_0^{1^2}}(p_0^1-p_m^1)^2 \\ &+ \tfrac{\partial^2 S}{\partial x_0^1\partial x_0^2}(x_0^1-x_k^1)(x_0^2-x_l^2)+\tfrac{\partial^2 S}{\partial x_0^1\partial p_0^1}(x_0^1-x_k^1)(p_0^1-p_m^1) \\ &+ \tfrac{\partial^2 S}{\partial x_0^1\partial p_0^2}(x_0^1-x_k^1)(p_0^2-p_n^2)+\tfrac{\partial^2 S}{\partial x_0^2\partial p_0^1}(x_0^2-x_l^2)(p_0^1-p_m^1) \\ &+ \tfrac{\partial^2 S}{\partial x_0^2\partial p_0^2}(x_0^2-x_l^2)(p_0^2-p_n^2)+\tfrac{\partial^2 S}{\partial p_0^1\partial p_0^2}(p_0^1-p_m^1)(p_0^2-p_n^2) \end{aligned} \tag{3.26}$$

Using the definition of the stability matrix M:

$$\begin{pmatrix} \delta p_t^1 \\ \delta p_t^2 \\ \delta x_t^1 \\ \delta x_t^2 \end{pmatrix} = \begin{pmatrix} m_{11} & m_{12} & m_{13} & m_{14} \\ m_{21} & m_{22} & m_{23} & m_{24} \\ m_{31} & m_{32} & m_{33} & m_{34} \\ m_{41} & m_{42} & m_{43} & m_{44} \end{pmatrix} \begin{pmatrix} \delta p_0^1 \\ \delta p_0^2 \\ \delta x_0^1 \\ \delta x_0^2 \end{pmatrix} \tag{3.27}$$

and the chain rule the partial derivatives in 3.26 are

$$\frac{\partial S}{\partial x_0^1} = -p_m^1 + p_{klnmt}^1 m_{33} \tag{3.28}$$

$$\frac{\partial S}{\partial x_0^2} = -p_n^2 + p_{klnmt}^2 m_{44} \tag{3.29}$$

$$\frac{\partial S}{\partial p_0^1} = m_{31} p_{klnmt}^1 \tag{3.30}$$

$$\frac{\partial S}{\partial p_0^2} = m_{42} p_{klnmt}^2 \tag{3.31}$$

$$\frac{\partial S^2}{\partial {x_0^1}^2} = m_{13} m_{33} \tag{3.32}$$

$$\frac{\partial S^2}{\partial x_0^1 \partial x_0^2} = m_{23} m_{44} \tag{3.33}$$

$$\frac{\partial S^2}{\partial x_0^1 \partial p_0^1} = m_{13} m_{31} \tag{3.34}$$

$$\frac{\partial S^2}{\partial x_0^1 \partial p_0^2} = m_{23} m_{42} \tag{3.35}$$

$$\frac{\partial S^2}{\partial {x_0^2}^2} = m_{24} m_{44} \tag{3.36}$$

$$\frac{\partial S^2}{\partial x_0^2 \partial p_0^1} = m_{14} m_{31} \tag{3.37}$$

$$\frac{\partial S^2}{\partial x_0^2 \partial p_0^2} = m_{24} m_{42} \tag{3.38}$$

$$\frac{\partial S^2}{\partial {p_0^1}^2} = m_{31} m_{11} \tag{3.39}$$

$$\frac{\partial S^2}{\partial p_0^1 \partial p_0^2} = m_{31} m_{12} \tag{3.40}$$

$$\frac{\partial S^2}{\partial {p_0^2}^2} = m_{42} m_{22} \tag{3.41}$$

The positions are also expanded as

$$\begin{aligned} x^1 &= x_t^1 + m_{33}(x_0^1 - x_k^1) + m_{34}(x_0^2 - x_l^2) + m_{31}(p_0^1 - p_m^1) + m_{32}(p_0^2 - p_n^2) \\ x^2 &= x_t^2 + m_{43}(x_0^1 - x_k^1) + m_{44}(x_0^2 - x_l^2) + m_{41}(p_0^1 - p_m^1) + m_{42}(p_0^2 - p_n^2) \end{aligned} \tag{3.42}$$

The integral over $\vec{p}_0$ from equation 3.24 fixes $\vec{x} = \vec{x}_t$. Solving the system of equations in 3.42 gives p_0 as

$$\begin{aligned} p_0^1 &= p_m^1 + \tfrac{1}{m_{32}m41 - m_{31}m_{42}}(-m_{42}(x^1 - x_t^1) + m_{32}(x^2 - x_t^2) \\ &+ (m_{33}m42 - m_{32}m_{43})(x_0^1 - x_k^1) + (m_{34}m42 - m_{32}m_{44})(x_0^2 - x_l^2)) \\ p_0^2 &= p_n^1 - \tfrac{1}{m_{32}m41 - m_{31}m_{42}}(-m_{41}(x^1 - x_t^1) + m_{32}(x^2 - x_t^2) \\ &+ (m_{33}m41 - m_{31}m_{43})(x_0^1 - x_k^1) + (m_{34}m41 - m_{31}m_{44})(x_0^2 - x_l^2)) \end{aligned} \tag{3.43}$$

The term in the exponent then becomes (with $\vec{p}_0$ given by 3.43 implicit)

$$\begin{aligned} & i(S(x_k^1, x_l^2, p_m^1, p_n^2) + (m_{33}p_{klmnt}^1 - p_m^1)(x_0^1 - x_k^1) \\ & +(m_{44}p_{klmnt}^2 - p_m^2)(x_0^2 - x_l^2) \\ & +m_{31}p_{klmnt}^1(p_0^1 - {}_m^1) + m_{42}p_{klmnt}^2(p_0^2 - p_n^2) + \tfrac{1}{2}m_{13}m_{11}(x_0^1 - x_k^1)^2 \\ & +\tfrac{1}{2}m_{24}m_{44}(x_0^2 - x_l^2)^2 + \tfrac{1}{2}m_{31}m_{11}(p_0^1 - p_m^1)^2 + \tfrac{1}{2}m_{42}m_{22}(p_0^2 - p_n^2)^2 \\ & +m_{23}m_{44}(x_0^1 - x_k^1)(x_0^2 - x_l^2) + m_{13}m_{31}(x_0^1 - x_k^1)(p_0^1 - p_m^1) \\ & +m_{23}m_{42}(x_0^1 - x_k^1)(p_0^2 - p_n^2) + m_{14}m_{31}(x_0^2 - x_l^2)(p_0^1 - p_m^1) \\ & +m_{24}m_{42}(x_0^2 - x_l^2)(p_0^2 - p_n^2) + m_{31}m_{12}(p_0^1 - p_m^1)(p_0^2 - p_n^2)) \\ & -\alpha(x_0^1 - x_k^1)^2 - \beta(x_0^2 - x_l^2)^2 - \gamma(p_0^1 - p_m^1)^2 - \epsilon(p_0^2 - p_n^2)^2 - \tfrac{i\nu\pi}{2} \end{aligned} \tag{3.44}$$

This is the contribution to the semiclassical Green function for each cell. The total Green function is the sum over these terms with a prefactor from the $|\partial x_t/\partial p_0|^{1/2}$ term which is $1/\sqrt{m_{31}m_{42} - m_{32}m_{41}}$.

The purpose of calculating the semiclassical Green function is to use it in (3.11) to build up a functional form that can then be used in an integral for some statistical

property such as the radial distribution function. It takes many trajectories for the Green function from cellular dynamics to cover all possible ranges, and calculating the statistical properties from this form is still a work in progress.

Chapter 4

Correlated Thomas-Fermi Method

There are many methods for calculating the ground states of chemical systems [17]. DFT has been at the forefront of these methods and as such improvements to DFT are currently pushing back the boundaries on the types of systems that it is possible to model in a reasonable amount of computing time and to a reasonable accuracy. At the same time however, the relative dominance of DFT in this area means that there are types of systems that we have made little progress in modeling. That is because of DFT routinely fails for some types of systems, the most prominent being strongly correlated systems. It is for this reason that we are interested in approximate methods for the ground state of strongly correlated systems.

Our work on strongly correlated systems starts from an insight into the Thomas-Fermi Approximation and the somewhat fuzzy idea which has taken on greater clarity with our work that strongly correlated systems are more suceptible to semiclassical approximations because they actually have a greater classical character. Because of the central importance of the Thomas-Fermi approximation to our work, we take

some time to review it first. Then we discuss our related method, which we call correlated Thomas-Fermi (CTF).

As we will show in the review of CTF in Section 4.2, this method hinges on an ability to determine which state in the spectrum of states for an analogous system of distinguishible particles is the first totally antisymmetric state, that is the ground state for a system of fermions. This is a new and interesting problem in it's own right that brings together disparate ideas from group theory, quantum mechanics, and combinatorics in a novel way. We discuss this problem in detail and propose different solutions in Section 4.7.

4.1 Review of Thomas-Fermi Theory

Thomas-Fermi theory has dual importance as a precursor to modern density functional theory and as a successful approximation in its own right. The TF approximation has been used for a wide variety of systems ranging all the way from atoms and molecules to stars [18], [19]. In this section we offer a short review of TF theory both from the standard perspective and from the perspective that allows us to formulate CTF (For further information on TF theory see [20]).

The Thomas-Fermi approximation started from an ansatz for an energy functional of the density [21]. The Thomas-Fermi ground state energy is broken down into a kinetic energy term, $T_s^{\text{loc}}[n]$ and an interaction term, $U[n]$, together with a term that calculates the energy due to the external potential $v_{\text{ext}}(\mathbf{r})$.

$$E^{\text{TF}}[n(\mathbf{r})] = T_s^{\text{loc}}[n(\mathbf{r})] + U[n(\mathbf{r})] + \int d\mathbf{r}\ n(\mathbf{r}) v_{\text{ext}}(\mathbf{r}) \quad , \tag{4.1}$$

The kinetic-energy term $T_s^{\rm loc}[n(\mathbf{r})] = \frac{3}{10}(3\pi^2)^{2/3}\int d\mathbf{r}\; n(\mathbf{r})^{5/3}$ is chosen to yield the exact energy for a non-interacting electron gas of uniform density. The electron-electron interaction term for Coulomb-interacting electrons has the standard Hartree form $U[n(\mathbf{r})] = \frac{1}{2}\int\int d\mathbf{r}d\mathbf{r}'\; n(\mathbf{r})n(\mathbf{r}')/|\mathbf{r}-\mathbf{r}'|$ (we use atomic units in this chapter). Looking at the Thomas-Fermi approximation through the lens of modern DFT we see that it is made up of a local density approximation to the non-interacting kinetic energy functional along with a Hartree term.

Minimizing the energy with respect to density variations, subject to the constraint that the number of particles N remains constant, $\int n(\mathbf{r})\; d\mathbf{r} = N$, leads to the Thomas-Fermi equation

$$\frac{3}{10}\left(3\pi^2 n(\mathbf{r})\right)^{2/3} + v_{\rm ext}(\mathbf{r}) + v_{\rm H}[n](\mathbf{r}) - \mu = 0 \quad , \tag{4.2}$$

where $v_{\rm H} = \delta U[n]/\delta n$ is the Hartree potential, and μ is the chemical potential that ensures that the number of particles is constant. The self-consistent solution of Eq.(4.2) produces a rough approximation to the true density. Details such as atomic shell structure are not produced in the approximation. Using this density in Eq.(4.1) gives an approximation to the ground state energy.

An alternative formulation of TF theory that makes clear its semiclassical nature uses a phase space based perspective [22]. The *classical* Hartree density of states $\rho_{\rm cl}(\varepsilon)$ is

$$\rho_{\rm cl}(\varepsilon) = \frac{1}{(2\pi)^3}\int d\mathbf{p}d\mathbf{r}\; \delta(\varepsilon - h_{\rm cl}(\mathbf{p},\mathbf{r})) \quad , \tag{4.3}$$

where the integrals are done over all of phase-space and $h_{\rm cl}(\mathbf{p},\mathbf{r})$ is the classical single-particle hamiltonian $h_{\rm cl}(\mathbf{p},\mathbf{r}) = p^2/2 + v_{\rm ext}(\mathbf{r}) + v_{\rm H}(\mathbf{r})$. The self-consistent solution

of:

$$N = \int_{-\infty}^{\varepsilon_F} \rho_{\rm cl}(\varepsilon)\ d\varepsilon \qquad \text{and} \qquad E^{\rm TF} = \int_{-\infty}^{\varepsilon_F} \varepsilon\rho_{\rm cl}(\varepsilon)\ d\varepsilon \tag{4.4}$$

leads to the same energy $E^{\rm TF}$ as before, Eq.(4.1). The Fermi energy ε_F coincides with the chemical potential $\mu = dE^{\rm TF}/dN$ of Eq.(4.2).

It is now clear how Pauli's principle is satisfied. We keep adding particles occupying each a volume h^3 of phase space ($(2\pi)^3$ in atomic units), until we have filled the available phase space.

This is a good approximation because $\rho_{\rm cl}(\varepsilon)$ is the first (Weyl) term in the semiclassical Gutzwiller expansion [23] of the Kohn-Sham density of states (see e.g. refs.[24]-[25]). Typically the smooth part of the Kohn-Sham staircase function $S_s(\varepsilon) = \sum_n \theta(\varepsilon - \varepsilon_n)$, where the ε_n are exact Kohn-Sham eigenvalues, is well approximated by its classical counterpart:

$$S_{\rm cl}(\varepsilon) \equiv \int_{-\infty}^{\varepsilon} d\varepsilon'\ \rho_{\rm cl}(\varepsilon') \quad , \tag{4.5}$$

as illustrated schematically in the left panel of Fig.4.1. This point is the crux of the semiclassical approximation that leads to Thomas Fermi theory. We further discuss its range of applicability with respect to CTF in Section 4.3.

Clearly there are two main aspects to the Thomas-Fermi approximation. The first part of the approximation is that interactions are treated in a mean-field manner. This is clear from the fact that it uses a Hartree type potential for the interaction term in Eq.(4.3). The second part of the approximation became clear when we looked at the phase space formulation of Thomas-Fermi theory. It is an inherently semiclassical approximation since the Gutzwiller expansion to the density of states is cut off after the first term. These approximations together lead to efficient calculations for even

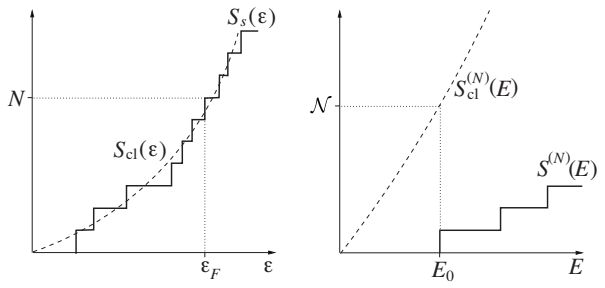

Figure 4.1: *Schematic diagram*, assuming a spectrum with no exact degeneracies. Left panel: The classical function $S_{\rm cl}(\varepsilon)$, Eq.(4.5) is a smooth approximation to the Kohn-Sham staircase function $S_s(\varepsilon)$. Right panel: The N-electron classical function $S_{\rm cl}^{(N)}(E)$ does *not* go through the quantum N-electron staircase $S^{(N)}(E)$, because the latter consists of antisymmetric states only. $S_{\rm cl}^{(N)}(E)$ is a smooth version of the quantum-mechanical problem when symmetry is disregarded (a much steeper staircase), and can be used to approximate the true ground-state energy E_0 via Eq.(4.8), if the number of states $\mathcal{N}$ below the first totally antisymmetric state is known.

quite large systems. The two approximations are however separate. It is possible therefore to remove one approximation while keeping the other.

For example it is possible to keep the mean field approximation, but improve upon the semiclassical part of the approximation. This could be done by including additional terms in the semiclassical Gutzwiller expansion. Ullmo et al [26] follow a related strategy for improving the Thomas-Fermi approximation. In our formulation of CTF we do the opposite. We allow the semiclassical approximation to stand, but improve upon the mean-field approximation by including explicit interactions. Of course any reduction in the level of approximation will lead to more intensive calculations, but the reward is greater accuracy.

4.2 Correlated Thomas-Fermi

The formulation of CTF follows from the phase space perspective of Thomas-Fermi theory as seen in Eq.(4.3) and Eq.(4.4). We want to include explicit interactions so we need to use the classical N-body density of states in place of the classical Hartree density of states. Employing the notation $\mathbf{R} \equiv (\mathbf{r}_1, ...\mathbf{r}_N)$, and $\mathbf{P} \equiv (\mathbf{p}_1, ...\mathbf{p}_N)$, the classical N-electron density of states $\rho_{\rm cl}^{(N)}(E)$ corresponding to the classical N-electron Hamiltonian $H_{\rm cl}(\mathbf{P}, \mathbf{R})$ is:

$$\rho_{\rm cl}^{(N)}(E) = \frac{1}{(2\pi)^{3N}} \int d\mathbf{P} d\mathbf{R}\ \delta(E - H_{\rm cl}(\mathbf{P}, \mathbf{R}))\ , \tag{4.6}$$

and the N-electron analog of the smooth staircase function of Eq.(4.5) becomes:

$$S_{\rm cl}^{(N)}(E) \equiv \int_{-\infty}^{E} dE'\ \rho_{\rm cl}^{(N)}(E')\ \ . \tag{4.7}$$

Unlike the analogous TF case, this function of energy does *not* go through the exact (quantum) N-electron staircase $S^{(N)}(E) = \sum_n \theta(E - E_n)$, where the E_n are the energy eigenvalues of the N-electron interacting system and θ is the Heaviside step function (see right panel of Fig.4.1). The Pauli principle forces the quantum staircase, $S^{(N)}(E)$, to only contain antisymmetric states. The classical Hamiltonian on the other hand does not have this same requirement. Nowhere in Eqs.(4.6)-(4.7) has antisymmetry been invoked. Classical particles are distinguishable, so $S_{\rm cl}^{(N)}(E)$ approximates the much steeper staircase comprised of states of all symmetries (not depicted in Fig.4.1). In order to find the ground state energy of a fermionic system, we must introduce symmetry at this latter stage of the calculation. We include symmetry by counting along the steeper classical staircase to the level with the correct symmetry. This is analogous to introducing the Pauli exclusion principle in standard Thomas-Fermi

theory by integrating up to the Fermi energy. It is however a different perspective than is usually taken when finding the ground state of a fermionic system. Instead of projecting the Hamiltonian onto the correct symmetry character of the permutation group, we include all symmetries of the permutation group and convert the problem into one of state-counting, that is, counting the number of states (of any symmetry) that have an energy lower than that of the first totally antisymmetric one. We call this number, the number of the first totally antisymmetric state among the set of states with all symmetries, $\mathcal{N}$. Another way to look at $\mathcal{N}$, is as the number that the fermionic ground state corresponds to in the spectrum of the same system replaced with distinguishible particles.

If we know $\mathcal{N}$, an approximation for the ground state energy is determined as the upper limit of an energy integral:

$$\int_{-\infty}^{E^{\mathrm{CTF}}} \rho_{\mathrm{cl}}^{(N)}(E)\, dE = \mathcal{N} \quad , \tag{4.8}$$

We call E^{CTF} the Correlated-Thomas-Fermi (CTF) approximation to E_0.

We have looked at a few toy systems to prove that given the correct $\mathcal{N}$ our method works. This is just a proof of concept, but it is useful because it proves that if we have a good approximation to $\mathcal{N}$ the CTF method would be complete.

We now turn to three different model systems for which we have also found $\mathcal{N}$ as proofs of concept.

Case 1. First, we consider N spinless electrons in a one dimensional harmonic trap of unit frequency, interacting via a harmonic potential of frequency Ω, which we

vary from 0 to 2. The Hamiltonian of this system is

$$H = \sum_{i=1}^{N} \left[-\frac{1}{2}\frac{d^2}{dx_i{}^2} + \frac{1}{2}x_i{}^2 \right] + \sum_{i<j}^{N} \frac{1}{2}\Omega^2 \left(x_i - x_j\right)^2 \tag{4.9}$$

The integral for the classical density of states in Eq 4.8 can be done analytically as should be expected since we are only dealing with harmonic potentials. It only takes a rotation of the coordinate system to put the Hamiltonian from 4.9 in a form that allows the the integral for the classical density of states to be relatively easily done. If the level curves of the potential in 4.9 are plotted it is clear that the potential is eliptical with one axis having a distinct length and all other axes having the same length. The distinct axis is along the line $x_1 = x_2 = \cdots = x_N$. So it is possible to rotate the coordinate system to decouple the oscillators, and all that is necessary to determine the Hamiltonian after such a rotation is to find the frequency along the distinct and the frequency along any other axis.

In other words the potential is

$$V = \sum_{i}^{N} \frac{1}{2}x_i{}^2 + \sum_{i<j}^{N} \frac{1}{2}\Omega^2 \left(x_i - x_j\right)^2 \tag{4.10}$$

but we know there is a coordinate rotation (that leaves $\vec{p}^2$ unchanged since it is just a rotation) to take the potential to the form

$$V = \frac{\omega_0{}^2}{2}x_1{}^2 + \sum_{i=2}^{N} \frac{\omega_1}{2}x_i{}^2 \tag{4.11}$$

So it is not necessary to find the rotation only to find ω_0 and ω_1. To do this we compare the $V = \frac{1}{2}$ level curve for the original and the rotated (uncoupled) potentials.

For the rotated level curve half the length of the distinct axis of the ellipse is given by solving for x_1 in the level curve equation with all other $x_i = 0$. This gives

$$1 \;=\; \omega_0{}^2 x_1{}^2 + \sum_{i=2}^{N} \omega_1 0^2 \tag{4.12}$$

$$1 = {\omega_0}^2 {x_1}^2 \tag{4.13}$$

$$x_1 = \frac{1}{\omega_0} \tag{4.14}$$

$$\tag{4.15}$$

The half length of the other axes can be found by setting all $x_i = 0$ except e.g. x_2. This gives

$$1 = {\omega_0}^2 0^2 + {\omega_1}^2 {x_2}^2 + \sum_{i=3}^{N} \omega_1 0^2 \tag{4.16}$$

$$1 = {\omega_1}^2 {x_2}^2 \tag{4.17}$$

$$x_2 = \frac{1}{\omega_1} \tag{4.18}$$

$$\tag{4.19}$$

Using these lengths, all that must be done is compare them to the lengths of the unrotated potential to find ω_0 and ω_1 since the lengths must be the same (it is only a rotation; the scale is unchanged).

For the original potential, the distict axis is along $x_1 = x_2 = x_3 = \cdots = x_N$. Plugging this into the $V = \frac{1}{2}$ level curve

$$1 = \sum_{i}^{N} {x_1}^2 + \sum_{i<j}^{N} \Omega^2 \left(x_1 - x_1\right)^2 \tag{4.20}$$

$$1 = N \frac{1}{2} {x_1}^2 \tag{4.21}$$

$${x_1}^2 = \frac{1}{N} \tag{4.22}$$

So the half length of the axis of the ellipse is

$$||(x_1, x_2, \cdots, x_N)|| = \sqrt{\sum_{i}^{N} x_i^2} \tag{4.23}$$

$$= \sqrt{\sum_{i}^{N} 1/N} \tag{4.24}$$

$$= 1 \tag{4.25}$$

Now all that remains is to consider an axis of the ellipse that is perpendicular to $x_1 = x_2 = x_3 = \cdots = x_N$. We can choose $x_1 = -x_2 = x_3 = -x_4 = \cdots = \pm x_N$ where the negative signs are on all even x_is. This gives

$$1 = \sum_{i}^{N} {x_i}^2 + \sum_{i=2 \text{ even}}^{N} \sum_{j<i}^{N} \Omega^2 (x_i - x_j)^2 + \sum_{i=1 \text{ odd}}^{N} \sum_{j<i}^{N} \Omega^2 (x_i - x_j)^2 \tag{4.26}$$

$$1 = N{x_1}^2 + \sum_{i=2 \text{ even}}^{N} \sum_{j<i \text{ odd}}^{N} \Omega^2 (x_1 + x_1)^2 + \sum_{i=1 \text{ odd}}^{N} \sum_{j<i \text{ even}}^{N} \Omega^2 (x_1 + x_1)^2 \tag{4.27}$$

$$1 = N{x_1}^2 + \sum_{i=2 \text{ even}}^{N} \sum_{j<i \text{ odd}}^{N} \Omega^2 4{x_1}^2 + \sum_{i=1 \text{ odd}}^{N} \sum_{j<i \text{ even}}^{N} \Omega^2 4{x_1}^2 \tag{4.28}$$

$$1 = N{x_1}^2 + \sum_{i=2 \text{ even}}^{N} \frac{i}{2} \Omega^2 4{x_1}^2 + \sum_{i=1 \text{ odd}}^{N} \frac{i-1}{2} \Omega^2 4{x_1}^2 \tag{4.29}$$

$$1 = N{x_1}^2 + \Omega^2 4{x_1}^2 \left(\sum_{i=2 \text{ even}}^{N} \frac{i}{2} + \sum_{i=1 \text{ odd}}^{N} \frac{i-1}{2} \right) \tag{4.30}$$

$$1 = N{x_1}^2 + \Omega^2 4{x_1}^2 \left(\sum_{i=2 \text{ even}}^{N} \frac{i}{2} + \sum_{i=1 \text{ odd}}^{N} \frac{i}{2} - \sum_{i=1 \text{ odd}}^{N} \frac{1}{2} \right) \tag{4.31}$$

$$1 = N{x_1}^2 + \Omega^2 4{x_1}^2 \left(\sum_{i=1}^{N} \frac{i}{2} - \sum_{i=1 \text{ odd}}^{N} \frac{1}{2} \right) \tag{4.32}$$

$$1 = N{x_1}^2 + \Omega^2 4{x_1}^2 \left(\frac{1}{2} \frac{N(N+1)}{2} - \frac{1}{2} \frac{N}{2} \right) \tag{4.33}$$

$$1 = N{x_1}^2 + \Omega^2 {x_1}^2 N^2 \tag{4.34}$$

$${x_1}^2 = \frac{1}{N + N^2 \Omega^2} \tag{4.35}$$

And the half length of the axis of the ellipse is

$$||(x_1, x_2, \cdots, x_N)|| = \sqrt{\sum_{i}^{N} x_i^2} \tag{4.36}$$

$$= \sqrt{\sum_i^N \frac{1}{N + N^2\Omega^2}} \tag{4.37}$$

$$= \sqrt{\frac{1}{1 + N\Omega^2}} \tag{4.38}$$

$$\tag{4.39}$$

Comparing the original and rotated ellipse gives equations for ω_0 and ω_1:

$$\frac{1}{\omega_0} = 1 \tag{4.40}$$

$$\omega_0 = 1 \tag{4.41}$$

and

$$\frac{1}{{\omega_1}^2} = \frac{1}{1 + N\Omega^2} \tag{4.42}$$

$$\omega_1 = \sqrt{1 + N\Omega^2} \tag{4.43}$$

Now it is relatively straightforward to take the integral for the density of states in the rotated coordinate system.

$$\rho(E) = \int \frac{d^N p}{h^N} \int d^N x \; \delta\left(E - \frac{p^2}{2m} - \frac{{x_1}^2}{2} - \sum_{i=2}^N {\omega_1}^2 \frac{{x_i}^2}{2}\right) \tag{4.44}$$

$$= \frac{1}{h^N} \int d\vec{\Omega} \int dp \; p^{N-1} \int d^N x \; \delta\left(E - \frac{p^2}{2m} - \frac{{x_1}^2}{2} - \sum_{i=2}^N {\omega_1}^2 \frac{{x_i}^2}{2}\right) \tag{4.45}$$

where $d\vec{\Omega}$ is the N-dimensional solid angle volume element. If S_N is the result of the angular integrals we have

$$\rho(E) = \int \frac{d^N p}{h^N} \int d^N x \; \delta\left(E - \frac{p^2}{2m} - \frac{{x_1}^2}{2} - \sum_{i=2}^N {\omega_1}^2 \frac{{x_i}^2}{2}\right) \tag{4.46}$$

$$= \frac{S_N}{h^N} \int d^N x \; p^{N-1} \frac{m}{p} \tag{4.47}$$

where $p = \sqrt{2m\left(E - \frac{{x_1}^2}{2} - \sum_{i=2}^{N} {\omega_1}^2 \frac{{x_i}^2}{2}\right)}$. Making the appropriate substition we have

$$\rho(E) = \frac{S_N}{h^N} m^{N/2} 2^{N-1} E^{N-1} \int d^N y \left(1 - {y_1}^2 - \sum_{i=2}^{N} {\omega_1}^2 {y_i}^2\right)^{N/2-1} \tag{4.48}$$

It is possible to do the y_1 integral now while considering the other variables constant with the substitution $y_1 = \sqrt{1 - \sum_{i=2}^{N} {\omega_1}^2 {y_i}^2}\ \eta_1$

$$\rho(E) = \frac{S_N}{h^N} m^{N/2} 2^{N-1} E^{N-1} \int d\eta_1 dy_2 \cdots dy_N \left(1 - \sum_{i=2}^{N} {\omega_1}^2 {y_i}^2\right)^{(N-1)/2} \tag{4.49}$$

$$\times \Theta\left(1 - \sum_{i=2}^{N} {\omega_1}^2 {y_i}^2\right) \left(1 - {\eta_1}^2\right)^{N/2-1} \tag{4.50}$$

The η_1 integral is now straightforward with the substition of $\eta_1 = sin\theta$. The y integral needs to be done in spherical coordinates, and can then be done with an analogous trigonometric substition.

$$\rho(E) = \frac{S_N}{h^N} m^{N/2} 2^{N-1} E^{N-1} S_{N-1} \int dy\ y^{N-2} \left(1 - {\omega_1}^2 y^2\right)^{(N-1)/2} \Theta\left(1 - {\omega_1}^2 y^2\right) \tag{4.51}$$

$$\times \int_{-\pi/2}^{\pi/2} d\theta \cos^{N-1}\theta \tag{4.52}$$

$$= \frac{S_N}{h^N} m^{N/2} 2^{N-1} E^{N-1} S_{N-1} \int_0^{\phi/2} d\phi\ \frac{1}{{\omega_1}^{N-1}} \sin^{N-1}\phi \cos^N \phi \tag{4.53}$$

$$\times \int_{-\pi/2}^{\pi/2} d\theta \cos^{N-1}\theta \tag{4.54}$$

$$\tag{4.55}$$

Using the results of the angular integrals and simplifying gives

$$\rho(E) = \frac{m^{N/2}}{h^N {\omega_1}^{N-1}} \frac{(2\pi)^N}{\Gamma(N)} E^{N-1} \tag{4.56}$$

It is extremely straightforward to do the energy integral in Eq. 4.8 to give

$$E_{\mathrm{CTF}} = \mathcal{N}^{1/N} {\omega_1}^{(N-1)/N} (N!)^{1/N} \tag{4.57}$$

where again $\omega_1 = \sqrt{1 + N\Omega^2}$.

Now all that remains is to find $\mathcal{N}$ from the analytical exact solution [27] (Note it is also very straightforward to find the exact solution from the rotated potential). From the solution we know that the energy of the first totally antisymmetric state is

$$E_0^f = \frac{\omega_1}{2}\left(N^2 - 1\right) + \frac{1}{2} \tag{4.58}$$

and the energy of an arbitrary state is given by

$$E_{\{n_i\}} = n_1 + \omega_1 \left(\sum_{i=2}^{N} n_i + \frac{N-1}{2} \right) + \frac{1}{2} \tag{4.59}$$

where the $\{n_i\}$ are the quantum numbers. The number of states below the first totally antisymmetric state, $\mathcal{N}$, can be found by comparing these two energies.

We need to know for how many states is $E_{\{n_i\}} < E_0^f$. That is

$$n_1 + \omega_1 \left(\sum_{i=2}^{N} n_i + \frac{N-1}{2} \right) + \frac{1}{2} \;<\; \omega_1 \left(\frac{N-1}{2} + \frac{N(N-1)}{2} \right) + \frac{1}{2} \tag{4.60}$$

$$n_1 + \omega_1 \sum_{i=2}^{N} n_i \;<\; \omega_1 \left(\frac{N(N-1)}{2} \right) \tag{4.61}$$

$$\frac{n_1}{\omega_1} + \sum_{i=2}^{N} n_i \;<\; \frac{N(N-1)}{2} \tag{4.62}$$

First we consider the case $n_1 = 0$. The sum is just an integer, which we can label M. Then we have

$$M \;<\; \frac{N(N-1)}{2} \tag{4.63}$$

$$\tag{4.64}$$

and the number of levels with energy less than E_0^f is

$$\sum_{M=0}^{N(N-1)/2-1} W(M) \tag{4.65}$$

Where $W(M)$ is the number of ways to get M from the sum. This is just a problem in combinatorics and it is equivalent to the number of ways M balls can be put in $N-1$ boxes which is

$$W(M) = \frac{(N+M-2)!}{(N-2)!M!} \tag{4.66}$$

Now while $\lceil \frac{n_1}{\omega_1} \rceil$ the number of level less than E_0^f is simply

$$\sum_{M=0}^{N(N-1)/2-1} W(M) \tag{4.67}$$

Following this logic the total number of levels less than E_0^f, $\mathcal{N}$ is given by

$$\mathcal{N} = \sum_{n_1}^{\lceil \omega_1 N(N-1)/2 \rceil} \sum_{M=0}^{N(N-1)/2-1-\lfloor n_1/\omega_1 \rfloor} W(M) \tag{4.68}$$

which is a function only of the number of particles N and Ω through ω_1.

Combining equations (4.68) and (4.57) gives the CTF approximation (using the exact $\mathcal{N}$) to the true groundstate energy.

Figure 4.2 shows this energy for two particles as a function of interaction strength. As discussed above the exact energy is known analytically [27]. For two particles the exact $\mathcal{N}$ is $\mathcal{N} = \lfloor \sqrt{1+2\Omega^2} \rfloor + 1$, where $\lfloor\ \rfloor$ stands for the floor function, which leads to steps in the energy $E(\Omega)$. Leaving out the floor function provides the most natural way of smoothing-out the CTF curve, and it is this smoothed out curve that is depicted as the solid line in Figure 4.2. We observe that the CTF results run very close to the exact curve along the whole range of interaction strengths, improving dramatically upon both the original Thomas-Fermi approximation and Sommermann-Weidenmueller approximation [28], which is another semiclassical approach that is also related to the Thomas-Fermi approximation.

Table 4.1: Exact and CTF ground-state energies for N fermions interacting via a harmonic interaction, $\sum_{i<j}^{N} \frac{1}{2}(x_i - x_j)^2$, with a harmonic confining potential.

N	Exact	CTF	%Error
3	8.500E00	8.963E00	5E-02
5	2.989E+01	2.987E+01	-9E-03
10	1.647E+02	1.645E+02	-1E-03
15	4.485E+02	4.487E+02	5E-04

We have also looked at systems with N up to 15 particles for $\Omega = 1$ (see Table 4.1). The accuracy of CTF increases with the number of particles. The error decreases from 0.05% for $N = 3$ to 5×10^{-4}% for $N = 15$.

Case 2. The next case we consider is three spinless electrons interacting via a quartic attraction (the interaction term between two electrons is of the form $k(x_i - x_j)^4$) with a harmonic confining potential. That is the Hamiltonian is

$$H = \sum_{i=1}^{3} \left[-\frac{1}{2}\frac{d^2}{dx_i{}^2} + \frac{1}{2}x_i{}^2 \right] + \sum_{i<j}^{3} \frac{1}{2}k\left(x_i - x_j\right)^4 \tag{4.69}$$

The density of states integral can again be done analytically using some creative substitutions.

$$\rho(E) = \int \frac{d^3p}{h^3} \int d^3x\ \delta\left(E - \frac{\vec{p}^2}{2} - \frac{1}{2}\vec{x}^2 - \sum_{i<j}^{3} \frac{1}{2}k\left(x_i - x_j\right)^4 \right) \tag{4.70}$$

With a rotation corresponding to the subtitions $x_1 = \frac{1}{\sqrt{6}}\left(y_1 - \sqrt{3}y_2 + \sqrt{2}y_3\right)$, $x_2 = \frac{1}{\sqrt{6}}\left(y_1 + \sqrt{3}y_2 + \sqrt{2}y_3\right)$, and $x_3 = \frac{1}{\sqrt{3}}\left(-\sqrt{2}y_1 + y_3\right)$ it is possible to decouple all but two of the coordinates:

$$\rho(E) = \int \frac{d^3p}{h^3} \int d^3y\ \delta\left(E - \frac{\vec{p}^2}{2} - \frac{1}{2}\vec{y}^2 - \frac{9}{2}k\left(y_1{}^2 + y_2{}^2\right)^2 \right) \tag{4.71}$$

$$= \frac{4\pi}{h^3} \int d^3y \sqrt{2\left(E - \frac{1}{2}\vec{y}^2 - \frac{9}{2}k\left(y_1{}^2 + y_2{}^2\right)^2 \right)} \tag{4.72}$$

where the p integral is done in spherical coordinates using the delta function. The resulting integral is most easily done in cylindrical coordinates.

$$\rho(E) = \frac{4\pi}{h^3}\int r dr d\theta dz \sqrt{2\left(E - \frac{1}{2}r^2 - \frac{1}{2}z^2 - \frac{9}{2}kr^4\right)} \tag{4.73}$$

The z integral can be done using the substitution $z = \sqrt{2(E - \frac{1}{2}r^2 - \frac{9}{2}kr^4}\ \sin\phi$

$$\rho(E) = \frac{8\pi^2}{h^3}\int dr 2r\left(E - \frac{1}{2}r^2 - \frac{9}{2}kr^4\right)\int_{-\pi/2}^{\pi/2} d\phi \cos^2\phi \tag{4.74}$$

$$= \frac{16\pi^2}{h^3}\int dr\ \left(Er - \frac{1}{2}r^3 - \frac{9}{2}kr^5\right)\left(\frac{\pi}{2}\right) \tag{4.75}$$

$$\tag{4.76}$$

It is important to note here that the r integral is not over all space, but only all classically allowed space; there should be a theta function to ensure this from the subsitution that was supressed for readability. So the maximum range of the r integral is r' defined by $E - \frac{1}{2}r'^2 - \frac{9}{2}kr'^4 = 0$. Taking the integral as well as the energy integral with $\hbar = 1$ gives

$$\frac{1}{6}\left(\frac{1}{116,640k^3}(1 + 72kE_{\mathrm{CTF}})^{5/2} - \frac{{E_{\mathrm{CTF}}}^2}{12k} - \frac{E_{\mathrm{CTF}}}{648k^2} - \frac{1}{116,640k^3}\right) = \mathcal{N} \tag{4.77}$$

When $\mathcal{N}$ is found from the exact diagonalization, the result for E_{CTF} can be found by finding the root.

In order to find $\mathcal{N}$ for this system it was necessary to do an exact diagonalization. We did this in the basis of harmonic oscillator states that are the eigenstates of the external potential without interactions. Finding the matrix elements in this basis is relatively straightforward since the potential can be written in terms of raising and lowering operators and then expanded

$$V_{ij} = k(x_i - xj)^4 \tag{4.78}$$

$$= \quad k\frac{\hbar^2}{4m^2\omega^2}(a_i{}^\dagger + a_i - a_j{}^\dagger - a_j)^4 \tag{4.79}$$

It is important to take note of the noncommutativity of raising and lowering operators when expanding. The commutator between raising and lowering operators

$$\left[a_i, a_i{}^\dagger\right] = 1 \tag{4.80}$$

can be use to simplify the expression. It is then straight forward to take the matrix elements between harmonic oscillator states. The full expression is too complicated to write down here.

It was possible to greatly reduce the resources necessary to diagonalize the Hamiltonian in a certain truncated basis by taking into account the permutation symmetry of the system. All that needs to be done is to use a symmetrized version of the basis and then matrix elements between basis elements of different symmetry character are zero. This results in a block diagonal hamiltonian with each block associated with a symmetry character based on the symmetry character of the basis vectors used to form it. Each block can then be diagonalized separately. This is discussed in much greater detail in Section 5.3.

Once the eigenstates are found exactly, $\mathcal{N}$ is found by counting the number of states with energy less than the energy associated with the first totally antisymmetric state (that is the lowest eigenvalue of the antisymmetric block).

Again, for the quartic system, we see that CTF runs very close to the exact curve for the whole range of values of k considered.

Case 3. Does the excellent performance of CTF reported so far have something to do with the integrability of the underlying classical dynamics (case 1) or its near-integrability (case 2)? In order to determine if the good results for our method is a

factor of the underlying classical dynamics being integrable (case 1) or nearly integrable (case 2) we have also calculated the CTF energies for a simple *non*-integrable system, 2 electrons interacting via a soft-Coulomb potential, $1/\sqrt{1+(x_1-x_2)^2}$, in a 1-d box of length L. In spite of the apparent simplicity of this model, the importance of ergodicity can be assessed as the length of the box is increased. Indeed, as concluded in ref.[29], this system displays hard chaos in the large-box limit, closely related to the fact that, due to the low electron density in that limit, the system becomes strongly correlated with the electrons localizing in opposite extremes of the box. Here the Hamiltonian is

$$H = -\frac{1}{2}\frac{d^2}{dx_1{}^2} - \frac{1}{2}\frac{d^2}{dx_2{}^2} + 1/\sqrt{1+(x_1-x_2)^2} \tag{4.81}$$

The density of states integral is again possible to do analytically in this case.

$$\rho(E) \;=\; \int \frac{d^2p}{h^2}\int d^2x\;\delta\left(E - \frac{p^2}{2m} - \frac{1}{\sqrt{(x_1-x_2)^2+1}}\right) \tag{4.82}$$

Where the coordinate integral is over the range of the box 0 to L. Using the delta function to take the p integral in circular coordinates gives

$$\rho(E) \;=\; \frac{m}{2\pi\hbar^2}\int_0^L dx_1\int_0^L dx_2\;\Theta\left(E - \frac{1}{\sqrt{(x_1-x_2)^2+1}}\right) \tag{4.83}$$

Making the substitution $x_1 = q + x_2$

$$\rho(E) \;=\; \frac{m}{2\pi\hbar^2}\int_0^L dx_2\int_{-x_2}^{L-x_2} dq\;\Theta\left(E - \frac{1}{\sqrt{q^2+1}}\right) \tag{4.84}$$

It is possible to calculate this integral by splitting it up into different regimes based on E. The step function changes at $E = \frac{1}{\sqrt{q^2+1}}$ that is $q = \sqrt{1/E^2-1}$ so the relevant ranges in E are $0 < E < \frac{1}{\sqrt{L^2+1}}$, $\frac{1}{\sqrt{L^2+1}} < E < 1$, and $E > 1$.

For $E < 1$ there is some point in the range of integration for which the step function is switches from 0 to 1. This point is $q = \pm\sqrt{1/E^2 - 1}$. The step function is 1 when q is outside these points. The integral then becomes

$$\rho(E) = \frac{m}{2\pi\hbar^2}\int_0^L dx_2\ \Theta\left(x_2 - \sqrt{1/E^2-1}\right)\int_{-x_2}^{-\sqrt{1/E^2-1}} dq \tag{4.85}$$

$$+ \frac{m}{2\pi\hbar^2}\int_0^L dx_2\ \Theta\left(L - x_2 - \sqrt{1/E^2-1}\right)\int_{\sqrt{1/E^2-1}}^{L-x_2} dq \tag{4.86}$$

The theta functions appear because it must be that $x_2 > \sqrt{1/E^2-1}$ and $L - x_2 > \sqrt{1/E^2-1}$ for the integrals to be nonzero.

$$\rho(E) = \frac{m}{2\pi\hbar^2}\int_0^L dx_2\ \Theta\left(x_2 - \sqrt{1/E^2-1}\right)\left(-\sqrt{1/E^2-1} + x_2\right) \tag{4.87}$$

$$+ \frac{m}{2\pi\hbar^2}\int_0^L dx_2\ \Theta\left(L - x_2 - \sqrt{1/E^2-1}\right)\left(L - x_2 - \sqrt{1/E^2-1}\right) \tag{4.88}$$

Now the theta functions change over the range of integration if $E > \frac{1}{L^2+1}$. For $E < \frac{1}{L^2+1}$ the step functions are always zero. So we have

$$\rho(E) = \frac{m}{\pi\hbar^2}\int_{\sqrt{1/E^2+1}}^L dx_2\left(-\sqrt{1/E^2-1} + x_2\right) \tag{4.89}$$

where we have used the change of variable $q_2' = L - q_2$ to show that the second half of the integral is the same as the first to pick up the factor of 2. The integral is now straightforward and gives

$$\rho(E) = \frac{m}{\pi\hbar^2}\left(\frac{L^2}{2} - \sqrt{\frac{1}{E^2}-1}L + \frac{1}{2}\left(\frac{1}{E^2}-1\right)\right) \tag{4.90}$$

For $E > 1$ the original theta function is always equal to 1 so the integral is

$$\rho(E) = \frac{m}{2\pi\hbar^2}\int_0^L dx_2\int_{-x_2}^{L-x_2} dq \tag{4.91}$$

$$= \frac{m}{2\pi\hbar^2}L^2 \tag{4.92}$$

$$\tag{4.93}$$

So we have for $E < \frac{1}{\sqrt{L^2+1}}$

$$\rho(E) = 0 \tag{4.94}$$

for $\frac{1}{\sqrt{L^2+1}} < E < 1$

$$\rho(E) = \frac{m}{\pi\hbar^2}\left(\frac{L^2}{2} - \sqrt{\frac{1}{E^2}-1}L + \frac{1}{2}\left(\frac{1}{E^2}-1\right)\right) \tag{4.95}$$

and for $E > 1$

$$\rho(E) = \frac{m}{2\pi\hbar^2}L^2 \tag{4.96}$$

$$\tag{4.97}$$

In order to find $\mathcal{N}$ for this system it was again necessary to do a numerical diagonalization. The basis used for this system was the particle in the box basis because that way the external potential was already diagonal. The interaction matrix elements were possible to find by numerical integration. This was relatively fast because the system is only one dimensional. Again, it was possible to speed up the diagonalization of the Hamiltonian by taking into account the permutation symmetry of the system. The Hamiltonian was partially diagonalized by using a symmetrized basis. Again see Section 5.3 for more details.

Table 4.2 shows the numbers obtained when the same value of $\mathcal{N} = 2$ is used for different box lengths. The performance of CTF improves as L increases, due to the increased localization leading to more classical character. This suggests that CTF might be particularly useful in the strongly-correlated regime.

The CTF approximation would not be complete without a word about spin. It turns out that the addition of spin does not change the approximation much. For

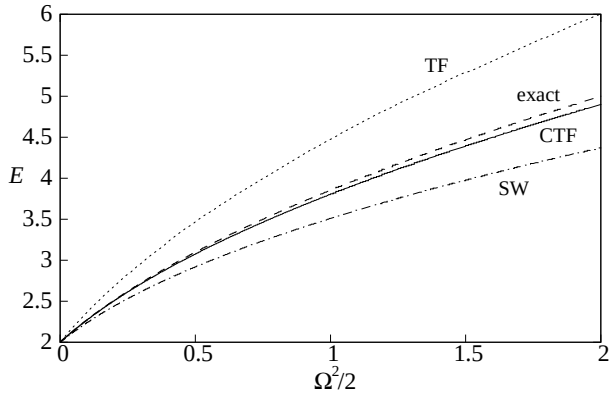

Figure 4.2: Ground-state energy for two spinless electrons interacting in one dimension via the potential $\frac{1}{2}\Omega^2(x_1 - x_2)^2$, calculated exactly (dashed line) and by different approximations: standard Thomas-Fermi (dotted); employing the antisymmetric staircase of SW [28] (dash-dot); and our CTF (solid).

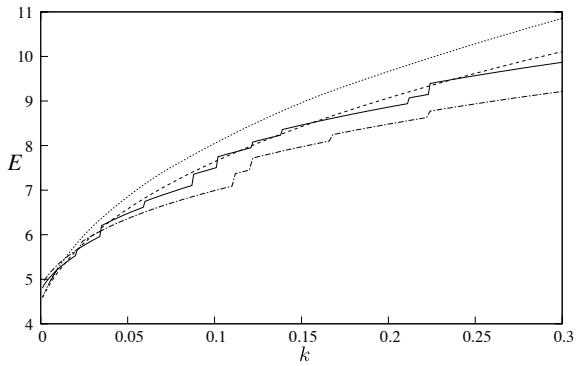

Figure 4.3: Ground-state energy for three spinless electrons interacting in one dimension via the potential $k(x_i - x_j)^4$, calculated exactly (dashed line) and by different approximations: standard Thomas-Fermi (dotted); our CTF method (solid); and CTF when the number of states $\mathcal{N}$ below the first totally antisymmetric state is calculated from perturbation theory (dot-dashed).

Table 4.2: Exact, TF, and CTF ($\mathcal{N} = 2$) ground-state energies for two electrons interacting via a soft-Coulomb potential $[(x_1 - x_2)^2 + 1]^{-1/2}$ and confined in a box of length L atomic units.

L	TF	CTF($\mathcal{N} = 2$)	Exact
1	1.37E+01	1.35E+01	2.56E+01
10	2.75E00	4.38E-01	5.12E-01
100	2.31E00	2.05E-02	2.20E-02
1000	1.99E00	1.40E-03	1.45E-03

particles that have spin, it is the combined spin and spatial part of the wavefunction that must be totally antisymmetric. The constraint that the spatial part of the wavefunction be antisymmetric is dropped. For spin $\frac{1}{2}$ particles such as electrons the spins can be either up or down so not all spatial symmetries are allowed. To find the ground state using CTF one must determine the symmetry of the spatial part of the ground state wavefunction and use that symmetry to find $\mathcal{N}$. That is $\mathcal{N}$ becomes the number of the first state of that symmetry in the spectrum of states with all symmetries included. In order to determine the spatial symmetry of the ground state it is necessary to use the pouring theorem of Lieb and Mattis [30].

It is important to remind the reader that these cases are just proofs of concept because we calulate $\mathcal{N}$ exactly. We are in effect cheating. In order for a complete CTF approximation we need a method for approximating $\mathcal{N}$. We address this in Section 4.7.

4.3 Applicability of CTF

Now we attempt a practical discussion of the usefulness and efficiency of the CTF method. We are replacing the quantum problem which scales exponentially with the number of particles with a classical one which scales polynomially. There may be some concern that the integral in Eq.(4.6) is over all phase space dimensions. However this is not a major drawback since Monte Carlo integration can be used which has a rate of convergence of $O(n^{1/2})$ where n is the number of points taken independent of dimension. This means that the integral itself scales well with increasing number of particles.

The question of range of applicability of the CTF method is an interesting one. The accuracy depends on how well the semiclassical energy levels from the Gutzwiller trace formula approximate the exact energy levels. The trace formula is

$$\text{Tr } G_{sc}(E) = \text{Tr } G_0(E) + \sum_j \text{Tr } G_j(E) \tag{4.98}$$

where $G_0(E)$ is due to zero length classical trajectories and the $G_j(E)$ terms are due to longer trajectories. If you read Chapter 2 you may remember that the trace of the Green's function is connected with the density of states by

$$-\frac{1}{\pi}\text{Im}\left(\text{Tr } G(E)\right) = \rho(E) \tag{4.99}$$

Using this with the trace formula gives

$$\rho_{sc}(E) = \rho_{cl}(E) + \delta\rho(E) \tag{4.100}$$

Where $\rho_{cl}(E)$ is the average part of the semiclassical density of states and $\delta\rho(E)$ is the oscillatory part. We expect therefore that $\rho_{cl}(E)$ approximates the exact average

density of states to the same degree of accuracy as $\rho_{sc}(E)$ approximates the exact density of states. We must investigate the derivation of the Gutzwiller trace formula to better understand the accuracy of CTF.

The derivation of the trace formula involves a stationary phase approximation to the exact Feynman path integral. Because the stationary phase approximation is the first term in an asymptotic expansion, an estimate for the error involved is not directly accessible. What we can say is that the approximation is better for quantum mechanical systems that behave more classically, that is with more localized particles, but it is never very bad. For higher energies the semiclassical energy levels must become better approximations, since the action is larger making the expansion parameter ($\hbar$) relatively smaller. The error in the staircase function is only picked up at low energies leading to a small constant error at higher energies. It is possible to determine how well CTF will do by looking at the localization of the particles in the ground state. For strongly interacting highly correlated systems the particles are more localized meaning CTF should work better for these systems.

If CTF gives insufficient accuracy it is possible to improve upon the semiclassical part of the approximation. It is possible to increase the accuracy of $\rho_{cl}(E)$ by adding higher order terms to the $\hbar$ expansion of the average density of states. Doing this will ensure that the integral of the resulting approximation to the average density of states goes through the exact staircase function.

4.4 Behavior of $\mathcal{N}$

In order to understand how $\mathcal{N}$ behaves for a large range of realistic interaction strengths we have analyzed systems with Gaussian interactions. Gaussian interactions are more realistic than the other types of interactions so far considered, but at the same time they are easier to deal with than interactions found in real systems such as Coulomb interactions because they are not singular at any point and many integrals involving them can be carried out analytically.

We consider systems with Hamiltonian

$$\hat{H} = \sum_{i=1}^{N} -\frac{1}{2}\nabla_i^2 + \frac{1}{2}\mathbf{x}_i^2 + \sum_{i<j}^{N} \alpha e^{-1/2(\mathbf{x}_i - \mathbf{x}_j)} \tag{4.101}$$

We want to know the behavior of $\mathcal{N}$ over an entire range of interactions strengths from weakly interacting systems, which means weakly correlated particles, to very strongly interacting systems, which means strongly correlated particles (approaching the strictly correlated limit as we discuss below). Therefore we need to consider the entire range of intereaction strengths, α from 0 to ∞.

In order to solve this system exactly we diagonalized the Hamiltonian numerically. We started with a basis of the eigenstates of the external potential. The external potential in 4.101 is harmonic, so the basis states we used were the tensor product of single particle harmonic oscillator states. The integrals for the Gaussian interactions are able to be done analytically but even with the increase in efficiency due to symmetrization as discussed in section 5.3, the diagonalization failed to give correct results for strong interactions.

The failure is due to the fact that for strong interactions the particles are strongly

correlated. Basis states made up of the tensor product of single particle states are necessarily uncorrelated. For tensor products of eignestates of the external potential, it is difficult to build up large correlations using linear combinations of these states. This is because most of the probability density is located around the center of the external harmonic potential. It takes very high states before the probablity density is able to move away from the center of the potential. However for strong interactions, it is possible to cause large correlations in the particles. For example one particle could be far from the center on one side of the external potential and another particle could be far from the center on the other side. If the interaction is repulsive and strong even at low energies, this type of state is possible. So we need to use a basis that would allow a wavefunction with particles localized on opposite sides of the potential more easily.

We use a distributed Gaussian (DG) basis for this purpose [31]. The basis functions for an N particle distributed Gaussian basis are of the form

$$\phi_{\beta,\vec{d}}(\vec{x}) = \exp\left(\frac{\beta}{2}\sum_{i}^{N}(x_i - d_i)^2\right) \tag{4.102}$$

This is just an N dimensional Gaussian centered at $\vec{d} = (d_1, \cdots, d_N)$ with a term specifying the width, β, that is equal to one over the variance. It is clear from 4.102 that the distributed Gaussian basis easily will allow for strongly correlated wavefunction since the linear combination of just two basis functions would be highly correlated if the two basis functions are localized far from one another.

The choice of β and $\vec{d}$ are important for the basis to work efficiently. It is possible to choose different β, but to keep things simple we only use a single width. This is all that is necessary because a sum of Gaussians with proper width and spacing can

approximate any function if the spacing is not too large. The relationship between β and $\vec{d}$ is an important one to get right however. If the Gaussians are too narrow relative to the spacings then they do not overlap very much and linear combinations of them cannot properly approximate arbitrary functions. If the width is too wide relative to the spacing then linear combinations of the basis functions cannot change very rapidly. This is again bad for the ability of the Gaussians to approximate arbitrary functions. The key is to get the relationship to be between these two extremes. The optimal point is near when the sums of the Gaussians becomes constant. If they are too narrow the sum will be wavy (see Figure 4.4) if they are too wide the sum will still be constant. So the best width relative to the spacing is at the width-spacing relationship that is just at this transition from a wavy sum to a constant sum. In order to have a good idea about this optimal relationship we plotted the sums of Gaussians with certain spacing and plotted the optimal width β as measured by the above criteria for a certain spacing Δ. We then did a simple quadratic fit because the data was clearly quadratic giving

$$\beta = .27 - .55\Delta + 1.26\Delta^2 \tag{4.103}$$

There is probably an elegant derivation for the actual optimal relationship between β and Δ but this served well for our purposes. (I'd really like to think some more about this some, but I really need to keep writing. If you have some ideas about this shoot me an e-mail.)

The result from this study for $\mathcal{N}$ is shown in Figure 4.5. For low interaction strengths, the order of the states is what one could have predicted using first order perturbation theory. For large interaction strengths the situation is more interesting.

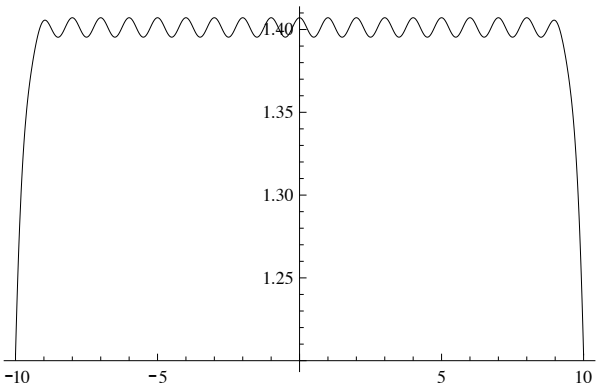

Figure 4.4: The sum of Gaussians spaced by one unit on the x-axis with slightly too narrow widths for the purposes of the DG basis. With slightly larger widths they would add up to be approximately constant and linear combinations would better be able to describe arbitrary functions.

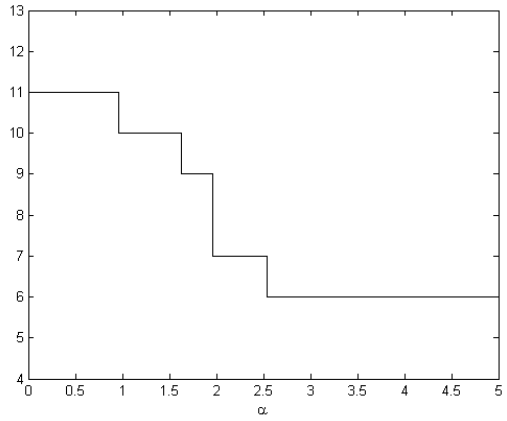

Figure 4.5: The behavior of $\mathcal{N}$ over the entire range of interactions strengths for three particles with Gaussian interactions. We studied systems with much stronger interactions but the $3! = 6$ limit extends to infinite interactions strengths as discussed in the text.

$\mathcal{N}$ reaches an asymptotic value for large enough interaction strengths. This value is just $N!$. This also could have been predicted by considering the strictly correlated limit [32]. The strictly correlated limit is essentially the limit of $\alpha \to \infty$. In this limit the kinetic energy term becomes neglible and so the ground state wavefunction is a delta function at the classical equilibrium postion, the position that minimizes the classical energy. If there is more than one position of equivalent energy such as in two or higher dimensions, the wavefunction is an average of delta functions at these points. Since a wavefunction made up of delta functions has no extent, it does not matter if the delta function carries a positive or negative sign in front of it. That means that states of all symmetries are equivalent in energy. In one dimension for example there are $N!$ possible places that you could place the delta function corresponding to the $N!$ permutations of N particles. The symmetrized wavefunctions are built from adding and subtracting these delta functions, but since the delta function has no extent, there is no overlap between different delta functions, and all of the ground state wavefunctions of each symmetry have the same energy.

When α is considered large, but not infinite, the delta functions that make up the ground state wavefunction resemble strongly peaked Gaussians. The extent of the wavefunctions leads to an energy level splitting because there is now some overlap to the functions being added and subtraced to form functions of the correct symmetry. The ordering of the states can be predicted using the same reasoning from [30]. States with more nodes are higher in energy and states with higher symmetry have fewer nodes. Out of the $N!$ degenerate states for $\alpha \to \infty$, the totally antisymmetric state is going to be the state with the most nodes for finite α and it is therefore the state

with the most energy out of these newly nondegenerate $N!$ states. By this reasoning it is clear that $\mathcal{N} = N!$ for large enough α.

The investigation of these two limits of $\mathcal{N}$ leads to clear ways to proceed with approximation for script $\mathcal{N}$.

4.5 Perturbation Theory for $\mathcal{N}$

Perhaps the most straightforward way of approximating $\mathcal{N}$ is by perturbation theory. It is trivial to find the number of energy levels below the first totally antisymmetric state for no interactions for most systems. If the interactions are treated as a perturbation, then the order of states can be approximated by perturbation theory. We mean just standard first order perturbation theory. That is for an N particle Hamiltonian with interactions such as

$$\hat{H} = \sum_{i=1}^{N} -\frac{1}{2}\nabla_i^2 + V_{\text{ext}}(\mathbf{x}_i) + \sum_{i<j}^{N} V_{ij}(\mathbf{x}_i - \mathbf{x}_j) \tag{4.104}$$

We take the perturbation to be the interactions

$$\hat{W} = \sum_{i<j}^{N} V_{ij}(\mathbf{x}_i - \mathbf{x}_j) \tag{4.105}$$

and we take $\hat{H}_0$ as the kinetic energy and external potential

$$\hat{H}_0 = \sum_{i=1}^{N} -\frac{1}{2}\nabla_i^2 + V_{\text{ext}}(\mathbf{x}_i) \tag{4.106}$$

Following the procedure of first order perturbation theory we find the unperturbed states $|\phi_n^0\rangle$

$$\hat{H}_0|\phi_n^0\rangle = E_n^0|\phi_n^0\rangle \tag{4.107}$$

and the first order energies

$$E_n^1 = \langle \phi_n^0 | \hat{W} | \phi_n^0 \rangle \tag{4.108}$$

The energies are then approximated as $E_n \approx E_n^0 + E_n^1$. If the $|\phi_n^0\rangle$s are properly symmetrized (see Section 5.3), then each E_n will have an associated symmetry. $\mathcal{N}$ is then found by counting the number of levels, E_n, below the lowest energy corresponding to a totally antisymmetric wavefunction.

This works well for weakly interacting systems, even though pertubation theory doesn't take into account avoided crossings. It is only when energy levels cross the first totally antisymmetric state when they should not have that an error is introduced. The order of energy levels both below and above this state doesn't matter. Because for low energies the spurious crossings (those that wouldn't have occured with a higher level of accuracy) don't occur, the approximation works very well. In fact before the interaction strength at which the levels start to cross $\mathcal{N}$ is exact in this approximation. Figure 4.6 shows how the results are good for weak interactions

We are concerned with strongly interacting systems however, because there are many methods that are able to approximate ground state energies for weakly interacting systems, and CTF has the potential to do well for strongly interacting systems. Of course for the case of strong interactions, which corresponds to a large perturbation $\hat{W}$, the results from first order perturbation theory are essentially worthless. Taking into account the fact that we need an approximation for $\mathcal{N}$ for systems with strong interactions in order for CTF to work for strongly correlated systems, we have developed an asymptotic expansion, analogous to first order perturbation theory, from the limit of interactions of infinite strength.

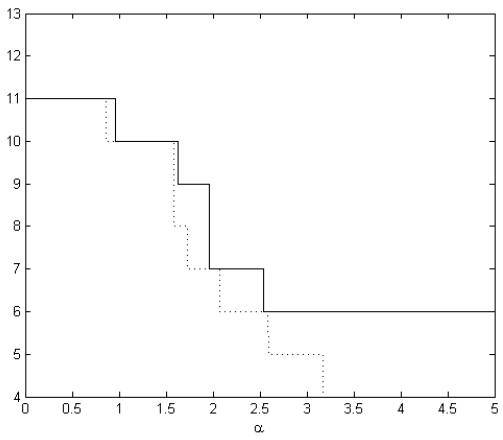

Figure 4.6: The approximation for $\mathcal{N}$ from perturbation theory. As expected it works well for weak interactions but fails for strong interactions.

4.6 Harmonic Approximation for $\mathcal{N}$

It is possible to estimate $\mathcal{N}$ in the strongly correlated limit in an analogous way to perturbation theory, which we discussed for the weakly correlated limit in the previous section. As discussed in section 4.4, in the limit of infinite correlation the ground state is formed by delta functions at the classical equilibrium points. Near the limit the wavefunction is sharply peaked around the classical equilibrium point. It is possible therefore to expand the potential about this point to second order. This leads to a harmonic approximation that is accurate for large α. The details are relatively straightforward, but we will discuss them here.

The first step is to find the classical equilibrium point which is $\vec{\nabla}V = 0$, where V is the total potential. For a generic system of N particles each in one dimension (higher dimensional systems are more complicated and will be discussed next) with

an external potential and interactions between the particles we have

$$V = \sum_{i=1}^{N} V_{\text{ext}}(\mathbf{x}_i) + \sum_{i<j}^{N} V_{ij}(\mathbf{x}_i - \mathbf{x}_j) \tag{4.109}$$

For the Gaussian system finding $\vec{\nabla} V = 0$ is straightforward.

Next the potential V is expanded to second order around the equilibrium point, $\vec{d}$, defined by $\vec{\nabla} V(\vec{d}) = 0$. The result is a harmonic potential. It is not in general N decoupled Harmonic oscillators. There will most likely be cross terms that couple the oscillators. So we need to decouple the oscillators with a rotation of the N coordinates. This is done by writing the potential in the form

$$\mathbf{x}^T \mathbf{A} \mathbf{x} + \mathbf{b}^T \mathbf{x} + c \tag{4.110}$$

where $\mathbf{A}$ is a $N \times N$ matrix, both $\mathbf{x}$ and $\mathbf{b}$ are $N \times 1$ column vectors, and c is just a constant (^{T} stands for transpose). Note that $\mathbf{b} = 0$ because the function was expanded about the point that gives $\vec{\nabla} V = 0$. The matrix that diagonalizes $\mathbf{A}$ gives the coordinate rotation that must be done in order to decouple the oscillators. All we really care about however are the frequencies of the decoupled oscillators. We can get these directly from the eigenvalues of $\mathbf{A}$, since the eigenvalues are the force constants.

Note that both the expansion and finding matrix $\mathbf{A}$ can be done at the same time since $\mathbf{A}$ is just the Hessian of the potential evaluated at the equilibrium point.

Once the oscillator frequencies are found finding $\mathcal{N}$ is straightforward. All that is necessary is to build the harmonic oscillator states with the correct frequencies. We call them

$$\psi_{\vec{n}}^{\vec{\omega}}(\vec{x}) = \prod_{i=1}^{N} \psi_{n_i}^{\omega_i}(x_i - d_i) \tag{4.111}$$

where the $\psi_{n_i}^{\omega_i}(x_i)$ are standard harmonic oscillator wavefunctions with an oscillator frequency ω_i and eigenvalue n_i. d_i is the ith component of $\vec{d}$, the equilibrium point.

The zeroth order approximation to the energy is given by the energy of the states $\psi_{\vec{n}}^{\vec{\omega}}$ in the harmonic potential. That is the sum of the eigenenergies typically associated with these states:

$$E_n^0 = \sum_i^N \hbar\omega_i \left(n_i + \frac{1}{2}\right) \tag{4.112}$$

This approximation is not enough to calculate $\mathcal{N}$. Each state is $N!$ fold degenerate meaning that if these states are symmetrized the symmetrized states will all be degenerate.

In order to calculate the first order approximation to the energy, symmetrized harmonic oscillator states must be built up and then the expectation value of the exact hamiltonian must be found for each state. So the first order energy of symmetry character s can be written as

$$E_n^s = \langle \psi_{\vec{n}}^{\vec{\omega}} | H P_s | \psi_{\vec{n}}^{\vec{\omega}} \rangle \tag{4.113}$$

where H is the full Hamiltonian and P_s is the projector onto symmetry character s (see Section 5.3).

As discussed above this method works well for large α. Figure 4.7 shows how this method works for three particles.

When looking at the wavefunctions, from the strongly correlated regime, the strength of the harmonic approximation stands out. Figure 4.8 shows how the correlated wavefunctions are made of projections onto symmetry characters of displaced harmonic oscillator states.

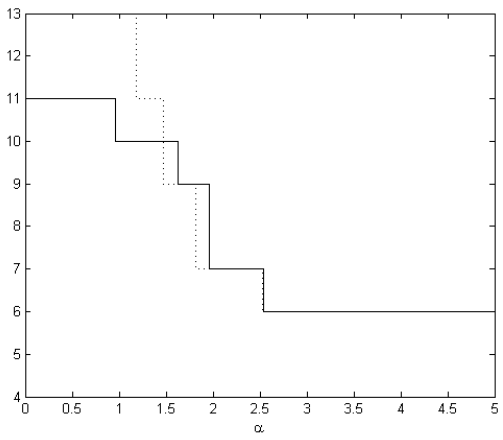

Figure 4.7: The harmonic approximation works well for strong interactions as expected.

4.7 Finding $\mathcal{N}$

The perturbation theory and harmonic approximation methods work best in different regimes. Using both pertubation theory and the harmonic approximation together therefore could be expected to cover the entire range of interaction strength. We expect it should be possible to interpolate between these two regimes to form an approximation for $\mathcal{N}$ over the whole range of interaction strengths. Figure 4.9 shows that together the perturbation and harmonic approximation give quite a good approximation for $\mathcal{N}$.

4.8 Particles in Higher Dimensions

The methods discussed in the previous section are directly applicable to higher dimensions. Working in higher dimensions leads to some problems and subtleties, however, that will be discussed in this section.

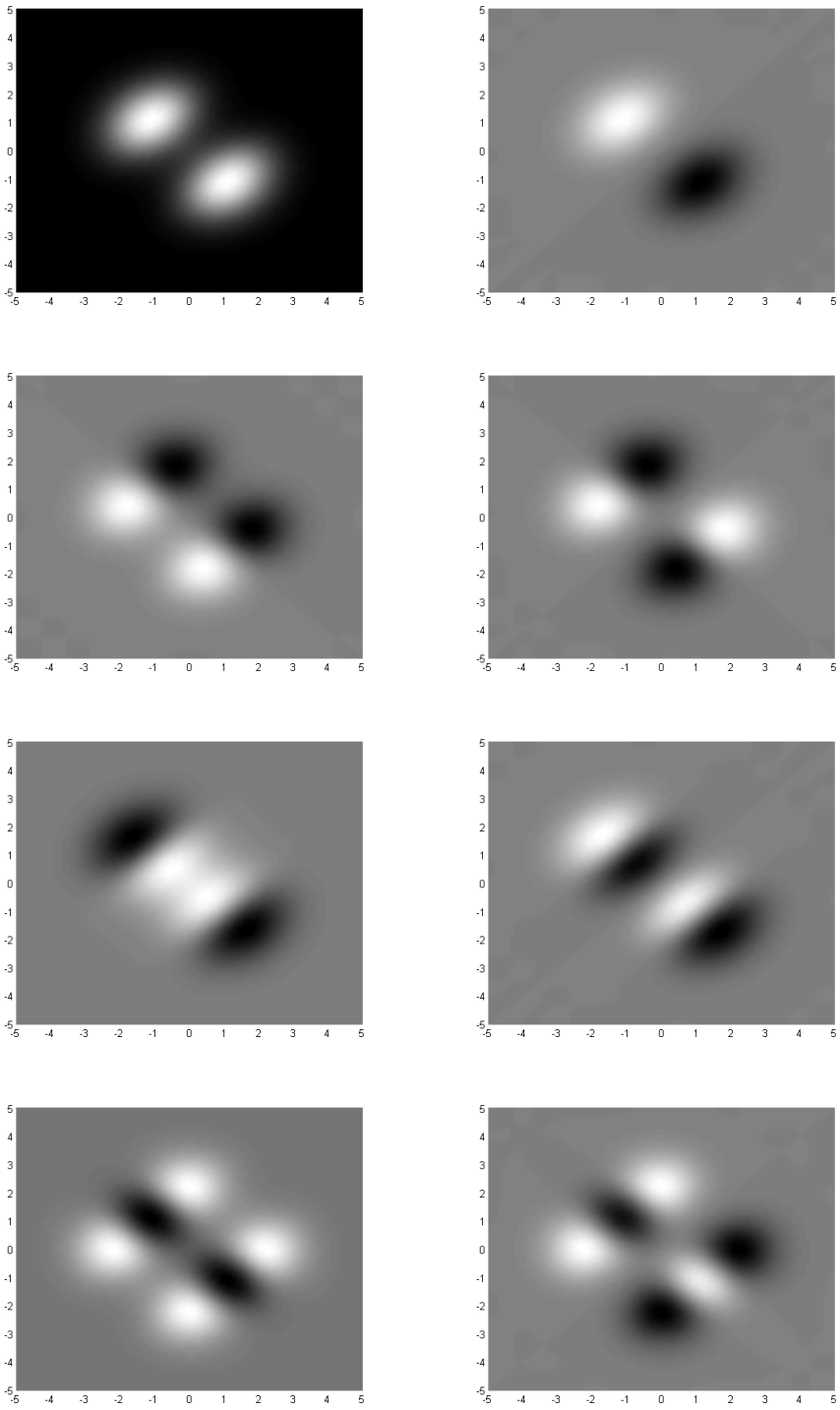

Figure 4.8: Exact wavefunctions for the first eight states of two particles with a strong Gaussian repulsion. The strong interaction forces the particle away from the center of the external potential, and the result is displaced harmonic oscillator type modes that are either symmetrized (left) or antisymmetrized (right) with respect to particle exchange.

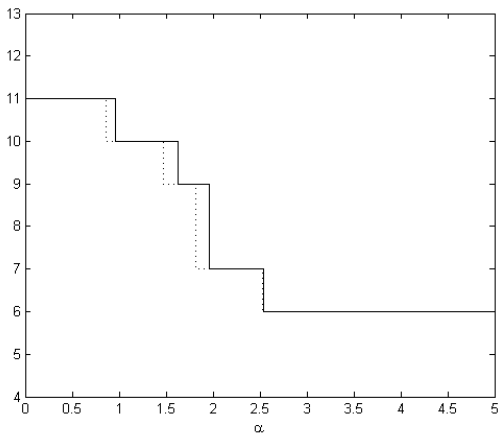

Figure 4.9: If the harmonic expansion and perturbation approximations for N are combined good results can be obtained over the entire range of interaction.

The distributed Gaussian basis works great for the entire range of interactions as discussed in section 4.4. But the DG basis is not optimized for the problem at all. It would work just as well for any potential. This is a good thing, but the trade off is in terms of computation time. Having Gaussians all over coordinate space as part of the basis means that it is easy to build up highly correlated wavefunctions, but at the same time, many of them will not be used. For higher dimensions this starts to be a problem since the basis size grows exponentially with the number of dimensions. One possible solution would be to only have the Gaussians where probablity density is expected. This requires knowing something about the solutions beforehand however.

We take another approach to find the $\mathcal{N}$ exactly in higher dimensions. Following the ideas in Sections 4.5 and 4.6 we break the range of interaction down into two regimes and use a basis that works in each regime. Using both bases at the same time should work well over the entire range of interactions.

We proceed very closely to the approximations in Sections 4.5 and 4.6. In the weak

interaction regime the basis we use is simply a truncated version of the eigenstates of the external potential H_0 from

$$H_0 = \sum_{i=1}^{N} -\frac{1}{2}\nabla_i^2 + V_{\text{ext}}(\mathbf{x}_i) \tag{4.114}$$

where the full Hamiltonian is

$$H = H_0 + \sum_{i<j}^{N} V_{ij}(\mathbf{x}_i - \mathbf{x}_j) \tag{4.115}$$

This is using the wavefunctions from zeroth order perturbation theory as a basis and works well for weak interactions independent of dimension.

For the strongly correlated regime we can use the zeroth order wavefunctions from the harmonic approximation. That is the $\psi_{\vec{n}}^{\vec{\omega}}$ from (4.116). For one dimension this is straightforward, but degeneracies in higher dimensions lead to some subtleties that we will look at next.

For either basis, we can symmetrize it (see Section 5.3) in order to block diagonalize the Hamiltonian and speed up the process of diagonalizing it.

For the Harmonic approximation in higher than one dimension finding the equilibrium point will present a problem for external potentials that are rotationally symmetric as we have been considering (actually the problem persists for any potential that leads to degeneracies in the classical groundstate and rotationally symmetric potentials are probably the easiest of this class to deal with). A rotationally symmetric external potential means the Hamiltonian is the same for any rotation of the entire coordinate system. This results in an infinite number of equivalent classical equilibrium points.

If one were to naively follow the procedure in Section 4.6 in more than one dimension (which of course was the first thing I tried), when diagonalizing the Hessian

matrix at least one of the eigenvalues is zero. The reason is the equilibrium point is not a true minima, but is instead a saddle point. Moving along a coordinate associated with a zero eigenvalue would keep the energy constant.

One possible solution to this degeneracy problem is to rewrite the Hamiltonian in coordinates that make the total angular momentum one of the canonical momenta and then remove that degree of freedom from the Hamiltonian. The Harmonic approximation could then be used on the resulting Hamiltonian. We do not take this approach here mainly because the resulting Hamiltonian is quite messy.

Instead we use a projector approach, and will explain the details for two dimensions. In two dimensions if a minimum position $\vec{d_0}$ for all the particles is found, another equivalent $\vec{d_0}$ can be found by rotating all the coordinates around the z-axis (if the two dimensions for each particle are taken to be in the xy plane). In polar coordinates, if the angle of one of the particles is fixed, a unique equilibrium point can be obtained for the rest of the particles and the radius of the fixed particle. It is therefore possible to use the harmonic approximation with one of the coordinates of the equilibrium point fixed say on the x-axis. This gives a unique equilibrium point $\vec{d_0}$. Although expanding the potential around this point still leads to a zero frequency, the frequency can be chosen arbitrarily, since it won't matter once we do the projection. So it is possible to form harmonic states $\psi^{\vec{\omega}}_{\vec{n}}$ (Now a $2N$ dimensional function)

$$\psi^{\vec{\omega}}_{\vec{n}}(\vec{x}) = \prod_{i=1}^{N} \psi^{\omega_{x\,i},\omega_{y_i}}_{n_{xi},n_{y_i}}(x_i - d_{xi}, y_i - d_{y_i}) \tag{4.116}$$

These states can be used as a basis to diagonalize the Hamiltonian, but it would not be a very good basis because it would not have the same rotational symmetry as the

actual eigenstates.

This can be rectified by forming linear combinations with the correct rotational symmetry. This is done by projecting onto the rotational states m (see Section 5.3). This is done with the projector

$$P_m = \frac{1}{2\pi}\int_0^{2\pi} d\phi\; e^{im\phi}\hat{R}(\phi) \tag{4.117}$$

where $\hat{R}(\phi)$ is the rotation operator that rotates all the coordinates simultaneously by ϕ. (Note that $e^{im\phi}$ are the characters of $\hat{R}(\phi)$ in irreducible representation m).

The new basis becomes $\{P_m|\psi_{\vec{n}}^{\vec{\omega}}\rangle\}$. We also want to project this basis onto the correct permutation symmetry character, but the two projections are independent; we can do that either before or afterward. Projection onto a certain symmetry of S_N works as discussed in Section 5.3, and it is easiest to consider the $|\psi_{\vec{n}}^{\vec{\omega}}\rangle$ as already symmetrized.

The matrix element we are concerned with is therefore

$$\begin{aligned}
\langle\psi_{\vec{n}}^{\vec{\omega}}(\vec{d}_0)|{P_m}^\dagger H P_m|\psi_{\vec{n}}^{\vec{\omega}}(\vec{d}_0)\rangle &= \langle\psi_{\vec{n}}^{\vec{\omega}}(\vec{d}_0)|H P_m|\psi_{\vec{n}}^{\vec{\omega}}(\vec{d}_0)\rangle &(4.118)\\
&= \frac{1}{2\pi}\int_0^{2\pi} d\phi\; e^{im\phi}\langle\psi_{\vec{n}}^{\vec{\omega}}(\vec{d}_0)|H\hat{R}(\phi)|\psi_{\vec{n}}^{\vec{\omega}}(\vec{d}_0)\rangle &(4.119)\\
&= \frac{1}{2\pi}\int_0^{2\pi} d\phi\; e^{im\phi}\langle\psi_{\vec{n}}^{\vec{\omega}}(\vec{d}_0)|H|\psi_{\vec{n}}^{\vec{\omega}}(\vec{d'}_0)\rangle &(4.120)
\end{aligned}$$

where $\vec{d}_0$ is the equilibrium position that the harmonic oscillator state is centered on, $\vec{d'}_0 = \hat{R}^{-1}(\phi)\vec{d}_0$, and we have used the hermitivity of the projector and the general property of projectors that $PP = P$. So the actual integrals that we need to perform are of the form

$$\langle\psi_{\vec{n}}^{\vec{\omega}}(\vec{d}_0)|H|\psi_{\vec{n}}^{\vec{\omega}}(\vec{d'}_0)\rangle \tag{4.121}$$

Even for three particles in two dimensions these integrals are time consuming to do. We have evaluated the integrals in terms of sums of Hermite polynomials in $\vec{d}$ but the sums become nested and even they become resource intensive. The integral over angles also needs to be done in addition to the integral in 4.121. Discretizing the angular integral actually leads to an interesting approximation where the resulting function will be some class in a discrete rotation group C_n rather than the continous rotation group. This is actually the same approximation as going from a continuous fourier transform to a discrete fourier transform (see Chapter 5).

4.9 Conclusion

Adding correlations to the standard Thomas-Fermi approximation makes things more complicated as we've discussed, but it leads to greater accuracy and it also has lead to some interesting questions about how to deal with particle exchange symmetry. Semiclassical methods usually do not have antisymmetry naturally built in because they are based on classical mechanics with its distinguishable particles. It is therefore necessary to bootstrap the antisymmetrization. We do this at an especially late stage in the approximation which allows us to think about the full symmetry of the Hamiltonian in all its grandeur. We use the symmetry to break states up into different symmetry classes and are able to think about the interesting different types of symmetry that exist apart from the comparatively mundane totally symmetric and totally antisymmetric. We follow this thread into the next chapter in which we talk about something that really is central to many-body systems of identical particles: permutation symmetry.

Chapter 5

Permutation Symmetry for Many-Body Systems

5.1 Introduction

Utilization of symmetry properties has a very long history in physics and chemistry. From Noether's Theorem [33] linking symmetries and conservation laws to asigning lines in chemical spectra, a system with some symmetry is not really solved until the results of its symmetry are understood. The first place to start with a difficult problem is to exploit symmetry properties in order to simplify it. For many body systems of identical particles there is always the associated permutation symmetry. Any N-body system of identical particles has symmetries related to the group of permutation transformations called the symmetric group, S_N. Understanding S_N is therefore vital to dealing with many body systems.

For quantum chemical systems the permutation symmetry is usually taken into

account at a very early stage in the calculation. Chemical systems are known to be fermionic and the wavefunction must therefore be totally antisymmetric. This requirement is usually realized by using a single slater determinant. We eschew this common technique in our work (mostly because it is not possible for us to do this directly). We've discussed an alternative way to deal with the symmetrization requirement in the previous chapter. We begin this chapter with a brief review of the symmetry group S_N. Then its applications to many body quantum systems in general and also to the specific problems dealt with herein are discussed.

5.2 Symmetric Group S_N

The symmetric group, S_N, is made up of permutations of N objects. All reorderings of N objects when applied successively are still a reordering so the group is closed. The permutation where all the objects keep their original order is the identity element. So clearly the permutations of N objects forms a group.

As an example consider $N = 3$. We label the objects 1, 2, and 3. We can write down all the group elements as

$$\begin{array}{ll} (123) & (132) \\ (213) & (231) \\ (312) & (321) \end{array} \tag{5.1}$$

The permutation (123) keeps the same order. (213) switches the first two etc. The combination of two permutations through the group multiplication is straightforward. For example (213)(321) means switch the first and third and then switch the first and second resulting in (213). So we have (213)(321) = (213). Note that for N greater

than 2 the group S_N is not commutatitve. Ordering of the permutations matter, therefore, and our notation is to take them from right to left as if they are operators acting on an actual set of objects.

In breaking down the different symmetry classes within S_N the concept of partitions of N particles becomes vital. Partitions of N are ways to break up N into positive integers. So a partition of N is a list of integers that when summed adds up to N. For example for $N = 4$ the possible partitions are

$$(1,1,1,1) \rightarrow 1+1+1+1=4 \tag{5.2}$$

$$(2,1,1) \rightarrow 2+1+1=4 \tag{5.3}$$

$$(2,2) \rightarrow 2+2=4 \tag{5.4}$$

$$(3,1) \rightarrow 3+1=4 \tag{5.5}$$

$$(4) \rightarrow 4=4 \tag{5.6}$$

$$\tag{5.7}$$

Standard notation is to write the partition so that the parts (the integers in the sum) are in decreasing order.

It is useful to have a visual representation for partitions. Young tableaux (sometimes called Young diagrams) are arrays of boxes that represent different partitions of N. The simplest way to write down certain partition is to write down columns of boxes of each part in the partition. For example for $(3,2,1,1)$, which is a partition of 7 the associated Young tableau $Y(3,2,1,1)$ is made up of a column of 3 boxes and then a column of 2 boxes and then two columns of one box each as seen in figure 5.1.

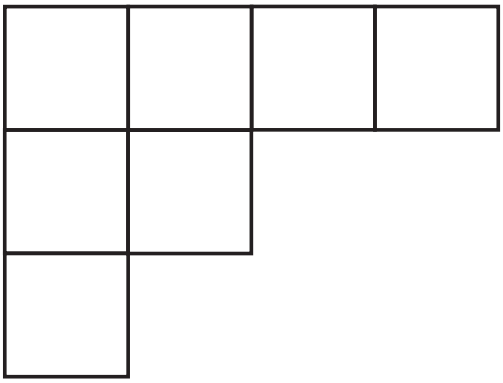

Figure 5.1: Young tableau corresponding to partition $(3, 2, 1, 1)$

The usefulness of the partitions and Young tableau is to characterize the symmetry classes of S_N. For example for (wave)functions in N variables each partition corresponds to a type of symmetry for that function. The purely vertical column for example corresponds to functions that are totally antisymmetric in the variables and the horizontal column corresponds to functions that are totally symmetric. It is possible to fill the Young tableaux with the numbers from 1 to N to make this idea clearer.

For example the Young Tableau in figure 5.4 would correspond to a totally antisymmetric wavefunction $\psi(x_1, x_2, x_3) = -\psi(x_2, x_1, x_3)$ and $\psi(x_1, x_2, x_3) = -\psi(x_3, x_1, x_2)$. (Note: Some references switch whether vertical columns correspond to antisymmetrization or symmetrization.) The Young Tableau in figure 5.3 could correspond to a wavefunction that is partially antisymmetric. That is $\psi(x_1, x_2, x_3) = -\psi(x_2, x_1, x_3)$

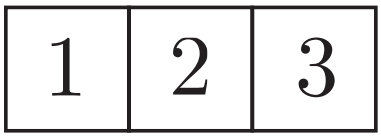

Figure 5.2: Totally symmetric

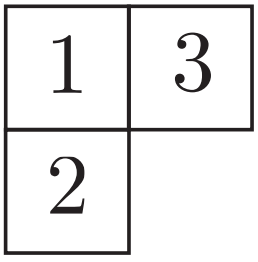

Figure 5.3: Partially antisymmetric

Figure 5.4: Totally antisymmetric

since 1 and 2 are in the same column, but switching the other variables does not lead to the same function or the same function with a negative sign.

To complete the example for $N = 3$ the Young Tableau in figure 5.2 corresponds to a totally symmetric wavefunction $\psi(x_1, x_2, x_3) = \psi(x_2, x_1, x_3)$ and $\psi(x_1, x_2, x_3) = \psi(x_3, x_1, x_2)$.

Another way to write permutations that will prove useful is the cycle notation. The cycle notation takes into account the fact that each number in a permuation necessarily is exchanged with another number which is then either exchanged with a third or exchanged back with the first. This means that the permutation can be written down by noting which objects are exchanged among themselves forming a cycle. For example the permutation (23154) means that 2 is put in the first place and is replaced by 3, which is in turn replaced by 1. So the objects labeled by 1, 2,

and 3 form a cycle because the are all exchanged among themselves: $2 \to 1 \to 3 \to 2$. The 4 and 5 objects are each exchanged with one another. This forms another cycle: $4 \to 5 \to 4$. It is possible therefore to write the partition (23154) in cycle notation by labeling each cycle separately as in $(23154) \to (123)(45)$. In cycle notation, for each cycle each number is replaced by the following number. This notation shows the cycle character of each partition, which will prove useful in determining the projectors onto different symmetry characters.

It should be noted here that permutations, cycles, partitions, and Young tableau are all very closely related. Permutations are the basic group elements of the symmetric group, but cycles, partitions, and Young tableau are really different ways to discuss the same structure in each permutation. Because the number of elements in each cycle must add up to the total number of objects being permuted, N, the partitions of N can be used to label the different types of cycles in S_N. That is why it is possible, as will be discussed next, to label the different symmetry characters by the different partitions since the symmetry characters are basically labeling how something changes under a permutation that can be broken down into a certain set of cycles. Young tableau are really just a graphical representation of the partitions of N, but as we shall see they have additional utility as a record keeping tool.

It is necessary for our purpose to be able to project onto a certain symmetry character of S_N (the same procedure works for any symmetry group). It is possible to build up the projector onto a certain symmetry class using the group table. The projector onto the symmetry class labeled α can be written

$$P_\alpha = \frac{n_\alpha}{g} \sum_j \zeta^\alpha \left(R_j\right)^* \hat{R}_j \tag{5.8}$$

where the sum is over all the elements of the group, $\zeta^{\alpha}(R_j)$ is the group table element associated with j, α, and R_j, and $\hat{R}_j$ is the operator that corresponds with R_j. Also g is the order of the group and n_α is the dimension of the irreducible representation of α.

It is necessary to know the group table to use the formula in 5.8. It is possible to calculate the group table for the symmetric group of any order using the Murnaghan-Nakayama formula. The Murnaghan-Nakayama formula is a recursive formula for the table elements that looks quite complicated, but in practice is not too difficult to use. As such first the formula will be presented and then a simple example will allow its use to become more clear.

The Murnaghan-Nakayama formula is

$$\zeta^{\alpha}(\pi) = \sum_{i,j,h^{\alpha}_{i,j}=k} (-1)^{l^{\alpha}_{i,j}} \zeta^{[\alpha]\backslash R^{\alpha}_{i,j}}(\rho) \tag{5.9}$$

where α is a partition of N, π is a permutation in S_N, ρ is a permutation in S_{N-k} with the same cycle structure as π except for a cycle of length k removed, $h^{\alpha}_{i,j}$ refers to the hook length, $l^{\alpha}_{i,j}$ refers to the leg length of the hook, and $[\alpha]\backslash R^{\alpha}_{i,j}$ is the partition α with the rim removed. Not all of these terms have been defined yet, but they will be presently and their use will become clear with an example.

The hook at some point in a Young tableau is the set of boxes to the left of the current box and down from the box with the current box included. The hook length is equal to the total number of boxes in the hook. For example for the Young tableau in figure 5.5 at the point (i,j)=(2,1) the hook is made up of the boxes with the line through them. The hook length is therefore 7. There is a separate hook for every box in the Young tableau.

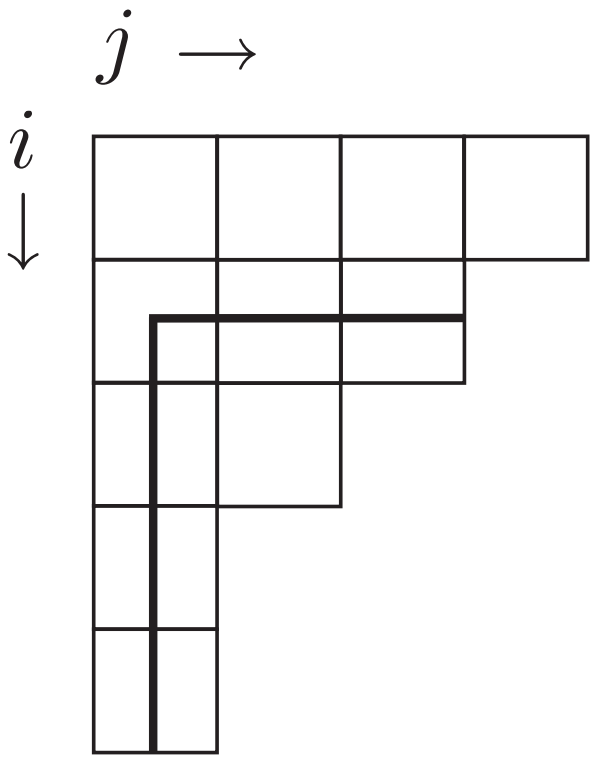

Figure 5.5: Example of a hook

The leg length of the hook is equal to the number of boxes below the corner box in the hook. Using the above example again, the box $(2, 1)$ is the one that the hook is labeled by. This is the corner box in the hook. There are three boxes below this box. Therefore the leg length of the hook in question is 3.

The rim of the hook are all boxes on the edge of the Young tableu between the two ends of the hook. The rim is found by including the two boxes on the end of the hook and all the boxes on a path between the two ends that stays on the edge of the Young tableau. So a procedure to find the rim is as follows. Start at say the bottom end of the hook and include that box in the set that makes up the rim. Now go right if possible and include that box in the rim set. If it is not possible to go right, go up and include that box. Now this procedure of trying to move right and then moving up if that's not possible must be repeated until at the right end of the hook.

Continuing with the example from Figure 5.5 the rim is made up of boxes labeled with an $\times$ in figure 5.6.

Now we have covered enough background into the elaborate art of Young tableaux to understand the Murnaghan-Nakayama formula. We calculate the group table element $\zeta^{(3,3,3)((1234)(56)(789))}$ from S_9 as an example. Note that the partition is written in cycle notation for convenient use with the Murnaghan-Nakayama formula. We can write it in standard permutation notation as $(1234)(56)(789) \rightarrow (234165897)$. In this example we will stick with the cycle notation.

The first step in the formula is to go over all boxes (i, j) in the Young tableau corresponding to partition $(3, 3, 3)$ with hook length of k where k is the length of the cycle that we are going to remove. The largest cycle in $(1234)(56)(789)$ is (1234) and

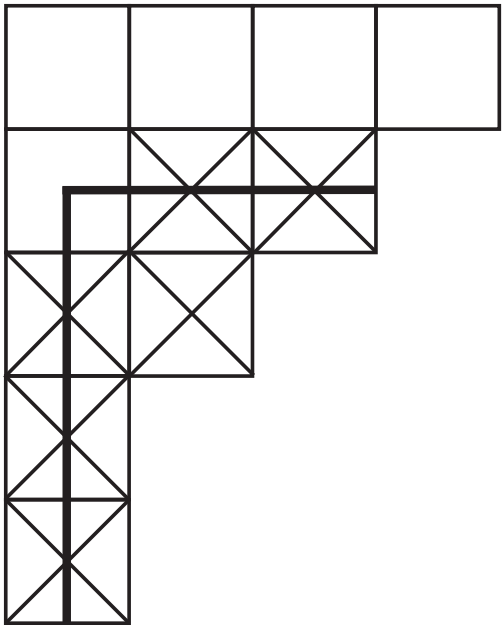

Figure 5.6: The rim associated with the hook is made up of the ×ed boxes.

has length 4. Removing the largest cycle makes subsequent step easier so we will remove that one (although the answer is of course independent of the order that we remove the cycles).

We need to find hook lengths of length $k = 4$. First we draw the Young tableau and look for hooks with hook lengths of 4 (see figure 5.7). In 5.7 we have labeled the two hooks of length 4. Since there are two hooks with $h^{\alpha}_{i,j} = 4$, the sum in 5.9 has two terms.

First we look at the term corresponding to the first hook with corner at $(i, j) = (1, 2)$. The leg length of the first hook is 2. So the the first factor is $(-1)^2 = 1$. The Young table with the rim removed is shown in figure 5.8 This corresponds to the partition $(3, 2)$. So the first term in the sum is $\zeta^{(3,2)}((56)(789))$.

Now we look at the term corresponding to the second hook with corner at $(i, j) =$

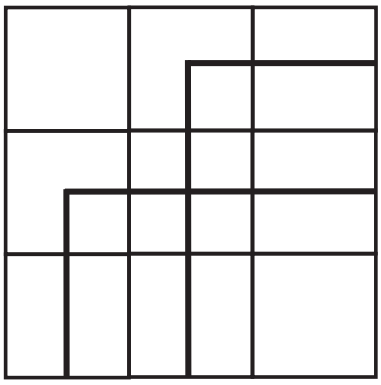

Figure 5.7: Two hooks of length 4

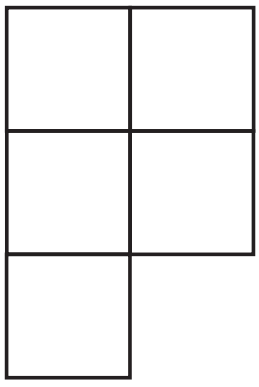

Figure 5.8: Table with the rim removed.

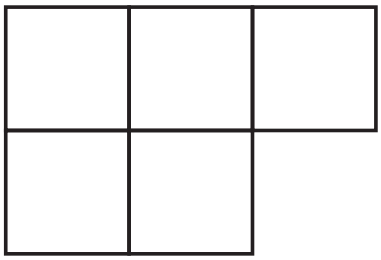

Figure 5.9: The other rim removed

$(2,1)$. The leg length is 1. So there is a $(-1)^1 = -1$ factor. The Young table with the rim removed is shown in figure 5.9. This corresponds to the partition $(2,2,1)$. So the second term in the sum is $-\zeta^{(2,2,1)}((56)(789))$.

Therefore we have

$$\zeta^{(3,3,3)}((1234)(56)(789)) = \zeta^{(3,2)}((56)(789)) - \zeta^{(2,2,1)}((56)(789)) \tag{5.10}$$

Next from each term we remove the cycle of length 3. There is one hook of length 3 in each term. The first term hook is at $(i,j) = (2,1)$ as shown in 5.10. The leg length is 1. The Young tableau with the rim removed is shown in 5.11. The partition associated with this Young tableau is $(1,1)$. So the first term can be written as $-\zeta^{(1,1)}((56))$.

The hook of length 3 from the second term is in figure 5.12. The leg length is 1. The Young tableau with the rim removed is in 5.13. The partition associated with

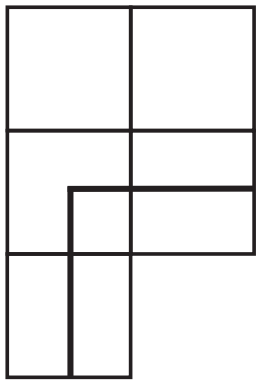

Figure 5.10: Next hook

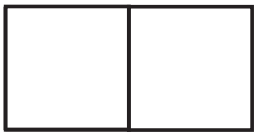

Figure 5.11: Rim removed

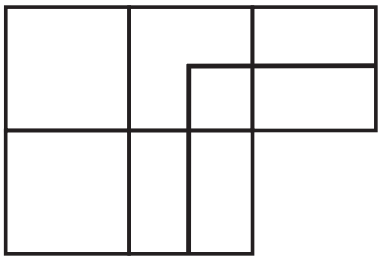

Figure 5.12: Hook of length 3.

this Young tableau is (2). So the second term can be written as $\zeta^{(2)}((56))$.

So far we have

$$\zeta^{(3,3,3)}((1234)(56)(789)) = -\zeta^{(1,1)}((56)) + \zeta^{(2)}((56)) \tag{5.11}$$

There is just one hook of length 2 (only the cycle of length 2 is remaining) for each term. The hook takes up both boxes of the remaining Young table in each term. The hook in the first term has a leg length 0. The second term has a leg length 1. So the second term picks up a negative sign. Once the rim is removed there is no remaining diagram so the group table element becomes

$$\zeta^{(3,3,3)}((1234)(56)(789)) = -\zeta(0) - \zeta(0) \tag{5.12}$$

And $\zeta(0) = 1$ giving

$$\zeta^{(3,3,3)}((1234)(56)(789)) = -2 \tag{5.13}$$

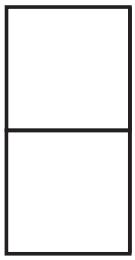

Figure 5.13: Rim removed

Table 5.1: Group table for S_3.

	(1,1,1)	(2,1)	(3)
(1,1,1)	1	1	1
(2,1)	2	0	-1
(3)	1	-1	1

This same procedure can be used to calculate all the group table elements (see [34]).

Using S_3 as an example, if the Murnaghan-Nakayama formula is carried out, the resulting group table is shown in Table 5.2.

Where the vertical partitions correspond to the symmetry classes and the horizontal partitions correspond to the cycle type of the permutation.

As an example of formula 5.8 we find the projector onto totally antisymmetric states for S_3. First it is helpful to group the permutations of S_3 by cycle type. $(1, 1, 1)$

corresponds to three one cycles, which is the identity element (123). $(2,1)$ corresponds to one cycle of length two meaning partitions that exchange two particles but leave the other alone. These permutations are (213), (132), and (321). The remaing partition (3) corresponds to length three cycles, (232) and (312). As discussed above the totally antisymmetric class corresponds to a single vertical column which corresponds to partition (3).

So the projector onto totally antisymmetric states is

$$P_{(3)} = \frac{1}{6}\left((123) - (213) - (132) - (321) + (232) + (312)\right) \tag{5.14}$$

This can of course be calculated from the standard equation for a projector onto totally antisymmetric space that has a positive sign in front of even permutations and a negative sign in front of odd permutations. But the symmetry characters that are not either totally symmetric or totally antisymmetric do not have such simple formulas, and these additional symmetry characters are important for our purposes.

5.3 Symmetrized Bases and Block Diagonal Hamiltonians

An immediate application of the topics discussed in the previous section is increasing the efficiency of diagonalizing the Hamiltonian in some truncated basis by using a symmetry adapted basis. As we will see, the use of such a symmetrized basis, creates a block diagonal Hamiltonian which means that instead of diagonalizing the whole Hamiltonian each block can be diagonalized separately. Diagonalizing the resulting several smaller matrices is more efficient than diagonalizing the original matrix.

Once the symmetrized basis is found it is straightforward to see that the Hamiltonian written in that basis must be block diagonal, but for many-particle bases built from the direct product of states, there are some subtle details that must be worked out. We use S_3 in this section when it is useful to look at a specific example because it is the smallest symmetric group that still has all the important details. First weshow that at the result of using a symmetrized basis is a block diagonal Hamiltonian.

If $|\phi\rangle$ and $|\psi\rangle$ are two vectors from the original basis, and P_α and P_β are projectors onto symmetry class α and β then $P_\alpha|\phi\rangle$ and $P_\beta|\psi\rangle$ are symmetrized basis vectors with the symmetry character associated with α and β respectively (assuming the result of the projection is not zero). Since the Hamiltonian commutes with the projectors (it must since it commutes with each of the group operators) the matrix element between the symmetrized vectors becomes

$$\langle\phi|P_\alpha H P_\beta|\psi\rangle = \langle\phi|H P_\alpha P_\beta|\psi\rangle \tag{5.15}$$

$$= \langle\phi|H P_\alpha|\psi\rangle\delta_{\alpha\beta} \tag{5.16}$$

where the fact that the projectors commute with the Hamiltonian and the general property of projectors, $P_\alpha P_\beta = P_\alpha\delta_{\alpha\beta}$, have been used. Therefore if the projectors are onto different symmetry characters the matrix element is zero. This results in a Hamiltonian made from blocks corresponding to the basis vectors of each symmetry character with the rest of the elements (those between basis vectors of different symmmetry) equal to zero. The matrix written in the symmetrized basis is block diagonal, and each block can now be diagonalized separately.

Usually it is not necessary to complete this block diagonalization because most applications deal with fermions or bosons and therefore only the totally symmetric or

totally antisymmetric blocks are considered. For our purposes, since we are coming from a semiclassical perspective, the classical nature in our methods means that it is necessary to consider states of all symmetries. It is not until a later stage of our calculation that the fermionic antisymmetrization is invoked.

Now we must discuss the details of actually forming a proper symmetrized basis. Since the basis vectors must be linearly independent and span the Hilbert space (truncated Hilbert space in actual applications) the resulting symmetrized basis must also be linearly independent and span the same space. This means that the same number of linearly independent symmetrized basis vectors must be formed from the original basis vectors.

This makes the formation of the symmetrized basis nontrivial. It is not possible to just take the original basis vectors and act with the symmetry projectors on them. This would not give the correct number of vectors. If the original basis has M vectors and there are S different symmetry classes then the total number of possible symmetrized vectors using this naive method is $M \times S$ which is obviously too many. When operated on by a projector some of the basis vectors give zero. So not all of the $M \times S$ possible vectors exist, but there are still more than M vectors because many of them are linearly dependent. In fact all but M of them must be linearly dependent. So one way to form the symmetrized basis is to generate all of the possible symmetrized basis vectors and then keep only M linearly independent ones. This is a lot more work than is necessary. Instead we could determine which vectors from the original basis we need to use to form the M symmetrized basis vectors.

We now discuss this problem of determining which vectors to use and the formation

of the symmetrized basis. First we must determine how many linearly independent vectors of each symmetry type there can be for a certain truncated basis. Since the total number of basis vectors must be the same for the unsymmetrized and symmetrized bases we can check whether the number for each symmetry is correct by adding them all up.

There are a few ways to determine the correct number of basis vectors for each symmetry character. One of the best ways is to first note that most symmetry classes in S_N can be further subdivided by symmetrizing the remaining $N-1$ particles. So the symmetry classes in S_N can be subdivided by using the symmetry classes of S_{N-1} (a subgroup of S_N). This can be done using projectors, but it is also helpful to see pictorally using Young Tableau.

We look at the S_3 example first using projectors. There are three symmetry classes for S_3 corresponding to the partitions $(1,1,1)$, $(2,1)$, and (3). We label the projectors onto these symmetry classes $S^{[3]}$, $N^{[3]}$, and $A^{[3]}$ respectively (standing for symmetric, antisymmetric, and neither). The superscript is noting that these projectors work in S_3.

The totally symmetric and antisymmetric projectors cannot be further subdivided because any two particles picked out of the three are already symmetric or antisymmetric under exchange. For $N^{[3]}$ however it is possible to assign a symmetry character to two of the particles using the subgroup S_{N-1} (it can be any two particles depending on how we pick the operators). We follow the convention established above by labeling the projector associated with $(1,1)$, $S^{[2]}$ and the projector associated with (2), $A^{[2]}$.

Next we write the projector $N^{[3]}$ as

$$N^{[3]} = N^{[3]}\hat{1} \tag{5.17}$$

$$= N^{[3]}\left(S^{[2]} + A^{[2]}\right) \tag{5.18}$$

$$= N^{[3]}S^{[2]} + N^{[3]}A^{[2]} \tag{5.19}$$

So we have split the $N^{[3]}$ space into two different spaces. And if we symmetrize the basis using $N^{[3]}S^{[2]}$ and $N^{[3]}A^{[2]}$ rather than just $N^{[3]}$ the $N^{[3]}$ block in the Hamiltonian is split into two blocks since the two new projectors in S_2 are projecting into different spaces that don't overlap (that is $N^{[3]}S^{[2]}N^{[3]}A^{[2]} = 0$).

The Young tableau are extremely useful here as a book keeping tool for higher order symmetric groups. In order to see which symmetry classes from the subgroup the full symmetry class can be split into, it is necessary to remove boxes from the original Young tableau from S_N such that a new Young tableau in S_{N-1} is formed. This leads to a tree of Young tableau along the subgroup chain from S_N to S_2. For S_3 the Young tableau tree (also called Young's lattice) is shown in figure 5.14

It is helpful to also see the larger tree for S_4. In analogy with S_3 we label the projectors associated with the partitions as $(4) \to S^{[4]}$, $(2,1,1) \to N_a^{[4]}$, $(2,2) \to N_b^{[4]}$, $(3,1) \to N_c^{[4]}$, and $(4) \to A^{[4]}$. The Young's lattice for S_4 is shown in figure 5.15.

Note that this pictoral method shows when projectors are zero without having to carry out the projector multiplication. For example in the case of S_4 the projector $N_a^{[4]}$ could be subdivided using S_3 a total of three times:

$$N_a^{[4]} = N_a^{[4]}\hat{1} \tag{5.20}$$

$$= N_a^{[4]}\left(S^{[3]} + N^{[3]} + A^{[3]}\right) \tag{5.21}$$

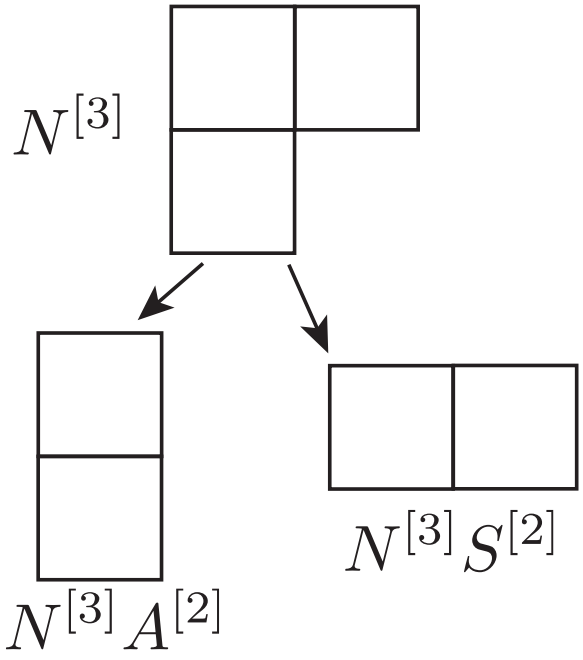

Figure 5.14: Young's lattice for S_3

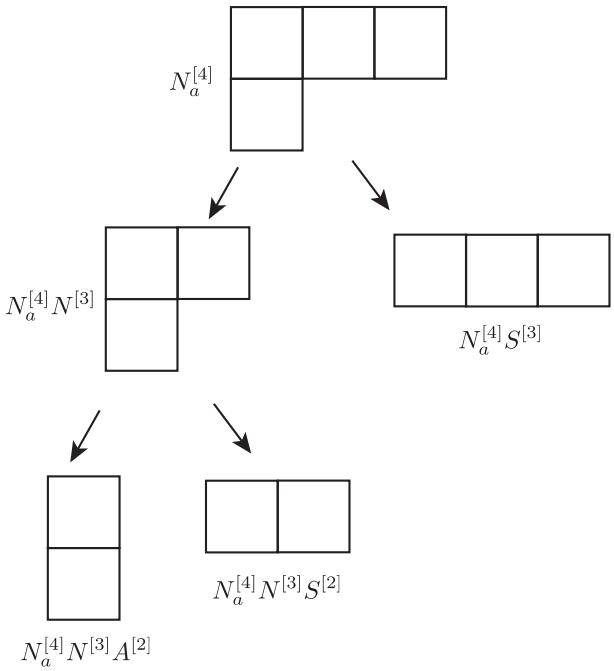

Figure 5.15: Young's lattice for S_4

$$= \quad N_a^{[4]} S^{[3]} + N_a^{[4]} N^{[3]} + N_a^{[4]} A^{[3]} \tag{5.22}$$

However $N_a^{[4]} A^{[3]} = 0$. So really we have

$$N_a^{[4]} \quad = \quad N_a^{[4]} S^{[3]} + N_a^{[4]} N^{[3]} \tag{5.23}$$

This can be seen graphically in the Young tableau notation because in order to have three particles all antisymmetric with respect to one another, they need to correspond to a column of three boxes. Because the Young tableau corresponding to $N_a^{[4]}$ does not have a column of three boxes this can't be done. The pictoral method for splitting up the projectors along the subgroup chain takes this into account.

Now we need to determine for orignal bases of interest how many linearly independent basis vectors of each symmetry type there are. It is again possible to use the Young tableau to make this process easier. For most applications the original basis consists of a tensor product of single particle states. For this type of original basis all that needs to be done to determine the correct number of basis vectors of each symmetry is to fill the corresponding Young tableau with the symbols for the single particle states in such a way that they are ordered across each row and down each column. The order is important because changing the order of symbols in a row or column does not result in a linearly independent vector since the rows and columns correspond to particles that are already symmetrized or antisymmetrized.

We first use S_3 as an example. For $N = 3$ there are three types of initial basis vectors. All the single particle states could be different: $|\alpha\beta\gamma\rangle = \phi_\alpha(x_1)\phi_\beta(x_2)\phi_\gamma(x_3)$. Two of the single particle states could be different: $|\alpha\alpha\beta\rangle = \phi_\alpha(x_1)\phi_\alpha(x_2)\phi_\beta(x_3)$. All the single particle states could be the same: $|\alpha\alpha\alpha\rangle = \phi_\alpha(x_1)\phi_\alpha(x_2)\phi_\alpha(x_3)$.

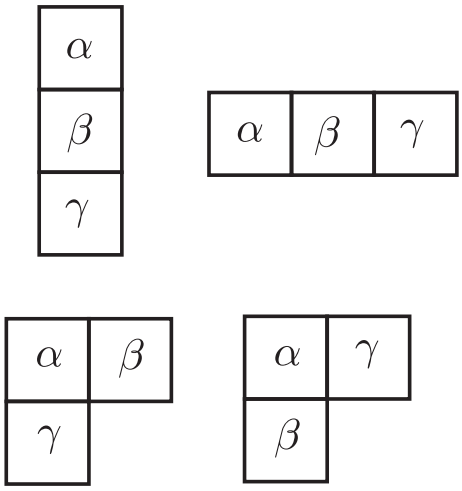

Figure 5.16: Ways to fill S_3 Young tableaux with three distinct particle labels.

For $|\alpha\beta\gamma\rangle$ the degeneracy is $3! = 6$, so we need to make 6 symmetrized vectors. The order that we assign to the symbols for the purpose of using the Young tableau technique is $\alpha < \beta < \gamma$. There is only one way to fill the tableau corresponding to totally symmetric and totally antisymmetric states (see Figure 5.16). There are two ways to fill each of the two other types of states, $N^{[3]}S^{[2]}$ and $N^{[3]}A^{[2]}$. So the 6 degenerate $|\alpha\beta\gamma\rangle$ states are split into 1 totally antisymmetric state, 1 totally symmetric state, 2 states in $N^{[3]}S^{[2]}$, and 2 states in $N^{[3]}A^{[2]}$.

For $|\alpha\alpha\beta\rangle$ the degeneracy is $3!/2! = 3$, so we need to make 3 symmetrized vectors. The order that we assign to the symbols for the purpose of using the Young tableau technique is $\alpha = \alpha < \beta$. It is not possible to fill the tableau corresponding to totally antisymmetric states because that would result in two of the same symbol in one column, which is not possible because columns stand for antisymmetrized particles.

There is one way to fill each of the other types of states, $N^{[3]}S^{[2]}$, $N^{[3]}A^{[2]}$, and $S^{[3]}$. So the 3 degenerate $|\alpha\alpha\beta\rangle$ states are split into 1 totally symmetric state, 1 state in $N^{[3]}S^{[2]}$, and 1 state in $N^{[3]}A^{[2]}$.

For $|\alpha\alpha\alpha\rangle$ the degeneracy is $3!/3! = 1$, so we need to make 1 symmetrized vector. It is only possible to fill the tableau corresponding to totally symmetric states because otherwise it would result in two of the same symbol in one column. So there is one way to fill the totally symmetric state. The single $|\alpha\alpha\alpha\rangle$ states becomes 1 totally symmetric state.

Now that we've determined how the original symmetry vectors are grouped into the new symmetric vectors it is only necessary to form the correct number of linearly independent symmetrized basis vectors. To do that just take the correct number of degenerate vectors and act with the appropriate projector. In order to make sure both vectors in each of the N symmetries is linearly independent the two states that are symmetrized for $N^{[3]}S^{[2]}$ or antisymmetrized for $N^{[3]}A^{[2]}$ should be different. That is if the S_{N-1} subgroup is chosen to be the first and second particle, two vectors that would have to produce linearly independent symmetrized vectors are $|\alpha\beta\gamma\rangle$ and $|\alpha\gamma\beta\rangle$. Because the first two particles are symmetrized, $|\alpha\beta\gamma\rangle$ and $|\beta\alpha\gamma\rangle$ would lead to the same symmetrized vector.

It proves useful to know the total number of symmetrized basis vector of each symmetry given an original basis built from the tensor product of p single particle states. For N particles, the total number of unsymmetrized basis vectors formed from the p single particle states is p^N. We want to know how these p^N states are split between the different symmetry characters. This is useful because it allows for the

preallocation of memory for the symmetrized basis, which allows for more efficient computations.

The best way to determine the total number of symmetrized vectors for each symmetry again uses the Young tableau. The total number of symmetrized vectors is equal to the number of ways that the Young tableau can be filled with the p states with the labels increasing across the row and down the column.

The reason this works out is as follows. Across a row the same state can be repeated. For the first box there are p ways to fill it. The second box has $(p+1)$ ways to fill it, and we must divide the total for both boxes by 2 to take into account that we only keep one possible ordering. This number, $p+1$, comes from the fact that we can fill the second box with any of the ps as long as we divide by two since we can only count one order. However that does not take into account having the same p in both boxes properly. For those Young tableau there is only one whereas the other combinations have two. To fix this we need to add one to the number of ps that can go in the second box. This additional one corresponds to another way of having the same p as in the first box. This doubles the number of tableau with the same p in the first and second box, which gives the correct number when divided by two. By similar reasoning the third box would have $(p+2)$ possible ways to fill it and we need to divide the total number of ways by 3!. So a three box row Young tableau has $p(p+1)(p+2)/3!$ ways of filling it.

When filling down a column the number of possible ways to fill the next box is one less than the number of ways to fill the previous box because the same p cannot be used twice in a column. Again the total number of ways to fill the tableau must

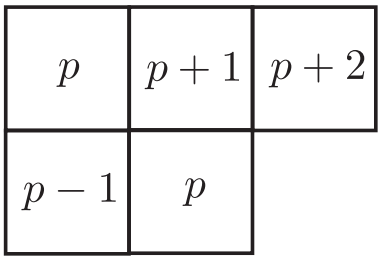

Figure 5.17: Using the Young tableau to determine the number of basis vectors

be divided by $N!$ to take into account only one ordering should be counted.

So in order to determine the number of basis vectors in general, fill the Young tableau with numbers starting with p in the upper left corner. Move down and across increasing the number in the previous box by 1 if moving across and decreasing it by one if moving down. Do this until the whole tableau is filled. The total number of states of that symmetry is the product of the numbers in the tableau times the number of subgroups for that symmetry divided by $N!$. See figure 5.17 for a pictoral representation for how this works.

5.4 Symmetrized FFT

When considering wavepacket methods for the calculation of $\mathcal{N}$ (see Section 4.7) the idea of exploiting the symmetry in the problem to make the wavepacket dynamics

more efficient arises naturally. If the wavepacket dynamics are done using the split operator method, which requires a Fourier transformation of the wavepacket back and forth between coordinate space and momentum space, a symmetrized fast Fourier transform (FFT) would prove useful eliminating elements that become unnecessary because of the symmetry. In this section we develop this idea. The theory is somewhat incomplete, but we present ideas for further study. The usual way to handle symmetry when using Fourier transformation is to use a reduced space called the irreducible Brillouin zone. The idea of symmetrized FFT would be another way of making efficiency gains due to symmetry. This idea has been implemented very recently for spherical symmetries [35],[36], meaning it is most likely an active area of research. We are more interested in geometrical and especially permutation symmetry.

The general idea of a symmetrized fast Fourier transform starts with understanding how a symmetrized Fourier transform would work. This is relatively straightforward and follows upon ideas discussed in the previous section. Next we need to determine the best way to discretize the problem in order to develop a symmetrized discrete Fourier transform. Finally, the last step, which is the hardest, is to determine the fastest possible way to sum over the discrete points in order to bring the discrete Fourier transform onto the level of standard fast Fourier transforms. FFTs are so efficient that it may be better to use an unsymmetrized FFT than to use a symmetrized discrete Fourier transform that does not have as efficient a summation scheme.

Firt we discuss symmetrization of a continous Fourier transform. The Fourier

transformation of $f(x)$ is written

$$F(\vec{k}) = \int_{-\infty}^{\infty} f(\vec{x}) e^{-i\vec{k}\cdot\vec{x}} d\vec{x} \tag{5.24}$$

and the inverse Fourier transform is

$$f(\vec{x}) = \frac{1}{2\pi} \int_{-\infty}^{\infty} F(\vec{k}) e^{i\vec{k}\cdot\vec{x}} d\vec{k} \tag{5.25}$$

So in Fourier transformation the function $f(\vec{x})$ is broken down into coefficients, $F(\vec{k})$, of plane waves $e^{i\vec{k}\cdot\vec{x}}$ that when integrated back together gives the original function $f(\vec{x})$. But what about if the problem has some symmetry so that $f(\vec{x})$ has some characteristic symmetry? Then it makes sense to think of $f(\vec{x})$ as the integral over symmetrized waves rather than unsymmetrized plane waves. To see how this works consider the arbitrary function $f(\vec{x})$ where the variable $\vec{x} = (x_1, x_2, x_3)$ is the position of three identical particles.

$$\begin{aligned} f(\vec{x}) &= \frac{1}{2\pi} \int F(\vec{k})(\hat{1}) e^{i\vec{k}\cdot\vec{x}} d\vec{k} && (5.26) \\ &= \frac{1}{2\pi} \int F(\vec{k})(S^{[3]} + N^{[3]} + A^{[3]}) e^{i\vec{k}\cdot\vec{x}} d\vec{k} && (5.27) \\ &= \frac{1}{2\pi} \int F(\vec{k}) S^{[3]} e^{i\vec{k}\cdot\vec{x}} d\vec{k} + \frac{1}{2\pi} \int F(\vec{k}) N^{[3]} e^{i\vec{k}\cdot\vec{x}} d\vec{k} && (5.28) \\ &\quad + \frac{1}{2\pi} \int F(\vec{k}) A^{[3]} e^{i\vec{k}\cdot\vec{x}} d\vec{k} && (5.29) \end{aligned}$$

Where we are using the notation for the projectors in S_3 from the previous section.

We have now written $f(\vec{x})$ as a sum (integral) over symmetrized waves. This is useful if we have some symmetrized function say $S^{[3]} f(\vec{x})$. In that case using the properties of projectors and Eq 5.29 we have

$$S^{[3]} f(\vec{x}) = \frac{1}{2\pi} \int F(\vec{k}) S^{[3]} S^{[3]} e^{i\vec{k}\cdot\vec{x}} d\vec{k} + \frac{1}{2\pi} \int F(\vec{k}) S^{[3]} N^{[3]} e^{i\vec{k}\cdot\vec{x}} d\vec{k} \tag{5.30}$$

$$+\frac{1}{2\pi}\int F(\vec{k})S^{[3]}A^{[3]}e^{i\vec{k}\cdot\vec{x}}d\vec{k} \tag{5.31}$$

$$= \frac{1}{2\pi}\int F(\vec{k})S^{[3]}e^{i\vec{k}\cdot\vec{x}}d\vec{k} \tag{5.32}$$

These results are quite easily generalizable to any symmetry group, and they show that if we know our function has some symmetry character, we know that only the symmetrized plane waves of that symmetry character are used in its spectral decomposition. For the case of continous Fourier transform this is not much benefit because we have gone from an infinite number of plane waves to a still infinite number of symmetrized waves. If we have a discrete Fourier transform the reduction in the number of wavevectors will be finite since we would only be dealing with a finite number to begin with.

Since the projector can be thought of to act on the function rather than the coordinates, the Fourier transform of $f(\vec{x})$ has the same symmetry as $f(\vec{x})$. This is most easily seen in Dirac notation where the Fourier transform is written

$$\langle\vec{k}|f\rangle = \int d\vec{x}\ \langle\vec{k}|\vec{x}\rangle\langle\vec{x}|f\rangle \tag{5.33}$$

Note that in Dirac notation the Fourier transform just involves the insertion of the completeness relation $1 = \int dx|x\rangle\langle x|$.

Say $f(\vec{x})$ is projected onto some symmetry, here we use $S^{[3]}$, we have

$$\langle\vec{k}|f\rangle = \int d\vec{x}\ \langle\vec{k}|\vec{x}\rangle\langle\vec{x}|S^{[3]}|f\rangle \tag{5.34}$$

Removing the completeness relation gives

$$\langle\vec{k}|f\rangle = \langle\vec{k}|S^{[3]}|f\rangle \tag{5.35}$$

Which shows that if $f(\vec{x})$ has some symmetry $F(\vec{k})$ must have the same symmetry.

Now we consider discretizing our problem. We will deal with S_N, but the same reasoning would apply to any type of symmetry group. One change between symmetry groups is that the grid should have the same symmetry as the problem. For S_N we take an N dimensional square grid. That is each $(1D)$ particle has its own linear grid that can be considered to be perpendicular to the other grids. To keep things as simple as possible we use S_2 as an illustrative example of how creating a symmetrized discrete Fourier transform could work.

There are many ways to think of the continous Fourier transform as a limit of the discrete transform [37]. It may be more elegant and far reaching to use one of these methods to connect the work done above for symmetrized continous Fourier transform with the development of a symmetrized discrete Fourier transform. However, here we take perhaps a more naive approach and write down the standard discrete Fourier transform and attempt to apply the same ideas that we used for continous transforms for the discrete version.

The standard form of the $1D$ Fourier transform is

$$X_k = \sum_{n=0}^{p-1} x_n e^{-\frac{2\pi}{N} ikn} \tag{5.36}$$

with the inverse

$$x_n = \frac{1}{p} \sum_{k=0}^{p-1} X_k e^{\frac{2\pi}{N} ikn} \tag{5.37}$$

Where the p grid points are labeled by n in real space and k in momentum space.

Since we want to consider S_2 we need the two dimensional transform. Luckily generalizations to higher dimensions are simple giving

$$X_{k_1,k_2} = \sum_{n_1=0}^{p-1} \sum_{n_2=0}^{N-1} x_{n_1,n_2} e^{-\frac{2\pi}{p} i(k_1 n_1 + k_2 n_2)} \tag{5.38}$$

with the inverse

$$x_{n_1,n_2} = \frac{1}{p^2} \sum_{k_1=0}^{p-1} \sum_{k_2=0}^{p-1} X_{k_1,k_2} e^{\frac{2\pi}{p} i(k_1 n_1 + k_2 n_2)} \tag{5.39}$$

In general it is not necessary to have the same number of grid points along each dimension, but since we want identical particles we choose the same number of grid points here.

If the numbers x_{n_1,n_2} are symmetrized with respect to the indices n_1 and n_2 we have

$$S^{[2]} x_{n_1,n_2} = \frac{1}{p^2} \sum_{k_1=0}^{p-1} \sum_{k_2=0}^{p-1} X_{k_1,k_2} S^{[2]} e^{\frac{2\pi}{p} i(k_1 n_1 + k_2 n_2)} \tag{5.40}$$

$$S^{[2]} x_{n_1,n_2} = \frac{1}{p^2} \sum_{\kappa=0}^{p(p+1)/2} X_\kappa \phi_\kappa^S(n_1, n_2) \tag{5.41}$$

where

$$\phi_\kappa^S(n_1, n_2) = \frac{1}{2} \left(e^{\frac{2\pi}{p} i(k_1 n_1 + k_2 n_2)} + e^{\frac{2\pi}{p} i(k_2 n_1 + k_1 n_2)} \right) \tag{5.42}$$

and each κ is associated with a pair of original points and serves to label the new symmetrized waves.

Additionally each of the original (n_1, n_2) pairs must be relabeled since some of them produce the same x_{n_1,n_2}. So really we have

$$S^{[2]} x_\eta = \frac{1}{N^2} \sum_{\kappa=0}^{p(p+1)/2} X_\kappa \phi_\kappa^S(n_1, n_2) \tag{5.43}$$

The number of points that the discrete transform needs to be taken on has been approximately reduced by a factor of 2.

All that needs to be done is to tabulate the (discrete) values of the $\phi_K(\eta)$ functions and you have a procedure for a $1D$ discrete Fourier transform that works in a subspace of the original $2D$ system.

In general for N particles the discrete plane waves can be symmetrized producing a number of symmetrized plane waves that can be calculated using Young tableau with the same procedure from section 5.3. In fact what is being done here is essentially the same thing as in section 5.3 except it is being applied to the Fourier tranform.

The drawback to this method is that it is not clear how to use factorization of the $\phi_K(\eta)$ functions to split the transform into two transforms that can then be split again as is done in the algorithm for FFT. This algorithm is important because it takes the algorithm from $O((p^N)^2)$ operations to $O(p^N \log p^N)$. It seems that it should be possible to come up with some grouping of the symmetrized waves that makes a similar algorithm possible and results in the same speed up.

As it is, however, the symmetrized discrete transform is an improvement over certainly the unsymmetrized naive discrete transform, but possibly even the FFT if N is large enough. As we see from section 5.3 the number of symmetrized waves of a certain symmetry character is $p^N/N!$ asymptotically. So if $x_{\vec{n}}$ has that symmetry character, using the symmetrized transform results in an improvement from $O(p^{2N})$ to $O(p^{2N}/(N!)^2)$. The FFT results in an improvement to $O(p^N \log p^N)$. However if N is considered to be the variable that is becoming large rather than p, the symmetrized discrete Fourier transform eventually will do better than the FFT. So for certain implementations the symmetrized transform should already be used instead of the fast transform.

The general effect for the symmetrized Fourier transform is actually opposite that of the FFT. In FFT the idea is to split a $1D$ transform into many nested transforms and nested transforms behave as multidimensional transforms. The symmetrized

Fourier transform is taking multidimensional tranforms and synthesizing them into $1D$ transforms with fewer elements (about $1/N!$ for S_N).

5.5 Conclusions

Group theory will continue to be a valuable tool and it is useful in a wide range of application because of the association between symmetries and groups. Much of the literature on groups is difficult for physicists to penetrate because of the different way that mathematicians explain things. Many of of the useful ideas that are actually stated in this chapter are usually obliquely mentioned as an afterthought to a theorem. For this reason much of the information in this chapter was gathered as a reference for physicists who would like to increase their knowledge on S_N and its applications.

Bibliography

[1] R.B. Laughlin, *Phys. Rev. Lett.*, **50**, 1395-1398 (1983).

[2] R.K. Pathria, *Statistical Mechanics*, 2nd edition, Butterworth-Heineman, Oxford (1996).

[3] M.V. Berry, *J. Phys. A: Math. Gen.*, **35**, 3025 (2002).

[4] M.V. Berry, *J. Phys. A: Math Gen.*, **10**, 2083 (1977).

[5] M. Srednicki, *Phys. Rev.* E, **50**, 888 (1994).

[6] J.D. Urbina and K. Richter, *J. Phys. A: Math. Gen.*, **36**, L495 (2003).

[7] R. Jancel, *Foundations of Classical and Quantum Statistical Mechanics*, Pergamon, Oxford (1969).

[8] H.M. Kleinert, *Path Integrals in Quantum Mechanics, Statistics, and Polymer Physics*, 2nd edition, World Scientific, Singapore (1995).

[9] D. Chandler and P.G. Wolynes, *J. Chem. Phys.*, **74**, 4078 (1981).

[10] D.M. Wang and J.B. Delos, *Phys. Rev. A* , **63**, 043409 (2001).

[11] M.V. Berry, *J. Phys.* A, **35**, 3025, (2002).

[12] A. Nakayama and N. Makri, *J. Chem. Phys.*, **125**, 024503 (2006).

[13] A. Nakayama and N. Makri, *J. Chem. Phys.*, **119**, 8592 (2003).

[14] J. Ciozlowski and K. Pernal, *J. Chem. Phys.*, **113**, 8434 (2000).

[15] M. Casula and D.M. Ceperley, *Phys. Rev. A*, **78**, 033607 (2008).

[16] E.J. Heller, *J. Chem. Phys.*, **94**, 2723 (1991).

[17] F. Jensen *Introduction to Computational Chemistry*, Wiley (2007).

[18] E. Lieb, *Rev. Mod. Phys.*, **53**, 603-641 (1981).

[19] A. Thorolfsson , et al, *Astrophys. J.*, **502**, 847-857 (1998).

[20] L. Spruch, *Rev. Mod. Phys.*, **63**, 151-209 (1991).

[21] L. H. Thomas, *Proc. Cambridge Philos. Soc.*, **23**, 542-548 (1927). E. Fermi, *Rend. Accad. Naz. Lincei*, **6**, 602 (1927).

[22] N.H. March and J.S. Plasckett, *Proc. Roy. Soc. A* **235**, 419 (1956).

[23] M. C. Gutzwiller, *Chaos in Classical and Quantum Mechanics*, Springer-Verlag, New York (1990).

[24] M. Brack and R.K. Bhaduri, *Semiclassical Physics*, Chapter 4, Westview Press, Boulder (2003).

[25] R.M. Dreizler and E.K.U. Gross, *Density Functional Theory: An Approach to the Quantum Many-Body Problem*, Chapter 5, Springer-Verlag, Berlin (1990).

[26] D. Ullmo, T. Nagano, S. Tomsovic, and H.U. Baranger, *Physical Review B*, **63**, 125339 (2001).

[27] M.A. Zaluska-Kotur, M.G. Gajda, A. Orlowski, and J. Mostowski, *Phys. Rev. A*, **61**, 033613 (2000).

[28] H.M. Sommermann and H.A. Weidenmueller, *Europhysics Letters*, **23**, 79-84 (1993).

[29] A. Wasserman, N.T. Maitra, and E.J.Heller, *Phys. Rev. A* , **77** 042503 (2008).

[30] E. Lieb and D. Mattis, *Phys. Rev.*, **125**, 164 (1962).

[31] I.P. Hamilton and J.C. Light, *J. Chem. Phys.*, **84**, 306 (1986).

[32] M. Seidl, P. Gori-Giorgi, and A. Savin, *Phys. Rev. A*, **75**, 042511 (2007).

[33] E. Noether, *Nachr. D. Knig. Gesellsch. D. Wiss. Zu Gttingen, Math-phys. Klasse*, **1918**, 235-257 (1929).

[34] G. James and A. Kerber, *The representation theory of the symmetric group*, Addison-Wesley Publishing Co, Reading, MA (1981).

[35] M.G. Reuter, M.A. Ratner, and T. Seideman, *J. Chem. Phys.*, **131**, 094108 (2009).

[36] M. Tygert, *J. Comp. Phys.*, **227**, 4260-4279 (2008).

[37] W.L. Briggs and V.E. Henson, *DFT: an owner's manual for the discrete Fourier Transform*, SIAM, Philadelphia (1995).